Doctoral Dissertation

NUMERICAL STUDY ON CHARACTERISTICS OF TIDAL CURRENT IN BENOA BAY, BALI-INDONESIA AND ITS ADJACENT AREA

I Gede Hendrawan

A dissertation submitted to the Department of Civil and Environment Engineering of Yamaguchi University in partial fulfillment of requirement for the degree of Doctor of Philosophy (PhD)

Department of Civil and Environmental Engineering
Graduate School of Science and Engineering
Yamaguchi University, Japan

January, 2014

ABSTRACT

Bali is one of the world tourism destination; and as a small island, Bali is surrounded by sea. Bali has a lot of beautiful marine destinations that are very attractive for the tourism activity such as diving, marine sport, and fishing. Bali famous tourism destination located in the coastline are Nusa Dua and Sanur. The seawater in Nusa Dua and Sanur is mostly influenced by the seawater from the Lombok Strait, Badung Strait and Benoa bay. In order to preserve those tourism destinations, it is important to know the characteristics of the seawater flow in the surrounding area.

The importance of Lombok Strait as one of the route of Indonesia Troughflow (ITF) would influence the dynamic of seawater in the adjacent area. Badung Strait has rough bottom topography and Lombok strait has a sill in the southern channel. This condition would have potentially triggered the mixing and upwelling in Lombok and Badung Straits. However, until now I have not found any research concerning the tidal upwelling in the Lombok strait.

Benoa bay is located in Bali and has connection with Badung Strait. Benoa bay is also a very famous place located near the tourism destination. Although in relation to the importance of Benoa bay, it has both economic and ecologic factor, there are still very few researches conducted to know the characteristics of the water circulation that occurred in the Benoa bay. From those backgrounds, I attempt to make an investigation of the tidal characteristics of the Benoa bay and its adjacent area using numerical model.

Firstly, the characteristics of the upwelling occurred around the Lombok sill was presented. This research was implemented numerically with Finite Volume Coastal Ocean Model (FVCOM). The numerical results indicated the occurrence of tidal upwelling over the Lombok sill. The upwelling occurred in the northern side of Lombok sill just after northward flow began; where the seawater temperature decreases to 20°C at 400 m depth and increases to 26°C at 300 m depth in the southern side of the sill. After the maximum and the end of northward tidal flow, the seawater downwelling occurred in the northern side of the sill and upwelling in the southern side of the sill. This caused the seawater temperature at 400m depth in the northern side increase to 22°C; whereas at 300 m depth in the southern side, the temperature reduces to 24°C. During the southward tidal flow, the tidal upwelling can be seen in the northern side of Lombok Sill; and just after southward flow begins, the seawater temperature decreases to 20_0C at 350m depth. Meanwhile, tidal downwelling occurred in the southern side of the sill and the seawater temperature becomes 26°C at 300m depth. The strong tidal

upwelling in the northern side of the sill and strong tidal downwelling in the southern side of the sill occurred after maximum southward tidal flow. It caused the temperature in the top of the sill decrease to 22°C. The upwelling occurred in the Lombok strait would bring high nutrient from deeper water to the surface. In addition, the tidal upwelling in Lombok strait will bring cooler water from deeper water to the surface. This cool water will decrease the evaporation, and has an impact for the local weather/climate.

Secondly, the water exchange of Benoa bay was presented. This research was also implemented numerically with FVCOM. For comparison, the numerical simulations were conducted for showing not only the present configuration of the bay but also the past one. Two past configurations were considered. One is the configuration with unreclaimed Serangan Island and the Benoa harbor, while the other is that with unreclaimed Serangan Island and no Benoa harbor. On the other hand, in this study we also make a new configuration for the Benoa bay, removing of the road that connecting the Benoa harbor with the main Island.

For the past configuration of Benoa bay, the water flow is divided into two routes, to the northern channel and to the southern channel. Relatively, the strong current occurred in both channel for the case of unreclaimed Serangan Island, the maximum tidal current was 0.45 m/s during ebb tide and 0.3 m/s during flood tide. The similar tidal current pattern can be seen for the case of Benoa bay without the Benoa harbor (original condition). Different mechanism occurred for the present condition. The seawater flow only has one channel, which is the southern channel with narrower channel. At the narrow strait in the bay mouth, the M2 tidal current reached 0.46 m/s during ebb tide and 0.31 m/s during flood tide. After made a new configuration of Benoa bay, seawater could flow from the northern channel between Benoa harbor and main Bali island, up to the outer (inner) bay during ebb (flood) tide, and the tidal current increase in the bay mouth becomes 0.66 m/s during ebb tide.

The characteristics of the seawater exchange were investigated by using the Langrangian particle method. The particle transport has a different pattern for three cases. The original configuration of Benoa bay could transport 80% particle from the inner bay to the outer bay, the only by four M2 tidal cycles. However, the particles only exported 60% and 50% for the case of Benoa bay with harbor and reclaimed condition respectively. The modification of present configuration could export more than 65% particles to the outer bay, after four tidal cycles. This case can give a better seawater exchange compared to the present configuration.

ACKNOWLEDGEMENT

I thank God for blessing, protecting and guiding me throughout my life. I thank him for giving me the strength despite all of the obstacles I have faced in my journey of life.

I would like to express the deepest gratitude and appreciation to my supervisors, Associate Professor Dr. Koji Asai, for inspiring guidance, encouragement, and constructive criticism for the period of taking a Ph.D course in Yamaguchi University. His technical guidance and unflagging encouragement will always be cherished

I would like to express deep appreciation to my thesis committee, Prof. Dr. Masahiko Sekine, Prof. Dr. Kesayoshi Hadano, Prof. Dr. Kakuji Ogawara, Assc. Prof. Dr. Koichi Yamamoto, and Prof. Dr. Tasuku Tanaka for providing considerable discussions and beneficial suggestions.

I would like to express deep gratitude to left of Prof. Dr. Yasuhiro Sugimori (former Director of Centre for Remote Sensing and Ocean Sciences (CReSOS), Udayana University-Bali, Indonesia). He has brought me to Japan and change my life by introducing me doing a research with his excellent knowledge. I have been very fortunate to know him as a wonderful person with a high responsibility and encourage me to continue to study and making a research. He also always gives a motivation by share his great experience to me.

I would like to convey my gratitude to Professor Dr. Made Bakta (former Rector of Udayana University) for supported my PhD study. I also would like to thanks Dr. Asai Laboratory member for their help in my PhD study and life in Yamaguchi. I would like to thank everyone in the Faculty of Marine Sciences and Fisheries, Udayana University-Bali, are acknowledged for their supports.

I would like to thank to the Government of Republic Indonesia through the National Education Ministry for granting me a PhD scholarship by mean of "Beasiswa

Unggulan". I thank the Centre for Remote Sensing and Ocean Sciences (CReSOS) Udayana University, which has supported me to pursue PhD degree in Yamaguchi University. I also thank Yamaguchi University, Graduate School of Science and Engineering which has accepted me as PhD student.

I dedicated this research to my parent Drs. I Nengah Teka Suriawan, S.H., M.Pd and Ni Wayan Rapig, SE who have never stopped to pray for me. I also dedicated this research to my beloved wife Ni Kadek Septia Sari, SH., M.Kn, and to my sons I Gede Krishnanda Sugi Mahendra and I Kadek Jyotisha Yama Mahendra for their understanding and encouragement. I am very much thankful to my brother and sister Made Agus Setiawan, S.Kom., M.Kom and Ni Komang Ayu Setiawati, S.Pd respectively for their many sacrifices and encouragement.

Finally, I would like to thank everybody who was important to the successful realization of this thesis, as well as expressing my apology that I could not mention personally one by one.

TABLE OF CONTENTS

LIST OF FIGURES

LIST OF TABLE

CHAPTER 1
GENERAL INTRODUCTION

1. General Background

The Ocean is a major buffer in moderating seasonal and climate changes in temperature (Mellor, 1996). Aside from their importance on climate, the ocean plays a major role in present day society and economics. Coastal region are used for a number of human activities, over sixty percent of the human population lies in the coastal zone. Coastal waters are also a major resource for human life as they contribute ninety percent of world fish catch (Kunthe, 2003).Coastal development has an implication to make a modification for the nature of the coastal region, such as mangrove ecosystem and direct result of pollutant amount from the human activities. Although the coastal region also provides important recreation resources, it is controlled by the influence of atmospheric and oceanic weather condition (Mellor, 1996). Furthermore, it also depends on the coastal quality, as in coastal water quality.

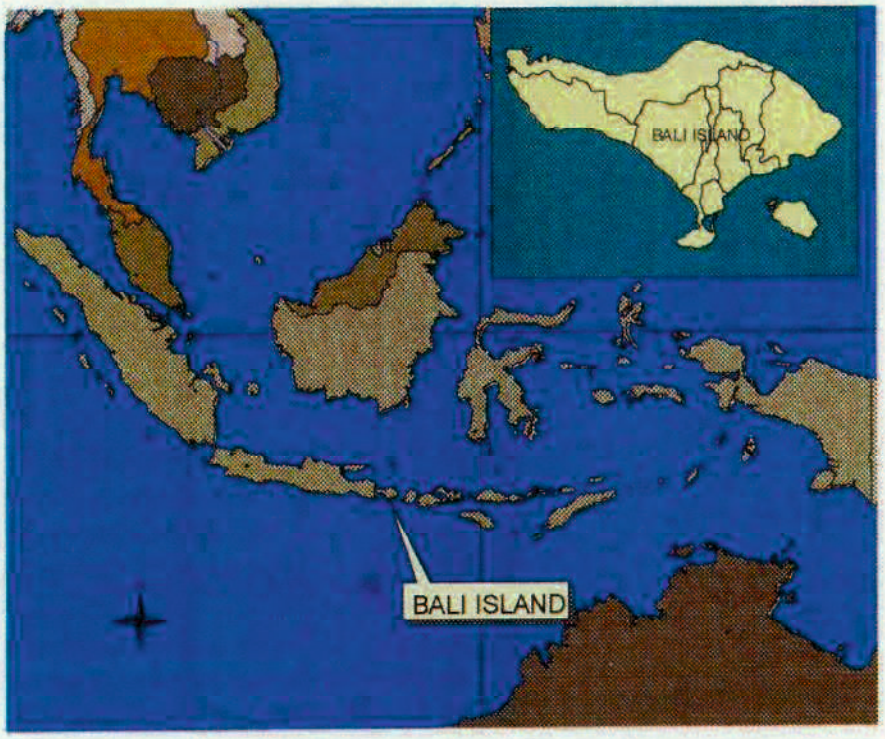

Figure 1.1 Indonesia and the island of Bali in the top right zoom displayed

(Sources: Integrated Coastal Zone Management Project Report in 2001)

The studies of tidally influenced coastal water have to include the hydrodynamics of coastal system. The coastal hydrodynamics control a variety of coastal processes including tidal flushing, pollutant dispersion, tidal currents, sedimentation, erosion, and water levels (Wood, 1999). Numerical models provide a cost-effective method for evaluating tidal hydrodynamics since they require limited data collection and may be utilized to numerically assess a range of management alternatives. Once the hydrodynamics of an estuary system are comprehended, computations regarding the related coastal processes become relatively straightforward extensions to the hydrodynamic modeling; for example, the spread of pollutants may be analyzed from tidal current information developed by the numerical models.

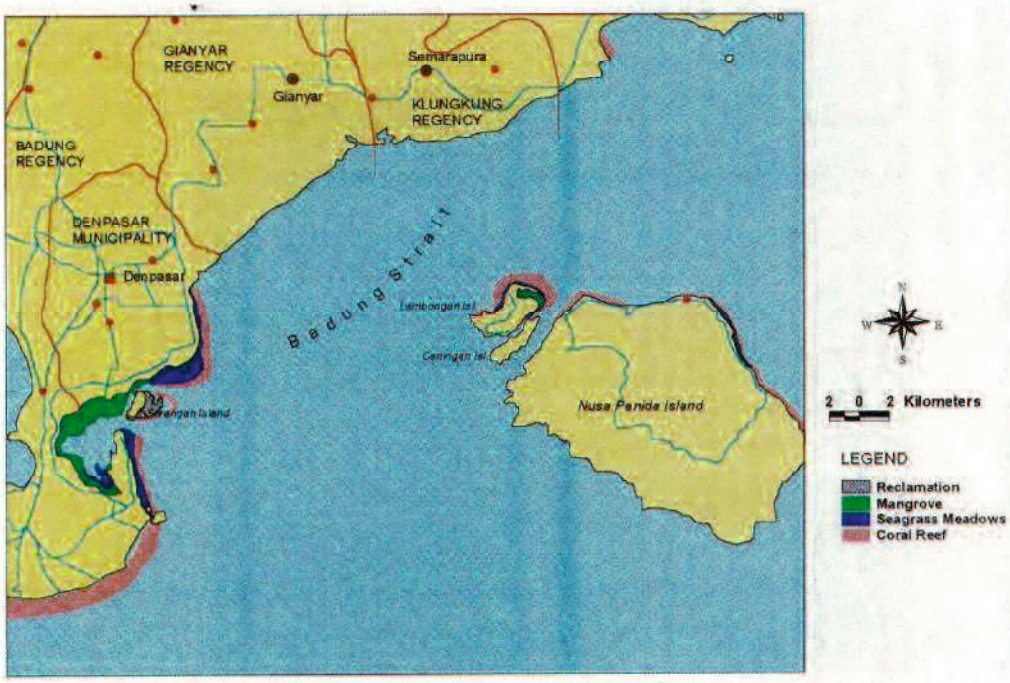

Figure 1.2. Major ecosystem on southeastern part of Bali

(Sources: Integrated Coastal Zone Management Project Report in 2001)

Bali is a small island located in the Indonesia (Fig. 1.1), that its coastal area has an important role for the people who live in Bali. The southeastern parts of Bali are coastal areas that have very high ecosystem diversity; such as mangrove, coral reef, and sea grass (Fig. 1.2). Hence, this area is very well known to utilize various activities that took advantage of environmental utilization, such as tourism, fisheries, and marine transportation. The coastal water could provide natural resources and environmental utilization that serves a critical role in supporting the life of surrounding community.

Economy growth in Bali, especially on southeastern part of Bali is mostly supported from tourism sector that utilizes the services of coastal and marine environments. Similarly, fishery activity also has an important role as a living foundation for the coastal communities. From marine transport point of view, the role is applied in freight and passenger services system that connects Bali to other islands in Indonesia and to other countries.

Lombok and Badung Strait are very important areas for the tourism activities such as diving and snorkeling, fishing activities such as fishing for local fishermen and seaweed cultivation, as well as inter-island maritime transport activities and international shipping lanes. Besides for various activities, these regions are also very attractive places from its marine sciences point of view. Other important location in the south-east of Bali is Benoa bay. It is a region with the largest mangrove ecosystem in Bali. Benoa bay is also used as a harbor, which is called Benoa harbor. It is the largest harbor for Bali, which used for fishing boats, passenger vessels, and cruise ships.

The importance of Lombok strait as the route of the Indonesia Troughflow (ITF) would influence the dynamic of seawater in the adjacent area. The internal wave generated by the sill in Lombok strait is well described by Susanto et.al (2005). The mixing processes in ITF route have been investigated by Hatayama (2004) in Dewakang sill (Makasar strait) and show the role of the sill. The rough bottom topography has an important role for the mixing and upwelling. These mixing and upwelling will control the local climate and also for the people who are interested in fishery.

Lombok strait is well known as one of the route for ITF and has a connection with Badung strait. Badung strait has rough bottom topography and Lombok strait has a sill in the southern channel. These topographical conditions would trigger the mixing and upwelling in Lombok and Badung strait. Therefore, it is very important to understand flow characteristics of Lombok and Badung strait in relation to the local impact for Bali as tourism destination and to the local fishermen. However, until now I have not found any research concerning the tidal upwelling in the Lombok strait. Upwelling is important for the nutrient; thus we must understand the mechanism of upwelling in Lombok Strait.

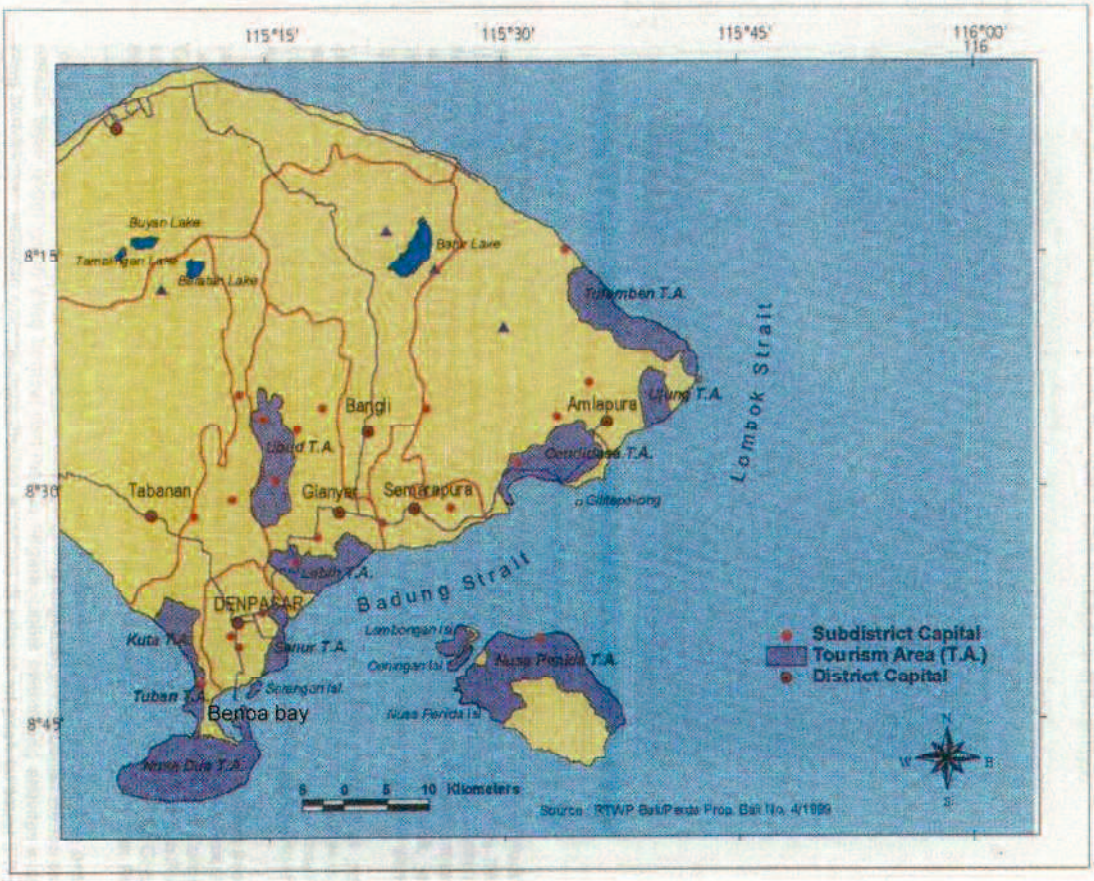

Figure 1.3. Southeastern part of Bali

(sources: Integrated Coastal Zone Management Project Report in 2001)

Benoa bay is located in Bali and has connection with the Badung strait (Fig. 1.3). Benoa bay is also a very famous place that located near tourism destination of Nusa Dua and Sanur. Recently, Benoa bay has been suffering from many of human activity, such as harbor activity and pollutant discharge from the river. The water quality in Benoa bay is also will controlled by the Badung strait. In the inner bay lies the harbor for national and international ocean traffic. Before the year of 1996, Serangan is only a small island located in the bay mouth and separated from the main island of Bali. It has two channels; southern channel between Tanjung Benoa and Serangan Island, and northern channel between Serangan Island and Bali Island. This original shape of Benoa bay made the seawater flow out from inner of bay without difficulty (Hendrawan, 2005). However, after the year of 1996, Serangan island being reclaimed and connecting Bali with Serangan Island. The reclamation of Serangan Island has changed the geometry of the Benoa bay. The bay mouth in the southern and

northern channel becomes narrower in approximately 400 m and 50 m respectively. It gave a serious impact for the water circulation (Hendrawan, 2005). The shape change has caused several ecological problems in the deterioration of water quality that characterized by an increase of BOD (biological oxygen demand) value, and an accumulation of oil spills, as well as a decrease of diversity index and abundance of macrozoobenthos in the inner of bay (see table.1). Until recently, only a few researchers have studied on the oceanic condition of Benoa Bay on either the general tidal flow characteristics or the seawater exchange. The residual current based on numerical study in Benoa bay have been done by Hendrawan et al (2005) and Koropitan (2005). However, these results did not provide enough explanation concerning the tidal current and restricted on two-dimensional circulations in the Benoa bay.

Table 1.1. Evidence of the impact on Reclamation of Serangan Island

Parameter	unit	Before Reclamation	After Reclamation
BOD	ppm	1 – 5*	7.5 – 10**
Oil spill	ppm	12 – 18*	62 – 366**
Macrozoobenthos Diversities index	-	1 - 2.56*	0 - 2.0***
Macrozoobenthos abundance	Ind/m^2	402 – 1268*	25 – 700***

note: * *:Sugirawan (1992)*
** *: Udayana University for the research affair (2000)*
*** *: Fitriana (2004)*

2. Environmental Setup

Figure 1.4 shows the bathymetry map obtained from Hydro-Oceanography Division Indonesian Navy (DISHIDROS-TNI AL). Benoa bay is shallow, where the deepest part in the inner part of the bay is less than 15 m and the outer part (towards the ocean) is less than 50 m. In the inner part of the bay, particularly in the nearest coastline, water depth varies from about 1 m to 5 m. The surroundings of the bay mouth and the east part of Benoa harbor have the stepped bottom topography with depth around 10 to 15 m.

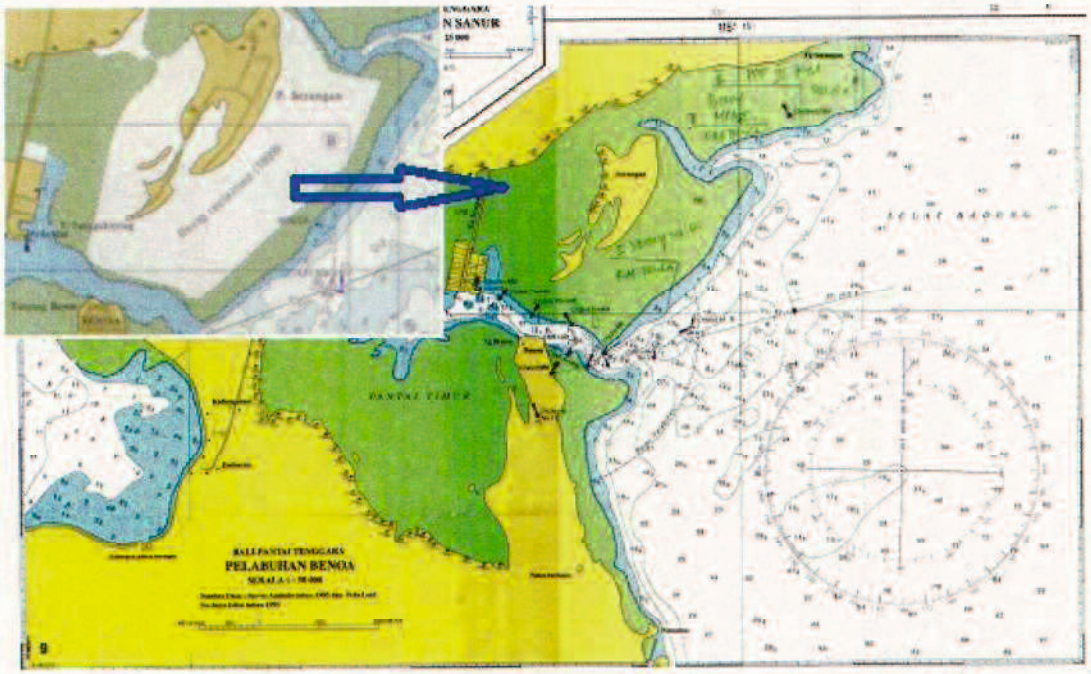

Figure 1.4 Bathymetry map of Benoa Bay (Sources: Dishidros map)

The seawater coming from Badung Strait controls Benoa bay. Badung Strait lies between Bali and Nusa Penida. Badung Strait is controlled by the seawater from Lombok Strait and Indian Ocean. Both of Badung Strait and Lombok strait has unique bottom topography. The northern part of Lombok strait is characterized by the deep water and shallower toward the sill in northern part between Nusa Penida and Lombok. From the sill toward the Indian Ocean, the bottom topography becomes deeper. Badung Strait is characterized by deep water column from the Lombok Strait toward the inner part of Badung Strait, and becomes shallow from the inner strait toward the southern part of Badung Strait. Those shapes of bottom topography may drive the tidal mixing and act as an input for Benoa bay.

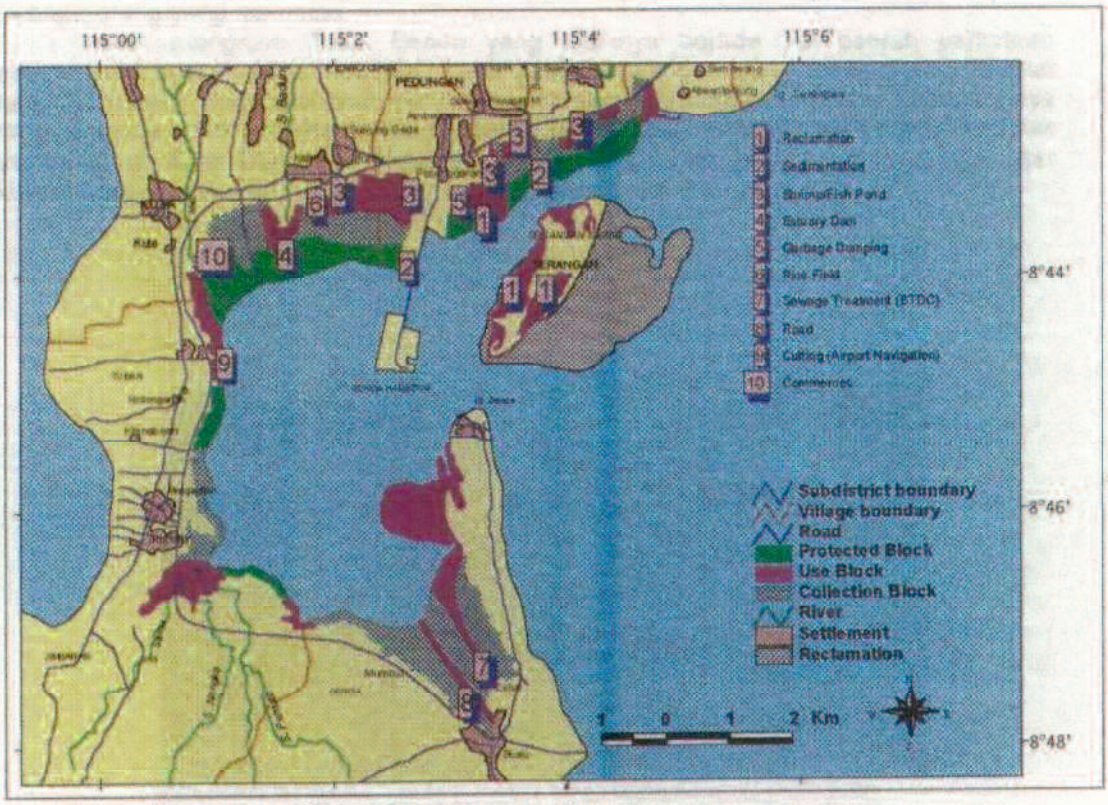

Figure 1.5 Ecological degradation in Benoa bay

(sources: Integrated Coastal Zone Management Project Report in 2001)

Recently, Benoa Bay has been suffered by a number of human activities (Fig. 1.5) and under the influence of the six rivers discharges: Badung, Mati, Sama, Telabah, Lolan and Rangda River. According to the report of Environmental Impact Assessment Agency of Bali Province, the fresh water discharged into the bay is less than 360 m^3/hours in each river. The harbor activity may also be a source of pollutant into the seawater, such as oil and several domestic activities. In the northeastern part of Benoa Bay (Suwung), it is used as garbage dump that the final garbage collection for two regencies in Bali, Denpasar city and Badung regency occur. This garbage dump is using the mangrove area and could be as a source for a number of pollutants within Benoa bay. There is a wastewater treatment in the region of Bali Tourism Development Centre (BTDC), which is located in the southern part of Benoa Bay. This facility may also be a source point of the pollutants discharging into the seawater and could degrade the seawater quality.

In general, the oceanic circulation within the Benoa Bay is controlled by inflows from Badung strait and Indian Ocean. The tides and tidal currents are typical of water

circulation in Benoa Bay. The type of tides in Benoa Bay is semi-diurnal, in which the M_2 is the dominant tidal component. During spring tide, the sea level in the inner bay can rise up to 2.5 m and drop about 2.1 m during neap tide.

Benoa bay has an important role for several habitats. Approximately 1,373 ha Mangrove grows along the coastline of Benoa bay. The mangrove ecosystem is located in the border of land and seawater. The mangrove habitats have an essential role for several marine species for live, since a variety of organism interact each other. In the outer of bay there are sea grass and coral reef habitats. Those habitats are important for not only our coastal environment but also as an attractive point for Bali tourism activities.

In order to ensure the mechanism of water transport which has an important role for the pollutant dispersion, we have to know the seawater circulation in Benoa bay. Unfortunately, not many scientific researchers have done what concerns the seawater circulation. Since Benoa Bay is mainly control by the tide, therefore it is important to understand the physical process of the tidal current field in order to discuss the water quality and the eco-system in Benoa Bay.

3. Previous Studies

The general characteristics of tide and tidal current in the Indonesian seas have been well described by Hatayama et al (1996). They also describe clearly that the tidal current are influenced by the coastal geometry such as the narrow strait. The tidal current also has an important role for transport and mixing processes in the Indonesian seas (Hatayama et al, 1996). A strong baroclinic M_2 tide were generated along the shelf slope break and over rough topography, particularly in straits (Robertson and Ffield, 2005).

The importance of Lombok strait as the route of Indonesia Troughflow (ITF) would influence the dynamic of seawater in the adjacent area. The intraseasonal variability appear most frequently and largest in magnitude for the pressure in the Lombok Strait (Potemra et al, 2002). Mitnik et al (2000) and Mitnik and Alpers (2000) suggested that the nonlinear solitary waves are generated by tidal current in the sill area between the islands of Lombok and Nusa Penida and their estimated propagation

velocity was 1.8-1.9 m/s. Susanto et al (2005) observed the high amplitude internal solitary wave in Lombok Strait.

The general oceanic circulation in Benoa bay has been analyzed using 2-dimensional numerical model (Hendrawan, 2005; Koropitan, 2005). They found that the development of Benoa harbor and the reclamation of Serangan Island have a significant role for the change of ocean current pattern. The seawater is relatively easy to be entered and exited from the bay before the harbor construction and the reclamation. However, the phenomena were changed after the constructions. The clockwise and anticlockwise eddy is formed by the M2 tidal residual current in the inner bay, while the clockwise eddy is formed in the bay mouth (Hendrawan, 2005).

The impact of harbor and Serangan reclamation indicated the accumulation of Biology Oxygen Demand (BOD) concentration and Chemical Oxygen Demand (COD) concentration in the inner bay (Koropitan, 2005). However, the BOD and COD concentration could be distributed to the outer bay without the existence of the harbor and reclaimed of Serangan island (Koropitan, 2005).The phosphate concentration in Benoa bay was found higher than the normal condition for the tourism and fisheries cultivation activity (Hendrawan and Ardhana, 2009). The phosphate sources in the Benoa bay are contributed by the river discharge, harbor activity, garbage dump, and wastewater sewerage treatment (Hendrawan and Ardhana, 2009). The concentration of phosphate is also accumulated in the inner of bay rather than transported toward outer bay (Hendrawan and Ardhana, 2009).

4. Aim and Objectives

As mentioned before, the role of Lombok sill and the seawater exchange of Benoa bay become more important for water environment, local climate, fishery and tourism. If we know a clear mechanism of tidal current and upwelling in the Lombok strait, this will be very helpful for the fisherman and the meteorologist concerning the local climate. If we have a clear knowledge of the water exchange of Benoa bay for the environment point of view, this knowledge will be very important for the government in order to maintain Benoa bay environment for tourism activity. The water exchange of Benoa bay and the up/down welling at Lombok sill is induced by the tidal current. Therefore, the tidal current has a very important role,

so that the aim of this study is to reveal the characteristics of the tidal current in the target sea area.

The many observation data are required to reveal the characteristics of the tidal current. Unfortunately, there are little observation data and it is expensive to conduct the filed observations. In this study, the approach of the numerical simulation is mainly used to achieve the aim of this study.

Based on the aim of this study, the objectives of this study are as follows;

1) To reveal the characteristics of the up/down welling at Lombok sill induced by the tidal current.
2) To reveal the characteristics of the seawater exchange in Benoa bay. Especially, the effect of the configurations of Benoa bay on the seawater exchange is focused.

The present study consists of 5 chapters. The first chapter includes a general introduction, a description of the study area, a review of earlier studies and the objective of the study. The second chapter presents the literature review. The description of Finite Volume Coastal Ocean Model (FVCOM) is also involved. The third chapter discusses the tidal upwelling in Lombok strait. The fourth chapter describes the characteristics of tidal current and identifications of seawater exchange in Benoa bay. The fifth chapter is conclusions of the entire study. It is followed by future studies.

References

Bali Local Government, The Environmental Impact Assessment Agency, 2001, Coastal and marine environment profile at South-east of Bali, Integrated Coastal Zone Magament Project Report.

Fitriana. YR., 2004., Keanekaragaman dan kelimpahan kominitas makrozoobenthos pada hutan mangrove hasil rehabilitasi di taman hutan raya ngurah rai, bali. Undergraduate thesis: Bogor Institute of Agriculture.

Hatayama, T., Awaji, T. and Akitomo, K. 1996, Tidal current in the Indonesian seas and their effect on transport and mixing, Journal of Geophysical Research, Vol.101, pp.12353-12373

Hendrawan, I.G. 2005, Barotropic Model to Calculate Water Circulation in Benoa Bay Bali, Master Thesis, Master Program of Environmental Study, Udayana University, Bali-Indonesia

Hendrawan, I.G.Nuarsa.W.,Sandi.W., Koropitan. A., Sugimori Y., 2005, Numerical Calculation for the Residual Tidal Current in Benoa Bay- Bali Island, International Journal of Remote Sensing and Earth Science.p.86-93

Hendrawan.I.G and Ardana.I.K.2009, Numerical Calculation of Phosphate Transport in Benoa Bay, Bali, International Journal of Remote Sensing and Earth Science.vol. 6. p39-45

Koropitan.A.F. 2005. Flow Pattern and Pollutant Distribution in Benoa Bay-Bali Island: A Numerical Model Experiment. Proceeding of the 4th Hokkaido Indonesian Student Association Scientific Meeting, Sapporo, 20 March 2005.

Kunte, P.D. 2003. Study of Sediment Transportation in The Bay of Kachchh, Using 3D Hydro-dynamic Model Simulation and Satellite Data (Doctor Dissertation). Doctoral Program at Center of Environmental Remote Sensing Chiba University, Japan

Mellor, G.L. 1996, Introduction to Physical Oceanography (text book), Springer, USA

Mitnik, L., and W. Alpers. 2000. Sea surface circulation through the Lombok Strait studied by ERS SAR. *Proceedings of the 5th Pacific Ocean Remote Sensing Conference (PORSEC 2000)*, 5-8. Dec 2000, Goa, India, Vol. I, Pp. 313–317

Mitnik, L., W. Alpers, & H. Lim. 2000. Thermal plumes and internal solitary waves generated in the Lombok Strait studied by ERS SAR. ERS-Envisat Symposium: Looking down to Earth in the New Millenium, 16-20 October 2000. Gothenburg, Sweden. SP-461. European Space Agency, Publication Division, Noordwijk, The Netherlands, Pp. 1-9

Potemra, J.T., 2002.Interaction between the Indonesian Seas and the Indian Ocean in Observations and Numerical Models, Journal of Physical Oceanography, Vol. 32, pp. 1838-1854

Robertson. R and AmyFfield. 2005, M2 BaroclinicTide in The Indonesian Seas, Oceanography, Vol. 18, No. 4, pp. 62-73

Sugirawan. IBK., 1992., Kondisi ekologi perairan muara sungai badung di teluk benoa ditinjau dari parameter fisika, kimia, biologi. Undergraduate thesis: Bogor Institute of Agriculture.

Susanto, R. D., Mitnik, L. and Zheng, Q. 2005, Ocean internal wave observed in the Lombok Strait, Oceanography, Vol.18, pp.80-87.

Wood, J.D., John S.R., Sean W.K. 1999, Two-Dimensional Hydrodynamic Modeling of Barnstable Harbor and Great Marsh, Barnstable, MA (Final Report), Applied Coastal Research and Engineering, Inc

CHAPTER 2
LITERATURE REVIEW

1. The Indonesian Seas

The Indonesian archipelago lies between two Ocean, i.e., the Pacific Ocean and the Indian Ocean. The Indonesian region is known as the "Maritime Continent". It is composed of more than 16,000 islands and with 81,000 km coastal perimeter. The Indonesian seas have a complex bottom topography and coastal geometry. It has an important role for the mixing in the ocean water. The ocean mixing and the connection of the Pacific Ocean and the Indian Ocean by the Indonesian seas play a role in maintaining of sea surface temperature (SST), further it will control the regional and global climate (Qu et al, 2005).

The Indonesian throughflow (ITF) is important for global climate since the warm water move from the Pacific to the Indian Ocean. This mechanism serves as the upper branch of the global heat conveyor belt. The upper thermocline of ocean water from the western Pacific Ocean pass through the Makassar Strait to either directly exit through the Lombok Strait or flow eastward into the Banda Sea. Another way is the ocean water from the western Pacific Ocean passes over the Lifamatola Passage into the Banda Sea, where these water masses are mixed due to tidal effects, Ekman pumping, and heat and fresh water flux at the ocean surface. From the Banda Sea the ITF exits Timor and Ombai passage.

The ITF pathway and topography of the channels are shown in the figure 2.1. The Lombok strait has rough bottom topography and a sill exist in the south channel with about 200 m deep. The input water from Pacific Ocean through Makassar Strait is 9 Sv and through Lifamatola is 1.5 Sv. The total outflow transport pass through Lombok Strait is 1.7 Sv, Ombai 4.5 Sv, and Timor 4.3 Sv. The heat transport of the ITF is about 0.5 - 1 PW (Godfrey,1996; Gordon, 2001; Vranes et al., 2002).

The seawater circulation and transport within the Indonesian Seas is most influenced by the monsoon. The southeast monsoon is predominant over the Indonesia during June-July-August (JJA) and enhances Ekman transport and the ITF transport. On the other hand, the ITF is reduced during December-January-February (DJF). The

Kelvin wave propagates from the eastern Indian Ocean to eastward along the Indonesian coastal. A coastally trapped Kelvin wave is made up during monsoon transition and serves to reduce the ITF transport. The northwest monsoon drives the downwelling along the southern of Java Sea to the Banda Sea and increases the sea level and reduces the ITF transport.

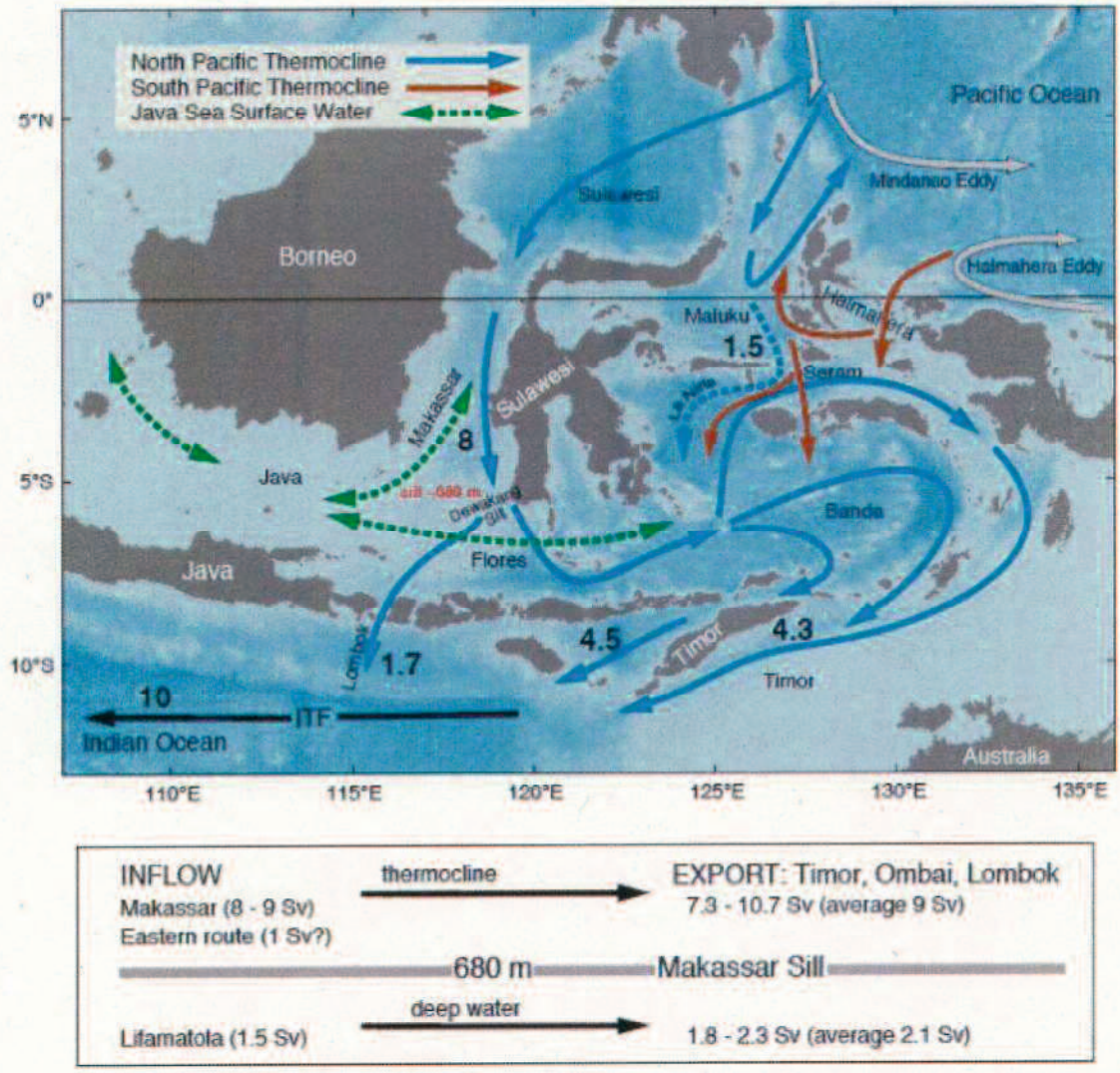

Figure 2.1 Indonesia Throughflow Pathway and transport (Gordon, 2005)

The Indonesian sea is a most attractive region for many researchers who investigate the role for the local, regional and global climatic system. In the connection with the ITF, the Indonesian sea receives the warm water from the western tropical Pacific Ocean. However the SST in the Indonesian sea is rather than lower the Pacific Ocean. It is driven by the tidal mixing (Ffield and Gordon, 1992). The tidal current in

the Indonesian sea has been investigated by a number of researchers (Wrytki, 1961; Hatayama et al, 1996; Robertson and Ffield, 2005), they suggested the strong tidal current in the Indonesian sea and play an important role for the transport and mixing.

2. The Seawater Dynamics

The Indonesia region is also known as "maritime continent". Ocean around Indonesia is very important for human life and influences on climate and weather conditions in Indonesia. The solar energy warms the seawater and the then warms the air above the ocean and generates the wind across the ocean. Moreover, the wind returns some energy to the ocean as waves and sea currents. The wave and sea current then contribute to the bay and the coastal dynamic.

Sea-level changes are long-term fluctuations of water level in a coastal zone. There are two reasons for sea-level changes as shown below (Kunte, 2003)..

1. Tectonic - uplift or sinking of a landmass. The actual amount of water in the ocean does not change, however an uplift or sinking of a portion of coast (or ocean bottom) shifts the shoreline up or down.
2. Eustatic-increase or decrease of the amount of water in the ocean. Major reason for such an increase or decrease is glaciations, like the Pleistocene Ice Age.

Sea-level changes create emergence and submergence of coastlines that start erosion, which causes sediment transportation (Kunte, 2003).

The tides move a large amount of water which has a frequency of four times a day, but the topography of the coastal areas has a little impact on the tides because the speed of the current is relatively low. In the narrow bay, tides have a greater power. It is called the tidal currents. The tidal currents could cause the erosion in coastal areas. In the sheltered bays and estuaries, the tides lose their speed and deposit the fine material (clay, silt) that bring by the water. Thus, bay slowly turns into a muddy flat, then to marshes.

The type of tide is determined by its frequency. This is because each location has different responses to generating tidal force. If the region has only one tide per day, then is said to be a diurnal tide. On the other hand, if the region has two tides per day, then is said to be a semi diurnal tide. Other tidal type is transitional between diurnal and semidiurnal type, which called mixed tides.

Tidal currents and waves sometimes play an important role in the dynamic system near the coast. When the sea surface water in the area is higher than in other areas, water flows from a higher elevation to a lower level, and then creating a tidal current. Significant currents generated by tides occur at the inlet of the lagoon and the entrance to the bay or harbor. Tidal current flow in such a water region when the tide is rising (flood tide) and flow out when the tide falls (ebb tide) (Kunte, 2003).

2.1 Wave

The description of a wave is still not clear and accurate, because the sea level is a complex field corresponding to the unstable and usually changing the pattern (Garrison, 1993). Wave is a natural raising and lowering the water periodically and can be found in all places around the world. Gross (1993) defines the wave as a surface water disturbance. While Sverdrup et al, (1946) defines a wave as something happens periodically, especially waves caused by the tidal.

Sea surface water is always in motion. This motion is mainly caused by the force of the wind that blows across the sea surface and generate waves and currents. The resulting wave forms tend uncertain and depend on several properties of the wave, where the wave height and period established. Formed wave will move out ward away from the center of origin and the wave propagates in all directions, as well as releasing energy. Propagation of these waves can travel thousands of miles before reaching a beach, where this type of wave is called "Swell".

Dissipation of wave energy (wave attenuation) results of the white-capping, the friction between molecules of water, air resistance, and wave-wave interaction of non-linear. Waves in shallow water dissipate energy by friction interaction with the sea floor and the breaking. Waves in shallow water can be refracted. In general, steeper the wave and the shallower the beach, the further offshore dissipation begins. As wave enters the shallow zone, the seabed friction will slows the wave propagation, especially near to the bottom. A wave become higher and steeper, tilt forward, and break in a swash as water runs up the beach slope. Thus the circular oscillation energy is translated into forward motion energy. Such a wave is called the wave of translation. Backwash is a reversed flow fed by retreating swash (Kunte, 2003).

In the open ocean, the waves travel as a straight line. However, when the wave enters shallow water, an irregularity in depth bend the wave front as it is slowed down in shallower areas and continues to travel fast in deeper areas. Bending of a wave due to differential speed of travel is called wave refraction (Kunte, 2003).

Although almost all of the waves due to wind, occasionally waves are created by undersea tectonic or volcanic event, like an earthquake or large lava flows at mid-ocean rift zone. Such waves are called seismic sea waves or tsunamis. They are characterized by very long wavelengths and wave heights (up to 30 m) as they reached the shoreline. Long period waves can travel across the ocean at speeds exceeding 800 kilometers per hour. Tsunamis can cause extensive damage at times (Kunte, 2003).

2.2 Current

The currents in the ocean are caused by two main factors, i.e. internal factors and external factors. Internal factors such as differences in seawater density, horizontal pressure gradient and friction. While external factors such the attractive force of sun and moon, the difference in air pressure, gravity force, tectonic force and wind. According to Bishop (1984), the main forces that play a role in the circulation of the water masses is the pressure gradient, Coriolis force, gravity, friction, and centrifugal force.

The primary driving force behind ocean currents is constant winds (for example, trade winds drive the equatorial current). Wind creates currents as it blows over the water surface, resulting a stress on the surface water particles and initiate the movement of water particles in the direction in which the wind blows. Thus, the surface currents created. When the current reaches the surface of the carrier, such as beaches, water tends to accumulate on the land (Kunte, 2003).

Of all flows, those flows near the coast have a great influence on the coastal landscape. The most important types currently in coastal areas is alongshore currents. Longshore current ("along the shore") is the current flowing in shallow water, parallel to the coastline, generally downwind. Longshore currents transport sediment along the coast, sometimes they are strong enough to erode the sea floor (Kunte, 2003).

2.3 Semi Diurnal and Diurnal Tide

Tides are oscillations of ocean waters due to the gravitational forces exerted by the moon and the sun upon the oceans. The rising tide is usually referred to as flood, whereas falling tide is called as ebb tide. Tidal currents are the horizontal water movements corresponding to the rise and fall (flood & ebb) of the tide. Pugh and Howarth (1983) defined tide as periodic vertical or horizontal movements which have coherent amplitude and phase relation-ship to some periodic geophysical force. In this case, his consider the movement of water, but movements of the atmosphere and of solid earth may also be tidal.

The high tide (the spring tide) occurs when the Earth, moon and sun are in a straight line. At the moment it will produce a highest tides and lowest tides. The spring tide occurs during the new moon and full moon. The low tide (the neap tide) occurs when the Earth, moon and sun form a perpendicular angle. At the moment, it will produce a lowest high tide and lowest low tide. The neap tide occurs at 1/4 and 3/4 month.

Equilibrium tides are understood as the tides which would occur in a non-inertial ocean covering the whole earth-globe. Many features related to the oceanic tides may be explained by the equilibrium theory, but a comparison with the observations indicates that there are also a number of considerable deviations. Although spring tides appear around the time of full moon and new moon, and neap tides at the quadrature and the heights of spring tides are considerably higher than those of neap tide, the observed tides show amplitudes which are generally much greater than those derived from the equilibrium theory (Sverdrup, 1978).

For the practical examinations of tidal phenomena, the harmonic theory of tides has been developed. The starting hypothesis of this theory of tides is similar to that for the dynamic theory; that the tidal fluctuations must be characterized by the same periods as the tide-generating forces. Through the harmonic theory, the basis was presented not only for the understanding of numerous tidal phenomena, but also for their prediction in time and space.

Tides consisted of various component which can be grouped by according to its cycle, as diurnal component (one high waters and one low waters per day), semi diurnal component (two high waters and two low waters per day), or quarternal component. All

of them will determine the type of tide in a coastal region. Some tidal constituents and their characteristic are shown in Table 2.1

Table 2.1 Component of the tide-producing forces

Name	Symbol	Period (hours)
Semidiurnal		
Principle lunar	M_2	12.42
Principle solar	S_2	12.00
Larger lunar elliptic	N_2	11.66
Luni-solar	K_2	11.97
Diurnal		
Luni-solar	K_1	23.93
Principle lunar	O_1	25.82
Principle solar	P_1	24.07

Sources: Schureman (1924; in Sverdrup, 1978)

2.4 Residual Current

The dominant motion in most coastal seas around the world is oscillatory flow driven by tides of the adjacent ocean basin. However, while a knowledge and understanding of the tidal dynamics of a sea is important, it is not sufficient to determine the transport of properties associated with the water, such as heat, dissolved salt, pollutants, suspended material, etc. While the tidal mean distribution of these is strongly influenced by the tidal oscillatory flow acting to disperse their concentration by a "tidal diffusion" process, their tidal mean transport is controlled by the residual current.

In coastal oceanography, where tides are predominant, the term residual is used to refer to the non-tidal part of the motion. In the context of time series of sea-level elevation or velocity, the residual is defined as the difference between the observed and tidally predicted parameter. This yields a time-varying residual, which should contain no energy at the discrete tidal frequencies. However, for theoretical consideration, it is more convenient to define the residual as the time mean.

The tide induced residual current is defined as the flow, which is caused non-linearity of tidal current in relation to horizontal boundary geometry and bottom topography. Residual current can be produced by wind drag on the sea surface, or driven by lateral density gradients due to non-uniform salinity or temperature distributions. However, they can also be generated by the tidal flow itself. It is the non-linear interaction of the oscillating tidal streams, leading to residual flows.

3. Numerical Model

A numerical model is a tool capable of integrating, by means of mathematical equation, the many diverse physical, chemical and biological processes involved in a coastal system. Due to its nature it can play a vital role in assessing the engineering feasibility of a proposed project as well as in assessing environment impacts of such development (Hadi, 2003).

They are two types of model that are often used in coastal studies namely physic and mathematical models. Physical model is a simplification of real world in a scale version. It is said to be physical because model elements are made of materials and hardware. In their application physical models have proved suitable for the investigation of coastal systems. Although physical models are a useful tool in studying coastal system, they have not been able to accurately describe the hydrodynamics and sedimentary processes in the coastal system. Lakhan and Trenhaile (1989; in Hadi, 2003) indicated that physical models can not duplicate any aspect of coastal system which are governed by numerous uncontrolled entities and attributes which are unpredictable in magnitude and duration.

Another set of models that can be used to study the coastal system are mathematical models. The mathematical models are the most widely used in system studies because of their generality, versatility and flexibility. According to Jacoby and Kowalik (1980; in Hadi, 2003) mathematical models can be classified according to different criteria, depending on the types of models data, parameters, mathematical relationship, solution technique, time related behavior and structure. The most widely used mathematical models in studying coastal system are numerical models.

For practical purposes, several types of model representations are used. Kremer and Nixon (1978, in Ae 2004) have summarized different types of models used in the

coastal studies. Of the wide range of models employed in the study of natural system, numerical models are more successful because of their generality, versatility and flexibility. Numerical models can solve both the linier and non-linier problems. To solve the equations of the model, numerical methods involving computational procedures have to be used. Model simulation can be considered as a mathematical, logic representation of a system, and then conducting experiments with the computerized system model on digital computer. Modeling is, therefore, the integrated development of mathematical equations, logical rules and constraints and a computer program embodying the equations, the logical rules and the solutions to them. On the other hand simulation is the experimental manipulation of the model on a digital computer. A simulation model has several advantages like as follow Kremer and Nixon (1978, in Ae 2004)

1. It permits controlled experimentation. A simulation model can be run a number of times with varying input parameters to test the behavior of the system under a variety of situations and conditions
2. It permits time compression. Operation of the system over extended periods of time can be simulated in only minutes with ultra fast computers
3. It permits sensitivity analysis by manipulation of input variables
4. It does not disturb the real natural system
5. It permits manipulation in term of real-time of minutes that would take years for the prototype.

4. Finite Volume Coastal Ocean Model (FVCOM)

The Finite-difference and finite element method have been widely used in ocean circulation model (Blumberg and Mellor, 1987; Blumberg, 1994; Haidvogel et al., 2000; Lynch and Naimie, 1993; Naimie, 1996). The finite-difference method has the advantage of computational and coding efficiency. The simple coastal region can be resolving by introducing an orthogonal or nonorthogonal curvilinear horizontal coordinate transformation into a finite-difference model. However the finite difference method is incapable of resolving the highly irregular inner shelf/estuarine geometries found in many coastal areas (Blumberg 1994; Chen et al. 2001; Chen et al. 2004a). In order to overcome these problems, the finite-element method has a greatest advantage

and can provide an accurate fitting of the complex coastal geometry. The P-type Finite-Element Method (Maday and Patera, 1988) or Discontinuous Galerkin Method (Reed and Hill, 1973; Cockburn *et al.*, 1998) has recently been applied to ocean and have shown promise in improving both computational accuracy and efficiency.

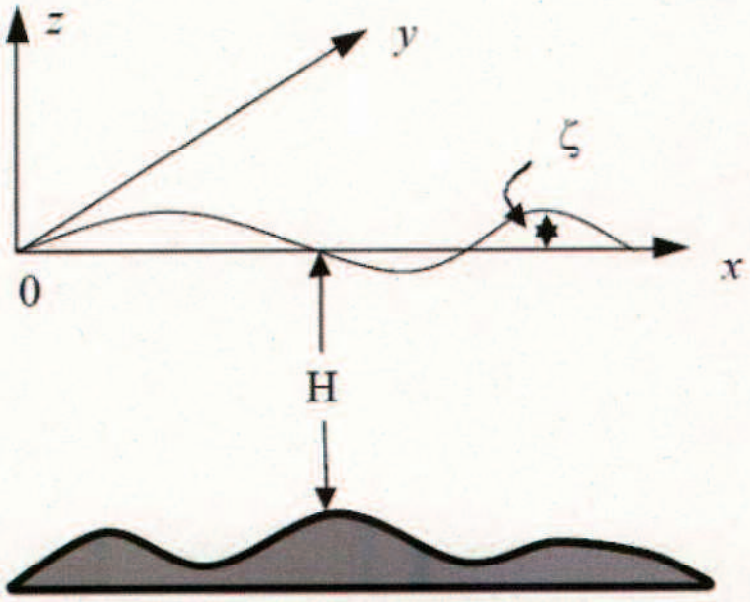

Figure 2.2 Illustration of the orthogonal coordinate system (Chen et al (2006)

Finite Volume Coastal Ocean Model (FVCOM) is a 3-D unstructured-grid, free-surface, primitive equation (Chen et al. 2003a; Chen et al. 2004b). Unlike the differential form used in finite-difference and finite-element models, FVCOM discretizes the integral form of the governing equations. Since these integral equations can be solved numerically by flux calculation (like those used in the finite difference method) over an arbitrarily-sized triangular mesh (like those used in the finite element method), the finite-volume approach is better suited to guarantee mass conservation in both the individual control element and the entire computational domain. From a technical point of view, FVCOM combines the best attributes of finite-difference methods for simple discrete coding and computational efficiency and finite-element methods for geometric flexibility. This model has been successfully applied to study several estuarine and shelf regions that feature complex irregular coastline and topographic geometry, including inter-tidal flooding and drying Chen et al (2006).

The governing equations consist of the following momentum, continuity, temperature, salinity, and density equations Chen et al (2006):

$$\frac{\partial u}{\partial t}+u\frac{\partial u}{\partial x}+v\frac{\partial u}{\partial y}+w\frac{\partial u}{\partial z}-fv=-\frac{1}{\rho_o}\frac{\partial p}{\partial x}+k_m\frac{\partial^2 u}{\partial z^2}+F_u \tag{2.1}$$

$$\frac{\partial v}{\partial t}+u\frac{\partial v}{\partial x}+v\frac{\partial v}{\partial y}+w\frac{\partial v}{\partial z}+fu=-\frac{1}{\rho_o}\frac{\partial p}{\partial y}+k_m\frac{\partial^2 v}{\partial z^2}+F_v \tag{2.2}$$

$$\frac{\partial p}{\partial z}=-\rho g \tag{2.3}$$

$$\frac{\partial u}{\partial x}+\frac{\partial v}{\partial y}+\frac{\partial w}{\partial z}=0 \tag{2.4}$$

$$\frac{\partial T}{\partial t}+u\frac{\partial T}{\partial x}+v\frac{\partial T}{\partial y}+w\frac{\partial T}{\partial z}=k_h\frac{\partial^2 T}{\partial z^2}+F_T \tag{2.5}$$

$$\frac{\partial S}{\partial t}+u\frac{\partial S}{\partial x}+v\frac{\partial S}{\partial y}+w\frac{\partial S}{\partial z}=k_h\frac{\partial^2 S}{\partial z^2}+F_S \tag{2.6}$$

$$\rho=\rho(T,S) \tag{2.7}$$

where x, y, and z are the east, north, and vertical axes in the Cartesian coordinate system; u, v, and w are the x, y, z velocity components; T is the temperature; S is the salinity; r is the density; P is the pressure; f is the Coriolis parameter; g is the gravitational acceleration; m K is the vertical eddy viscosity coefficient; and $Kh$is the thermal vertical eddy diffusion coefficient. Fu ,Fv, T F , and S F represent the horizontal momentum, thermal, and salt diffusion terms. The total water column depth is $D=H+\zeta$, where H is the bottom depth (relative to z = 0) and ζ is the height of the free surface (relative to z = 0).

The surface and bottom boundary conditions for temperature are:

$$\frac{\partial T}{\partial z}=\frac{1}{\rho c_p K_h}[Q_n(x,y,t)-SW(x,y,\zeta,t)],\quad at\ z=\zeta(x,y,t) \tag{2.8}$$

$$\frac{\partial T}{\partial z}=\frac{A_H\tan\alpha}{K_h}\frac{\partial T}{\partial n},\quad at\ z=-H(x,y) \tag{2.9}$$

where Q_n (x, y, t) is the surface net heat flux, which consists of four components: downward shortwave, longwave radiation, sensible, and latent fluxes, SW(x, y,0,t) is the shortwave flux incident at the sea surface, and c_p is the specific heat of seawater. A_H

is the horizontal thermal diffusion coefficient, α is the slope of the bottom bathymetry, and n is the horizontal coordinate shown in Figure 2.2 (Pedlosky, 1974; Chen *et al.*, 2004b).

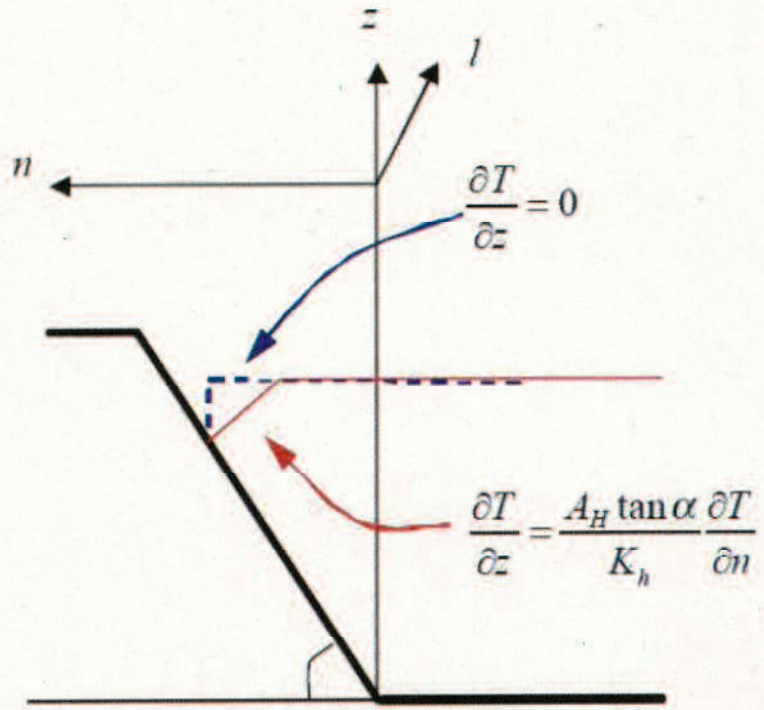

Figure 2.3 Schematic of the no-flux boundary condition on the bottom slope (Chen et al 2006)

The longwave, sensible and latent heat fluxes are assumed here to occur at the ocean surface, while the downward shortwave flux $SW(x, y, z, t)$ is approximated by:

$$SW(x,y,z,t) = SW(x,y,0,t)[\mathrm{Re}^{\frac{z}{a}} + (1-R)e^{\frac{z}{b}} \qquad (2.10)$$

where a and b are attenuation lengths for longer and shorter (blue-green) wave length components of the shortwave irradiance, and R is the percent of the total flux associated with the longer wavelength irradiance. This absorption profile, first suggested by Kraus(1972), has been used in numerical studies of upper ocean diurnal heating by Simpson and Dickey (1981a, b) and others. The absorption of downward irradiance is included in the temperature (heat) equation in the form of

$$H(x,y,z,t) = \frac{\partial SW(x,y,z,t)}{\partial z} = \frac{SW(x,y,0,t)}{\rho c_p}[\frac{R}{a}e^{\frac{z}{a}} + \frac{1-R}{b}e^{\frac{z}{b}}] \qquad (2.11)$$

This approach leads to a more accurate prediction of near-surface temperature than the flux formulation based on a single wavelength approximation (Chen *et al.*, 2003b).

The surface and bottom boundary conditions for salinity are:

$$\frac{\partial S}{\partial z} = \frac{S(\hat{P} - \hat{E})}{K_h \rho} \cos\gamma, \; at \; z = \zeta(x, y, t) \tag{2.12}$$

$$\frac{\partial S}{\partial z} = \frac{A_H \tan\alpha}{K_h} \frac{\partial S}{\partial n}, \; at \; z = -H(x, y) \tag{2.13}$$

where $\hat{P}$ and $\hat{E}$ are precipitation and evaporation rates, respectively. $\gamma = 1/\sqrt{1 + |\nabla\zeta|^2}$. Note that a groundwater flux can be easily added into the model by modifying the bottom boundary conditions for vertical velocity and salinity.

The surface and bottom boundary conditions for u, v, and $w$are:

$$K_m(\frac{\partial u}{\partial z}, \frac{\partial v}{\partial z}) = \frac{1}{\rho_o}(\tau_{sx}, \tau_{sy}), \; w = \frac{\partial \zeta}{\partial t} + u\frac{\partial \zeta}{\partial x} + v\frac{\partial \zeta}{\partial y} + \frac{E - P}{\rho}, \; at \; z = \zeta(x, y, t) \tag{2.14}$$

$$K_m(\frac{\partial u}{\partial z}, \frac{\partial v}{\partial z}) = \frac{1}{\rho_o}(\tau_{bx}, \tau_{by}), \; w = -u\frac{\partial H}{\partial x} - v\frac{\partial H}{\partial y} + \frac{Q_b}{\Omega}, \; at \; z = -H(x, y) \tag{2.15}$$

where (t_{sx} ,t_{sy}) and (t_{bx} , t_{by}) $= C_d\sqrt{u^2 + v^2}(u, v)$ are the x and y components of surface wind and bottom stresses, Q_b is the groundwater volume flux at the bottom and Ω is the area of the groundwater source. The drag coefficient C_d is determined by matching a logarithmic bottom layer to the model at a height z_{ab} above the bottom, *i.e.*,

$$C_d = \max\left(k^2 / \ln(\frac{z_{ab}}{z_o})^2, 0.0025\right) \tag{2.16}$$

where k= 0.4 is the von Karman constant and z_o is the bottom roughness parameter.

The kinematic and heat and salt flux conditions on the solid boundary are specified as:

$$v_n = 0; \frac{\partial T}{\partial n} = 0; \frac{\partial S}{\partial n} = 0 \tag{2.17}$$

Where v_n is the velocity component normal to the boundary, and n is the coordinate normal to the boundary.

It should be pointed out here that in most popular finite-difference models, the bottom boundary conditions (2.9) and (2.13) for temperature and salinity are simplified as $\frac{\partial T}{\partial z} = \frac{\partial S}{\partial z} = 0$. One reason for this is the difficulty in the finite-difference method of

calculating accurately α and $\frac{\partial T}{\partial z}$ and $\frac{\partial S}{\partial z}$over an irregular bottom slope. The error caused by inaccurate calculation of these two terms in a finite-difference approachmight be larger than their real values. This simplification is generally sound for much ofthe continental shelf in the coastal ocean where the bottom topography is smooth with small slope, but over the shelf break and continental slope where the bottom slope can be quite large, this simplification can destroy the nature of the dynamics of the bottom boundary layer and result in overestimation of vertical mixing and horizontal and vertical velocities. An example for the importance of the exact expression of the no normal flux condition at the bottom given in (2.9) and (2.13) can be seen in Chen *et al.* (2006a). In the finite-volume approach, the bottom slope and gradients of temperature and salinity for an irregular bottom shape can be directly calculated using a simple Green's theorem. Therefore, FVCOM can provide an accurate tracer flux at the bottom using (2.9) and(2.13). This is one of the advantages for using FVCOM in both coastal and deep ocean applications. The clear and fully guidance of using FVCOM can be found in Chen et al (2006).

5. Bathymetry Data

The bathymetry data in the Indonesian seas are majorly provided by the Division of Hydro Oceanography (DISHIDROS) of Indonesian Navy. The seafloor data providing by the DISHIDROS has a good accuracy for the Benoa bay, they was provided the bathymetry map with scale 1:10000. Though it was enough for the model design in Benoa bay, yet in this study is also considering the bathymetry map that was provided by the PT Pelabuhan Indonesia (PELINDO) III, Department of Public transportation Indonesia. They were provided the seafloor data with the scale of 1:2500. In order to obtaining the better accuracy of model calculation, in this study we use the both of bathymetry data DISHIDROS data and PELINDO data. These data then were filling the model area in the Benoa bay. The missing areas that were didn't coverage by those of data are filled by the interpolation method.

Meanwhile the bathymetry data that used for the Lombok strait are provided by the DISHIDROS. The bathymetry map provided by them has a good resolution with the map scale is 1:200000. This bathymetry map was coverage for the Lombok strait and Badung strait. In relation to the numerical calculation of the Lombok sill, those of

bathymetry map was accurate enough since the wide area of the Lombok strait and its sill. This bathymetry data are also interpolated by its mesh for the model calculation.

References

Ae,L.S. 2004. Simulation of Eco-dynamic Model in Tokyo Bay And its Comparison With Satellite Data, (Doctor Dissertation) Doctor Program in Center of Environmental Remote Sensing. Chiba University. Japan

Bishop, J.M. 1984. Aplied Oceanography. John Willey and Sons, Inc. New York

Blumberg, A. F., A primer for Ecom-si. *Technical Report of HydroQual, Inc.*, 66 pp, 1994

Blumberg, A.F., Mellor, G.L., 1987. A description of a three-dimensional coastal ocean circulation model.In Three-dimensional Coastal Ocean Model, N.S. Heaps, Ed., Coastal.Estuar. Sci., **4**, 1-6.

Chen, C. H. Liu, R. C. Beardsley, 2003a. An unstructured, finite-volume, three-dimensional, primitive equation ocean model: application to coastal ocean and estuaries. *J. Atm.&Oceanic Tech.*, 20, 159-186

Chen, C, G. Cowles and R. C. Beardsley, 2004b. An unstructured grid, finite-volume coastal ocean model: FVCOM User Manual. SMAST/UMASSD Technical Report-04-0601, pp183.

Chen, C., J. Zhu, E. Ralph, S. A. Green, and J. Budd, 2001. Prognostic modeling studies of the Keweenaw current in Lake Superior. Part I: formation and evolution. *J. Phys. Oceanogr.*, 31, 379-395.

Chen, C. J. Zhu, L. Zheng, E. Ralph and J. W. Budd, 2004a. A non-orthogonal primitive equation coastal ocean circulation model: application to Lake Superior. *J. Great LakesRes.*,30, 41-54.

Chen, C, R. C. Beardsley, and P. J. S. Franks, 2003b. J. V. Keuren, Influences of the diurnally varying heat flux on stratification and residual circulation on Georges Bank. *J. Geophys.Res.*, 108(C11), 8008, DOI 10.1029/2001JC001245

Chen, C., H. Huang, R. C. Beardsley, H. Liu, Q. Xu, and G. Cowles, 2006a. A finite-volume numerical approach for coastal ocean circulation studies:

comparisons with finitedifference models. *Journal of Geophysical Research*

Cockburn, B, S. Hou, and C. W. Shu, 1990. TVB Runge-Kutta local projection discontinuous Galerkin finite element method for conservation laws IV: the multidimensional case, *Math Comp.*,**54**, 545-581.

Ffield, A. and Gordon, A. L., 1992, Vertical mixing in the Indonesian thermocline, Journal of Physical Oceanography, Vol.22, pp.184-195.

Garrison, T.,1993, Oceanography: An Invitation to Marine Science,Wadsworth Publishing Company, Belmont

Gross, M. 1990.Oceanography sixth edition. New Jersey : Prentice-Hall.Inc.

Gordon, A. L., 2005, Oceanography of the Indonesian seas and their throughflow, Oceanography, Vol.18, pp. 14-27

Godfrey, J.S., 1996. The effect of the Indonesian throughflow on ocean circulation and heat exchange with the atmosphere: A review. Journal of Geophysical Research. Vol. 101, pp 12217–12238

Gordon, A.L. 2001.Interocean Exchange.Chapter 4.7.Pp. 303–314 in *Ocean Circulation and Climate*, G. Siedler, J. Church, and J. Gould, eds. Academic Press.

Hadi,S. 2003. Role of Numerical Modeling in Coastal Management, Proceedings Symposium on Coastal Zone Management.LPPM-Institute Teknologi Bandung. 28 July

Haidvogel, D. B, H. G. Arango, K. Hedstrom, A. Beckmann, P. M. Rizzoli, A. F. Schepetkin, 2000. Model evaluation experiments in the North Atlantic Basin, Simulation in nonlinear terrain-following coordinates. *Dyn.Atmo.Oceans.*, 32, 239-281.

Hatayama, T., Awaji, T. and Akitomo, K. 1996, Tidal current in the Indonesian seas and their effect on transport and mixing, Journal of Geophysical Research, Vol.101, pp.12353-12373

Howarth,M.J.andPugh,D.T. 1983. Observations of Tides Over The Continental Shelf of North-West Europe: Johns.B.,editor. Physical Oceanography and Coastal and Shelf Seas.Elseiver Publishing Company Inc. Amsterdam.p.135-187.

Kraus, E. B., 1972: Atmosphere-Ocean Interaction. *Clarendon Press*, 275pp

Kunte, P.D. 2003. Study of Sediment Transportation in The Bay of Kachchh, Using 3D Hydro-dynamic Model Simulation and Satellite Data (Doctor Dissertation). Doctoral Program at Center of Environmental Remote Sensing Chiba University, Japan

Lynch, D. R., and C. E. Naimie, 1993. The M2 tide and its residual on the outer banks of the Gulf of Maine, *J. Phys. Oceanogr.*, 23, 2222-2253

Maday,Y. and A. T. Patera, 1988. Spectral element methods for the incompressible Navier- Stokes equations. In: State-of-the art surveys in computational mechanics, A. K. Noor, editor, ASME, New York.

Naimie, C. E., 1996. Georges Bank residual circulation during weak and strong stratification periods: prognostic numerical model results. *J. Geophys. Res.* 101(C3), 6469-6486

Pedlosky, J., Longshore currents, upwelling and bottom topography.*J. Phys. Oceanogr.*, 4, 214- 226, 1974.

Qu, T. et al., 2005, Sea Surface Temperature and its Variability in the Indonesian Region, Oceanography Vol. 18, No. 4, pp 50-61

Reed, W. H., and T. R. Hill, 1973. Triangular and methods for the neutron transport equation, Tech. Report LA-UR-73-479, Los Alamos Scientific Laboratory.

Robertson. R and Amy Ffield. 2005, M2 BaroclinicTide in The Indonesian Seas, Oceanography, Vol. 18, No. 4, pp. 62-73

Simpson, J. J. and T. D. Dickey, 1981a: The relationship between downward irradiance and upper ocean structure. *J. Phys. Oceanogr.*, 11, 309-323.

Simpson, J. J. and T. D. Dickey, 1981b: Alternative parameterizations of downward irradiance and their dynamical significance. *J. Phys. Oceanogr.*, 11, 876-882.

Sverdrup,H.U., Martin,W.J., Richard,H.F. 1978. The Oceans (Their Physics, Chemistry, and general biology).Modern Asia Edition. Prentice-Hall Inc- Charles E.TuttleCompany . Japan

Vranes, K., A. L. Gordon, and A. Ffield (2002), The heat transport of the Indonesian Throughflow and implications for the Indian Ocean heat budget, Deep Sea Res., Part II, Vol. 49 (7–8),pp 1391–1410

Wyrtki, K. 1961. Physical oceanography of the Southeast Asian waters, Naga Report 2.Scripps Institution of Oceanography.

CHAPTER 3
THE TIDAL UPWELLING OF THE LOMBOK STRAIT

1. Introduction

Several studies concerning the dynamics of seawater flow in Indonesian Seas have been investigated (Ffield and Gordon, 1992; Hatayama et al, 1996; Ffield and Gordon, 1996; Robertson and Ffield, 2005). Seawater flow has a complicated system in the Indonesian basin due to the complex coastline geometry and the rough of sea bottom topography (Gordon and McClean, 1999; Gordon, 2005). The tidal current enhances the vertical mixing and transport in Indonesian Seas (Hatayama et al 1996; Ffield and Gordon, 1996), which have an important role in connecting the Pacific Ocean and the Indian Ocean. Mainly, the seawater flows from the warm Pacific Ocean to the Makasar Strait.

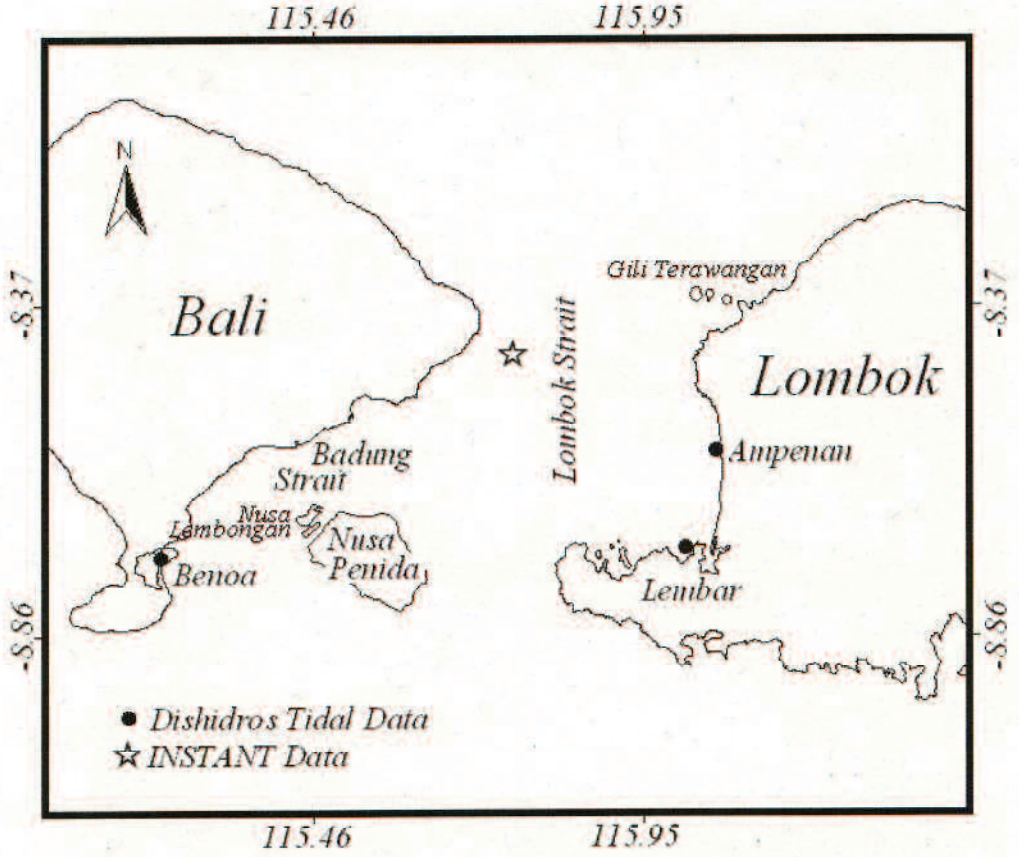

Figure 3.1 Chart of the Lombok Strait and the Location of Observation Data for Current and Tidal Elevation by INSTANT Project and DISHIDROS Respectively.

Lombok Strait is separated by Bali and Lombok as shown in Figure 3.1, and is an important pathway for the Indonesia Throughflow (ITF) (Gordon and McClean, 1999; Susanto *et al*,2005). In the south part of the Lombok Strait there are small islands namely, Nusa Penida, Ceningan and Lembongan. These islands and Bali form another water pathway in the Lombok Strait called the Badung Strait. In the northeastern channel too there are small islands called Gili Terawangan.

The Lombok Strait has step bottom topography from the North to the South channel (Figure 3.2). From the inner to the north part of the Lombok Strait there is a deep-water channel with depth ranging from 400 m up to 1400 m. Meanwhile, there is a sill formed in the southern channel between Nusa Penida and Lombok (after here we call it the Lombok Sill). On the top of the Lombok Sill, the water deep is 190 m. At the south part of the Lombok Sill toward the southern channel the bottom increases reaches 800 m. Moreover, in the Badung Strait pathway, the water depth is almost shallower than 200 m.

Tidal current has an important role for the water exchange processes through a strait (Awaji *et al*, 1980; Nakamura *et al*, 2000). Awaji *et al* (1980) experiments suggest that the amplitude and phase lag of the tide rapidly changes spatially and the vicinity of the strait cause the exchange of an extremely large amount of water through the strait. Nakamura *et al* (2000) also suggested the topographical impact on the water exchange through a deep strait makes the amount of the mean transport become significant.

In previous studies, the strong tidal current was investigated in the vicinities of the narrow passage in the Lombok Straits (Hatayama *et al*, 1996) by using 1/12 x 1/12 degree spatial resolution of the barotropic model for the entire area of Indonesian Seas. However, this resolution is quite coarse to clearly understand the tidal current system in the Lombok Strait. The high amplitude internal solitary wave was also examined using the satellite data. It was found that internal waves were generated by the interaction of successive semidiurnal tidal flows with the sill south of Lombok Strait (Susanto*et al*, 2005).

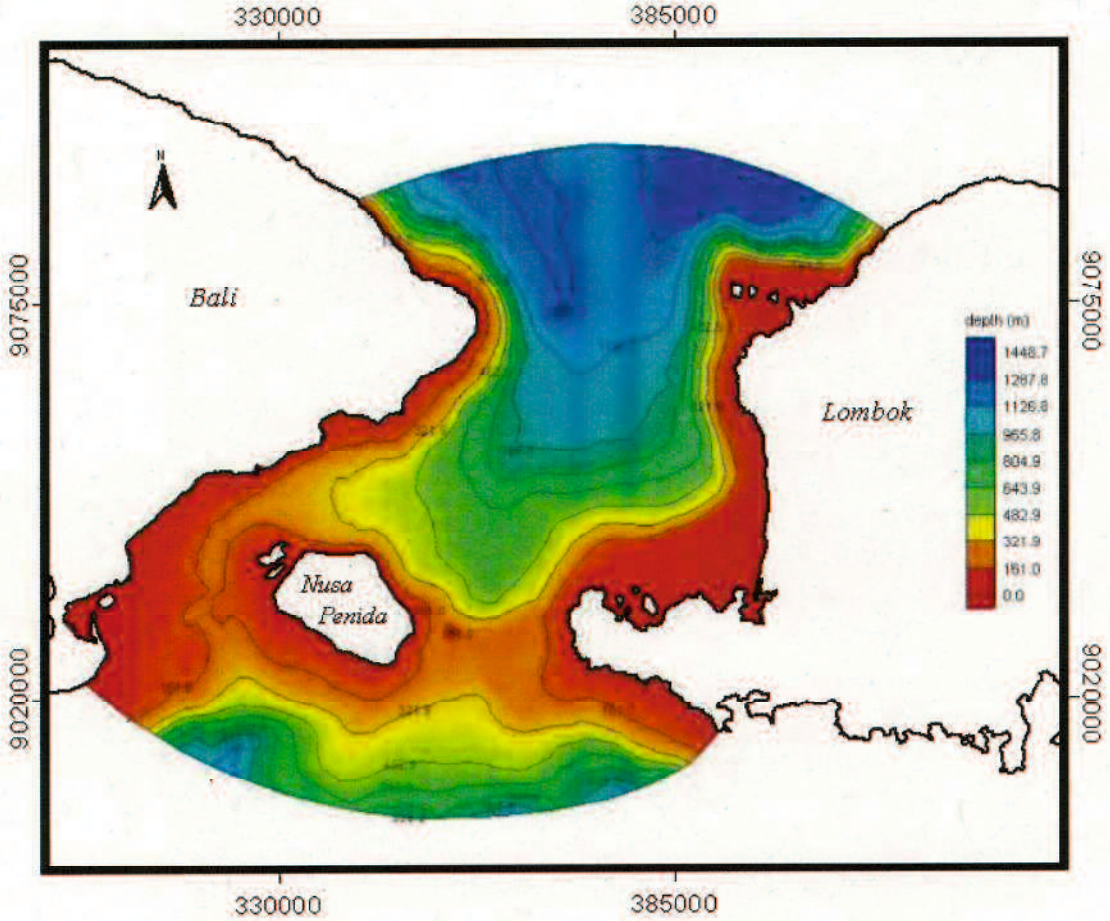

Figure 3.2 Seawater depth of Lombok Strait (sources: Dishidros map)

The mechanisms of upwelling have an important role for coastal productivity, whereby the seawater has a rich nutrient rose from the deeper waters (Wenju, 1988). It processes also can contribute to climate modification because the cold water will also raise to the upper layer. The upwelling processes can occur in the stepped and rough of sea bottom topography such as a vicinity of sill. The tidal mixing was investigated by Hatayama (2004) in the vicinity of sill at Makasar Strait and the tidal upwelling induced by tidal mixing front over sloping bottom topography well analyzed in the Yellow Sea (Lu, 2010).

Although there are several studies concerning the tidal mixing and the internal wave in Indonesian seas, discussion of the growth of short tide-induced upwelling passing through the Lombok Strait are very little. Firstly, the characteristics of tidal current pass through of the Lombok Strait and the Badung Strait by using a numerical calculation is presented. A numerical calculation is then presented to analyze features

revealed from the role of the stepped bottom topography and the vicinity of south sill induced tidal upwelling in the Lombok Strait.

2. The Ocean Mechanism in the Lombok Strait

The Lombok Strait is a sea channel in the southern part of the Indonesian Archipelago between Bali and Lombok. Lombok Strait is one of the important Indonesia Throughflow (ITF) passage. The seawater from the Pacific Ocean entering the Indonesia seas with cool and fresher water is passing through the Lombok Strait toward the Indian Ocean (Gordon, 2005). The seawater in the Indonesian seas is mostly influence by the monsoon. During the summer season the upwelling is revealing in the south of Java and Bali, and the downwelling is occurring during the winter season (Qu et al. 2005). These upwelling and the downwelling are also intruding into the Lombok and Badung Strait and also influence by the Kelvin wave (Potemra et al., 2002).

The strong tidal current occurred in the Indonesian sea is highly influenced by the rough of bottom topography and complex coastline geometry (Robertson and Ffield, 2005). The strong tidal current influences the ocean mixing in the basin and will alter the temperature in the surface layer become cool and high nutrient (Robertson and Ffield, 2005). The cooler surface layer has an implication to reduce the ocean evaporation and precipitation. The Lombok Strait and Badung Strait also has rough bottom topography (Figure 2.2). Furthermore, both straits also have a relatively narrow passage and complex coastal geometry. The shape of the Badung Strait and Lombok Strait could modulate the ocean mixing, where the ocean mixing is important for our local climate.

Murray and Arif (1988) found that the seawater transport in the Lombok Strait is minimum on February to through May about 1 Sv (1 Sv = 10^6 m^3/s), and maximum from July to September about 2 Sv. The mean annual transport passing through the Lombok Strait into the Indian Ocean is 1,7 Sv (Murray and Arif, 1988). The measured flow was dominantly southward, and about 80% of seawater is transported in the upper layer (less than 200 m) (Murray and Arif 1988).

The propagation of the tidal wave from the pacific and Indian ocean influences the Indonesian seas (Schiller, 2004). Thus, the Lombok strait is most influenced by the tidal wave from the Indian Ocean due to the location adjacent. Hatayama et al (1996)

found the strong tidal current generated by M2 component in the Lombok Strait. Furthermore, water properties flowing through the Lombok Strait could be modified by the strong tidal mixing.

3. Model Design

The hydrostatic three-dimensional (3D) Finite Volume Coastal Ocean Model (FVCOM) developed originally by Chen *et al* (2006) was used in this study. FVCOM is a second order approximation model and is based on the finite volume method and the three dimensional primitive equation. The three dimensional momentum and continuity equations are given in equation (3.1), (3.2) and (3.3).

$$\frac{\partial \zeta}{\partial t}+\frac{\partial Du}{\partial x}+\frac{\partial Dv}{\partial y}+\frac{\partial \omega}{\partial \sigma}=0 \tag{3.1}$$

$$\begin{aligned}&\frac{\partial uD}{\partial t}+\frac{\partial u^2 D}{\partial x}+\frac{\partial uvD}{\partial y}+\frac{\partial u\omega}{\partial \sigma}-fvD \\ &=-gD\frac{\partial \zeta}{\partial x}-\frac{gD}{\rho_o}[\frac{\partial}{\partial x}(D\int_{\sigma}^{0}\rho d\sigma')+\sigma\rho\frac{\partial D}{\partial x}]+\frac{1}{D}\frac{\partial}{\partial \sigma}(K_m\frac{\partial u}{\partial \sigma})+DF_x\end{aligned} \tag{3.2}$$

$$\begin{aligned}&\frac{\partial vD}{\partial t}+\frac{\partial uvD}{\partial x}+\frac{\partial v^2 D}{\partial y}+\frac{\partial v\omega}{\partial \sigma}+fuD \\ &=-gD\frac{\partial \zeta}{\partial y}-\frac{gD}{\rho_o}[\frac{\partial}{\partial y}(D\int_{\sigma}^{0}\rho d\sigma')+\sigma\rho\frac{\partial D}{\partial y}]+\frac{1}{D}\frac{\partial}{\partial \sigma}(K_m\frac{\partial v}{\partial \sigma})+DF_y\end{aligned} \tag{3.3}$$

Whereas x,y, and σ are the east, north, and vertical axes in the σ-coordinate system; u,v, and ω are the x,y,σ velocity components; D is the total depth equal to the sum of mean depth H and the surface elevation ζ; ρ_o reference density; f is the Coriolis parameter; g is the gravitational acceleration; K_m is the vertical eddy viscosity coefficient; F_x, F_y represent the horizontal momentum diffusion terms. The Mellor and Yamada level 2.5 turbulent closure schemes as modified by Galperin et al (1988) is used for vertical mixing in this model. The horizontal diffusion coefficient adopted from Smagorinsky eddy parameterization method (Smagorinsky, 1963) is applied.

The dimension of model domain is about 100 km x 80 km with two open boundaries in the northern and the southern channels. The triangle meshes were applied to give a better horizontal resolution along coastal line and over the sill (Figure 3.3). It varied from 1 km in the coastline expanding to 3 km near the open boundary. The

vertical grid is made of 30 sigma levels, uniformly distributed from the surface to the bottom. In order to reduce the artificial wave reflection at the two sides of open boundaries, the sponge layer was applied in this model.

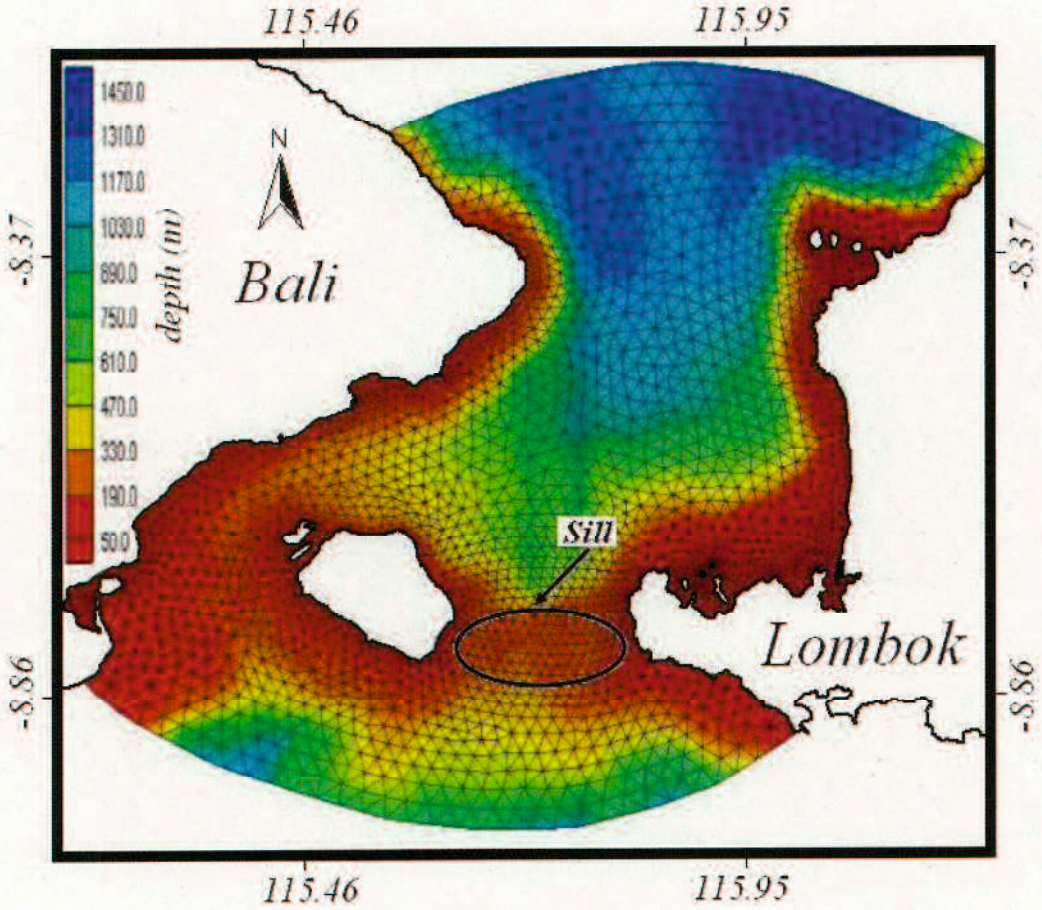

Figure 3.3 Model mesh

In the first step, the model is forced at both sides of open boundaries by the four major semidiurnal (M2, S2) and diurnal (O1, K1) tidal components. These tidal components were obtained from the ORI.96 ocean tidal model (Matsumoto *et al.* 1995). The first step calculations are intended to be able to determine the accuracy of our model.

The semidiurnal M2 component is a dominant of tidal component in the Lombok Strait, it was forced about 70%. Furthermore to investigate the internal mode of tide-induced upwelling in the Lombok Strait, we ran the 3-D model with the predominant M_2 tidal component.

In order to validate of our calculations, we used the observation data that were obtained from the International Nusantara Stratification and Transport (INSTANT)

program (for acoustic current meter) and Division of Hydro Oceanography (DISHIDROS) of Indonesian Navy (for tidal component data at 3 stations) (Figure 3.1). The initial vertical distribution of temperature and salinity were specified by a linear function of depth. The initial value of surface and bottom profile for salinity and temperature were derived from Murray *et al* (1990) observed data.

4. Tide and Tidal Current

4.1. Model Validation

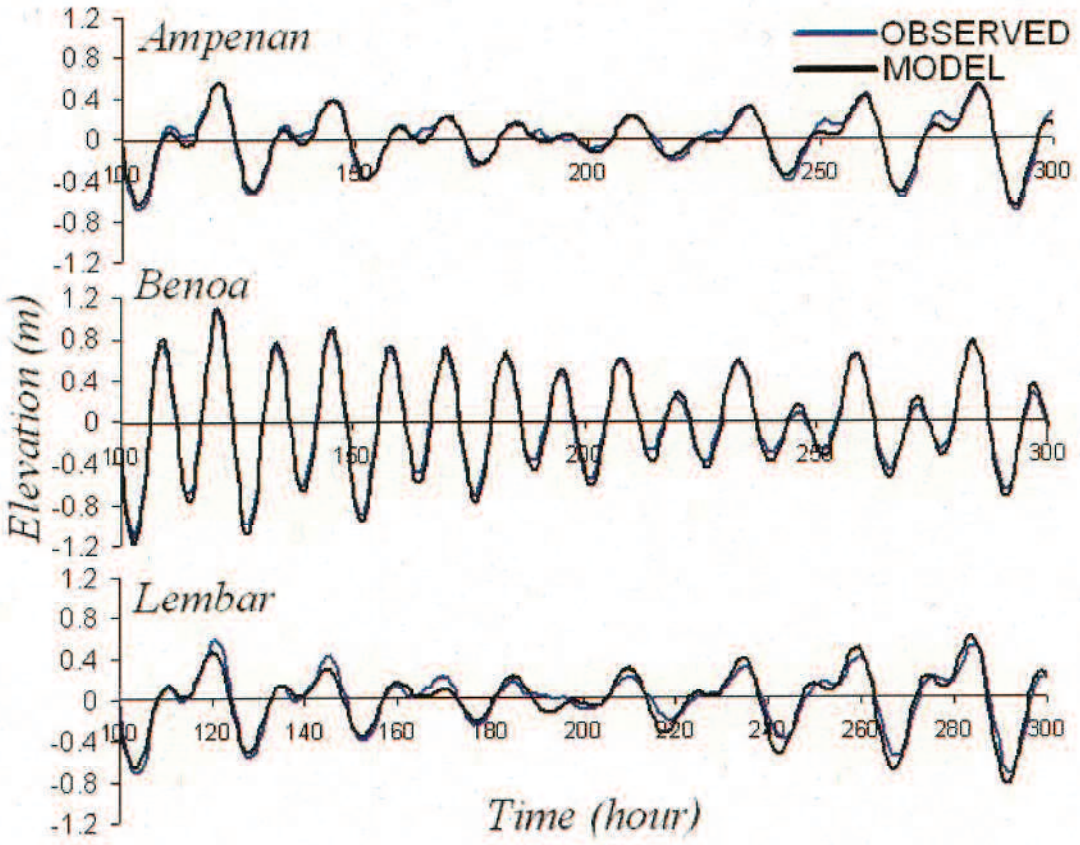

Figure 3.4 Comparison of model and observed tidal elevation at 3 stations.

In order to validate the model calculation, a comparison between the observed tidal elevation and tidal current and the model results are presented. Figure 3.4 shows the verification of tidal elevation, the observed tidal elevation of four major semidiurnal (M2, S2) and diurnal (K1, O1) components were directly compared with 200 hours model simulated tidal elevation. The calculated tidal elevation shown a good agreement with the observation data provided by DISHIDROS. The mean absolute error of tidal

elevation at Ampenan, Benoa and Lembar tidal gauge station is about 0.05 m, 0.06 m and 0.08 m respectively. The model versus DISHIDROS data of tidal amplitude and tidal phase of four primary tidal components (M2, S2, K1 and O1) are represented in Table 2.1 and Table 2.2 respectively. The comparison between DISHIDROS data and model calculated amplitudes and phases at three tidal stations show a good agreement. The standard deviation for M2, S2, K1 and O1 tidal simulations is 0.05 m and 0.02 m, 0.03 m and 0.01 m in amplitude and 3°, 14°, 8° and 10° in phase, respectively.

Figure 3.5 shows the comparison of model predicted tidal current with the observation data obtained from the INSTANT project. Around 48 hours of the INSTANT data from 23:00 PM of January 10th - 22:00 PM of January 12th 2004 was verified by the numerical data. It gave a similar shape for the northward and eastward component of the velocity. The current velocity component for x-direction indicates that the model results are somewhat underestimated from the observed data, though little overestimated for y-direction.

Table 3.1 Model-data amplitude comparison of tidal component.

	M2			S2			K1			O1		
Stations	ζo	ζm	$\Delta\zeta$	ζo	ζm	$\Delta\zeta$	ζo	ζm	$\Delta\zeta$	ζo	ζm	$\Delta\zeta$
Benoa	0.71	0.68	0.03	0.33	0.33	0.00	0.25	0.27	-0.02	0.12	0.13	-0.01
Lembar	0.27	0.31	-0.04	0.16	0.13	0.03	0.36	0.34	0.02	0.24	0.24	0.00
Ampenan	0.25	0.31	-0.06	0.15	0.14	0.01	0.31	0.35	-0.04	0.22	0.24	-0.02
Std dev			0.05			0.02			0.03			0.01

note: ζ: amplitude is in meter; ζo: data; ζm: model; $\Delta\zeta$: ζo- ζm

Table 3.2 Model-data phase comparison of tidal component.

	M2			S2			K1			O1		
Stations	θo	θm	$\Delta\theta$	θo	θm	$\Delta\theta$	θo	θm	$\Delta\theta$	θo	θm	$\Delta\theta$
Benoa	287	285	2	355	347	8	301	301	0	276	292	-16
Lembar	308	312	-4	317	329	-12	284	293	-9	264	266	-2
Ampenan	309	312	-3	339	325	14	300	293	7	268	265	3
Std dev			3			14			8			10

Note: θ: phase in degree; θo: data; θm: model; $\Delta\theta = \theta o - \theta m$

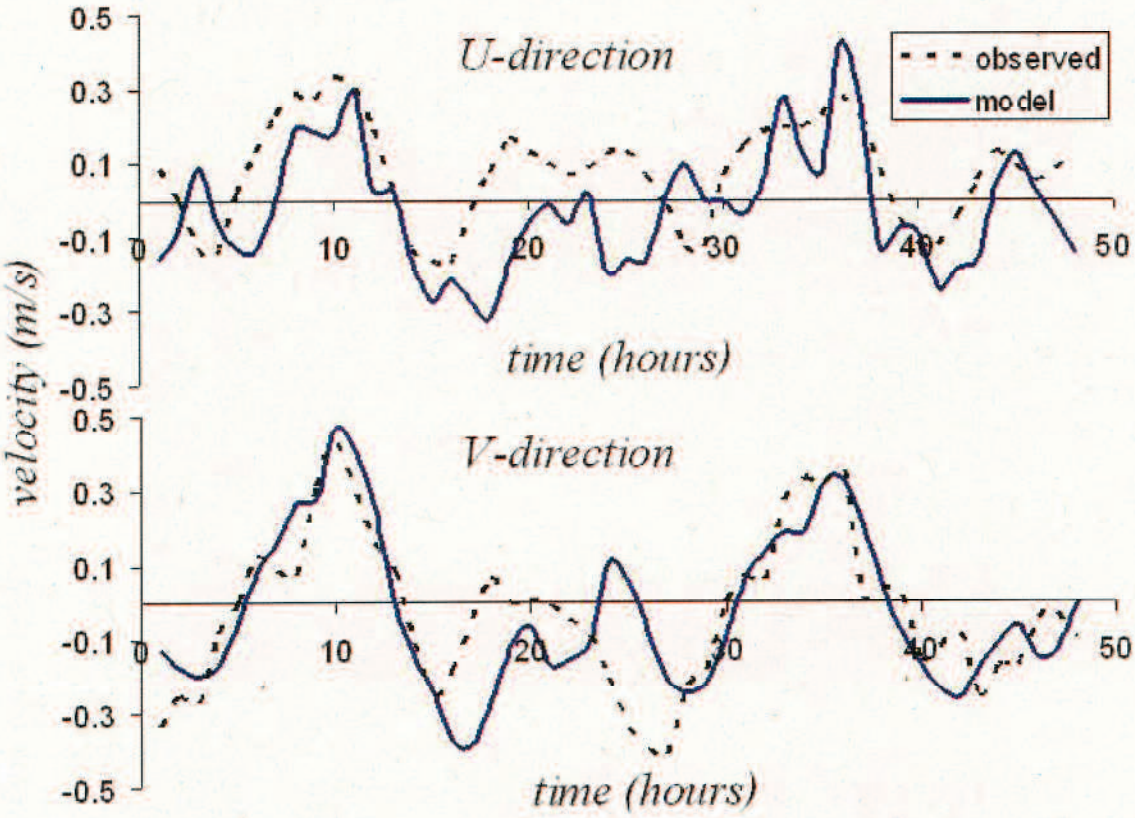

Figure 3.5 Comparison between observed and simulated tidal current at 250 m depth.

4.2 Tidal Current Pattern

The simulated tidal current in the Lombok Strait and Badung Strait are shown in Figure 3.6 and Figure 3.7. It was evidently shows the tidal current pattern generated by semidiurnal (M2, S2) and diurnal (O1, K1) components. The tidal flow field in Lombok Strait is characterized by strongly southward and northward flow over Lombok Sill and Badung Strait.

The Northward tidal currents are flowing from the southern open boundary entering the Lombok Sill and Badung Strait (Figure 3.6a and 3.6b). The flow of the tidal current that has a collision with Nusa Penida is divided into eastward and westward flow and flowing into Lombok Sill and Badung Strait. The alongshore current are revealed along the coastline of Bali, flowing from the south part to the northeast of Bali. The northward current in the Badung Strait does not enter the water into the Benoa bay. In the inner part of the Lombok Sill an opposite direction of near surface northward tidal current occurred (Figure 3.6a). The near surface layer of northward tidal current

flows eastward from the north side of Nusa Penida and along the southeast coastline of Bali. Meanwhile, small clockwise eddy in the inner part of Lombok Sill and an anticlockwise circulation in the Badung Strait occurred in the mid-depth layer (Figure 3.6b). The strongest northward tidal current can reach 4 m/s in the Lombok Sill and 2.5 m/s in the Badung Strait.

The near surface and mid-depth southward tidal currents (Figure 3.7a and 3.7b) enter the Lombok Sill and Badung Strait from the inner part of Lombok Strait. The northward and the southward currents are revealed to be the alongshore current along the coastline of Bali. These flow from northeast to the south part of Bali, and show the amount of water entering of the Benoa bay. The apparent strong tidal current occurred over the Lombok Sill, where it could reach 4.5 m/s around the Lombok Sill and 3 m/s in the Badung Strait.

A 3-D stratified model predicted the increase of tidal current across the Lombok sill and Badung Strait. It was also mentioned by Murray *et al* (1990) and Susanto *et al* (2005) that the relatively strong currents was found over the Lombok Sill and was about 2 ~ 4 m/s.

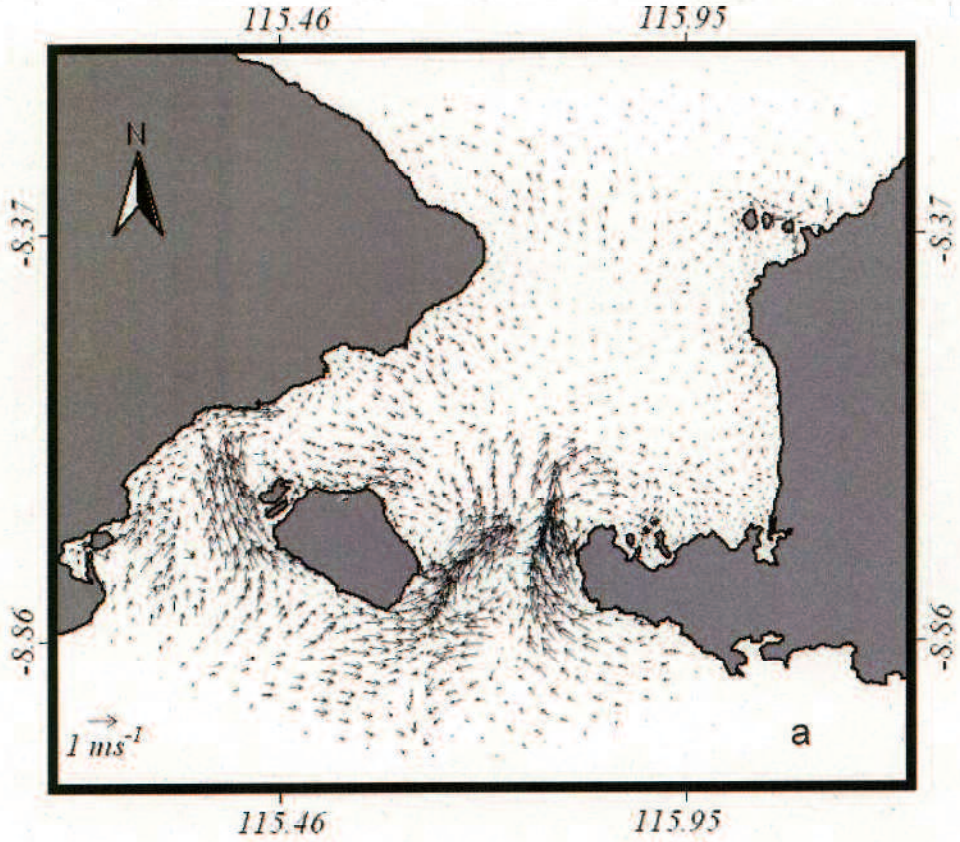

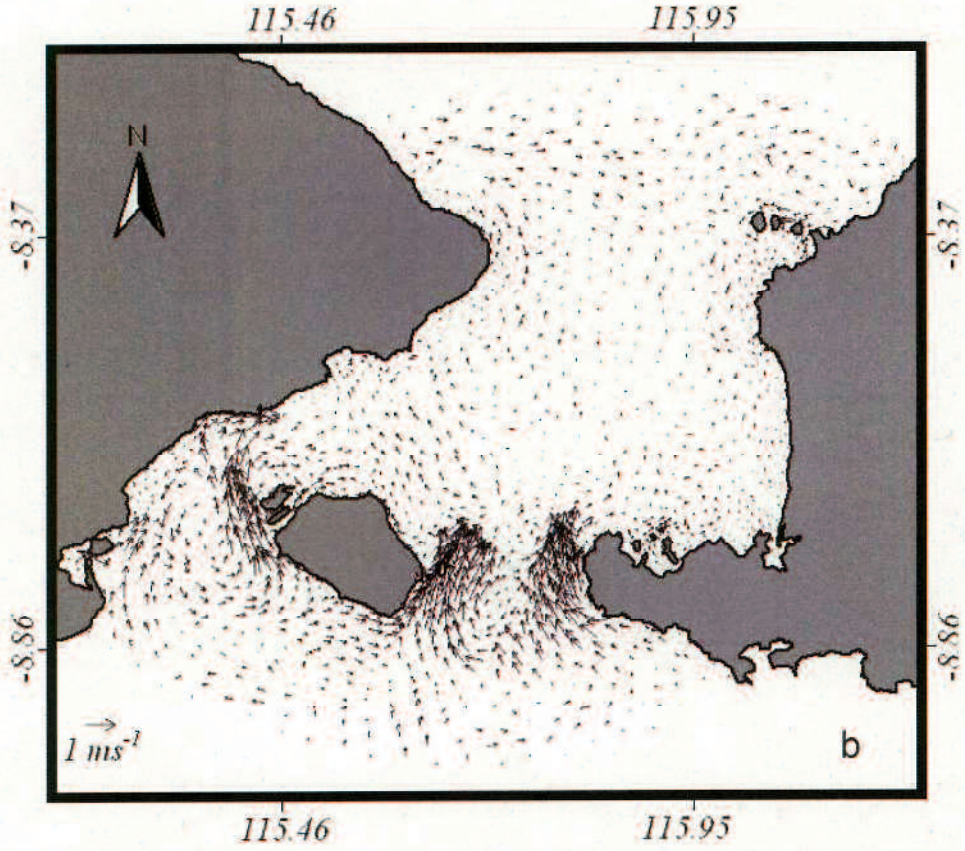

Figure 3.6 Northward tidal current patterns a) at near surface, b) at mid-depth.

The M2 and S2 tidal amplitude gradually increase from the north of the Lombok Strait to the south (Figure 3.8). It was clearly shown that the intensity of the tidal amplitude rapidly increasing in the vicinity of the sill and at the narrow passage of Badung Strait for both M2 and S2 tidal component.

From the simulation result, the tidal current pattern could be divided into two main routes as shown in Figure 3.9. The northward flow is propagated from southern open boundary to the Lombok Sill and Badung Strait. Meanwhile, the southward flow enters the Lombok Sill and Badung Strait from northern open boundary.

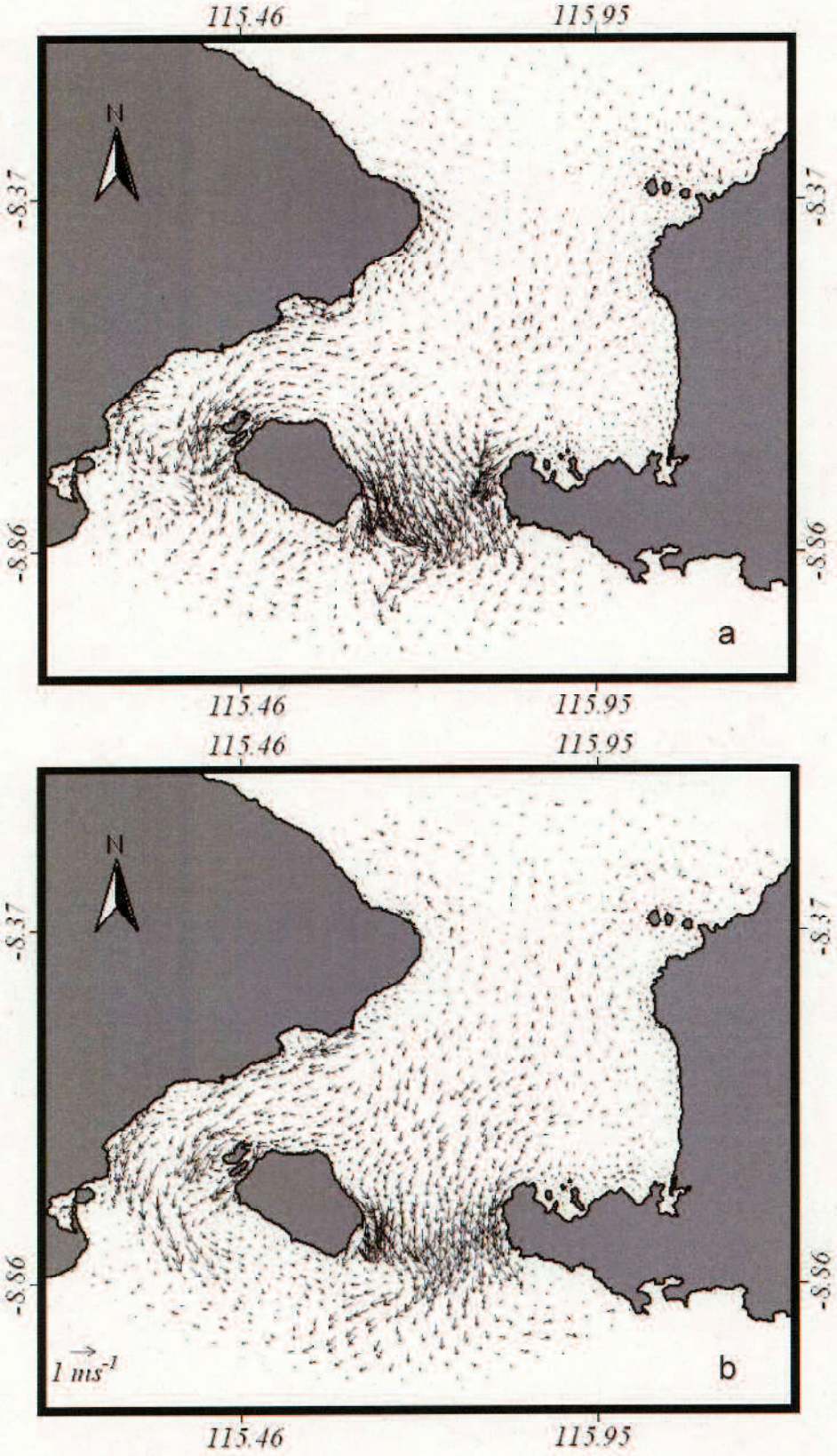

Figure 3.7 Southward tidal current patterns a) at near surface, b) at mid-depth layer.

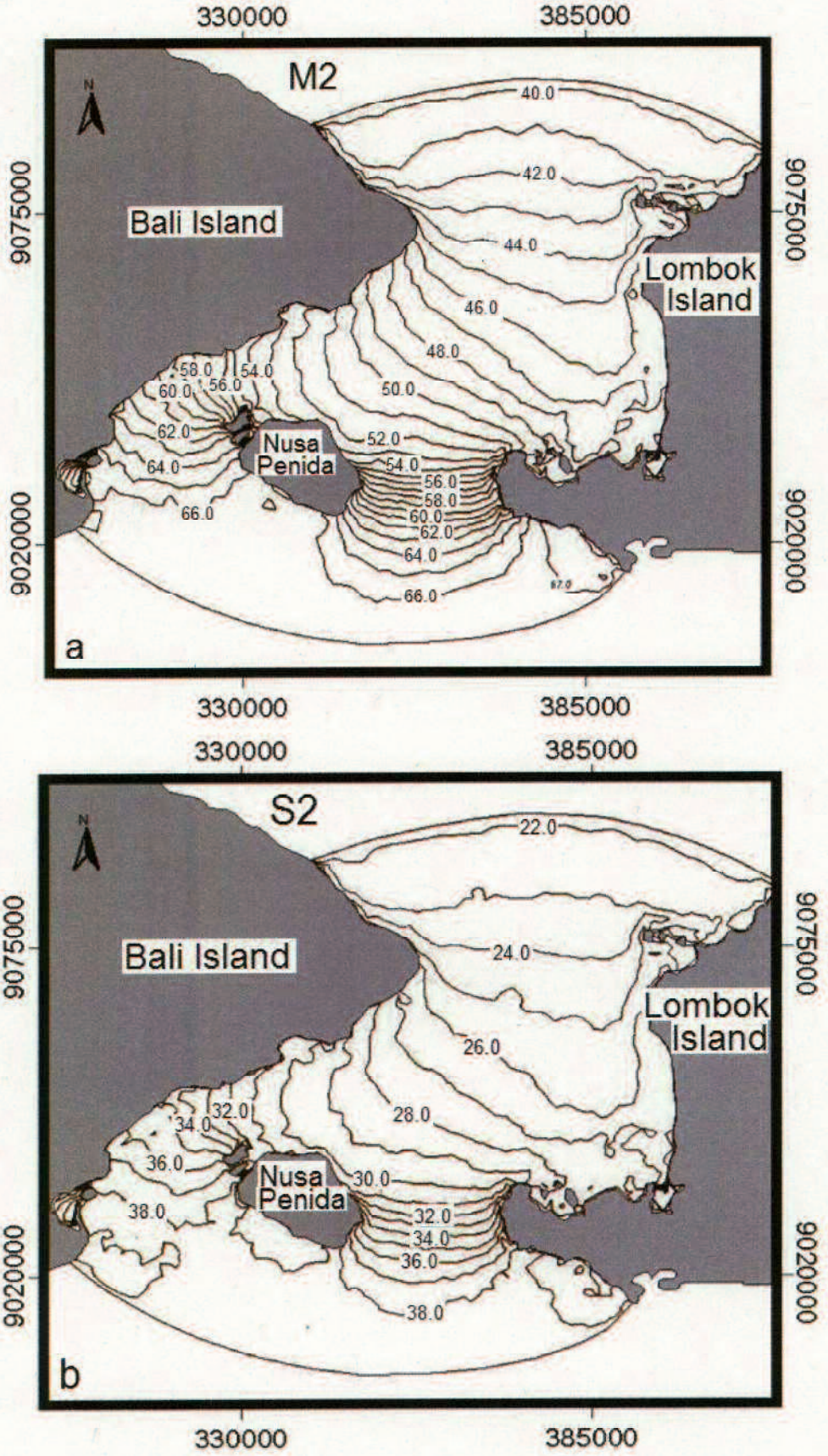

Figure 3.8 Co-amplitude of M2 and S2 tidal components.

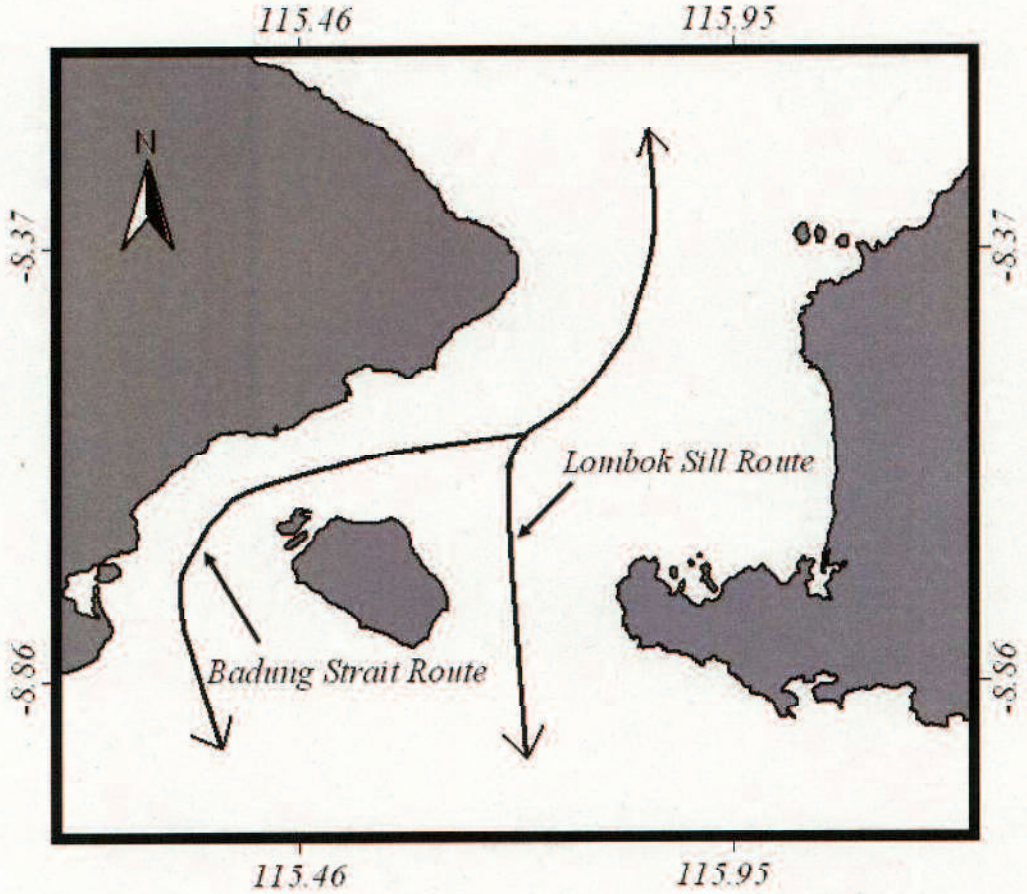

Figure 3.9 Two main routes of tidal flow in the Lombok Strait.

Figure 3.10 shows the kinetic energy along the Lombok Sill route from the northern open boundary to the southern open boundary. The horizontal axis, which is x-distance, goes from north to south. Here after, in the other figures in this chapter the x-distance has the same direction as the figure 3.10. The southward and northward tidal currents generate high kinetic energy in the vicinity of Lombok Sill. The surface layer kinetic energy for southward and northward flows is nearly zero from the northern open boundary to the northern side of Lombok Sill; though it dramatically increases in the vicinity of the Lombok Sill up to 0.7 m^2/s^2 for the northward current and to 0.78 m^2/s^2 for the southward current. It also occurs in the mid-depth layer, where the southward flow the kinetic energy could reach up to 0.45 m^2/s^2. On the other hand, relatively small fluctuation occurs during northward current, which reached about 0.1 m^2/s^2. In the near bottom layer, somewhat high kinetic energy occurs in the x-distance 34.5 km for both southward current and northward current, which reached 0.3 m^2/s^2, and increased dramatically over the top of Lombok Sill up to 0.68 m^2/s^2 for southward current.

However, a small fluctuation occurred over the Lombok Sill for northward current, which is 0.3 m^2/s^2.

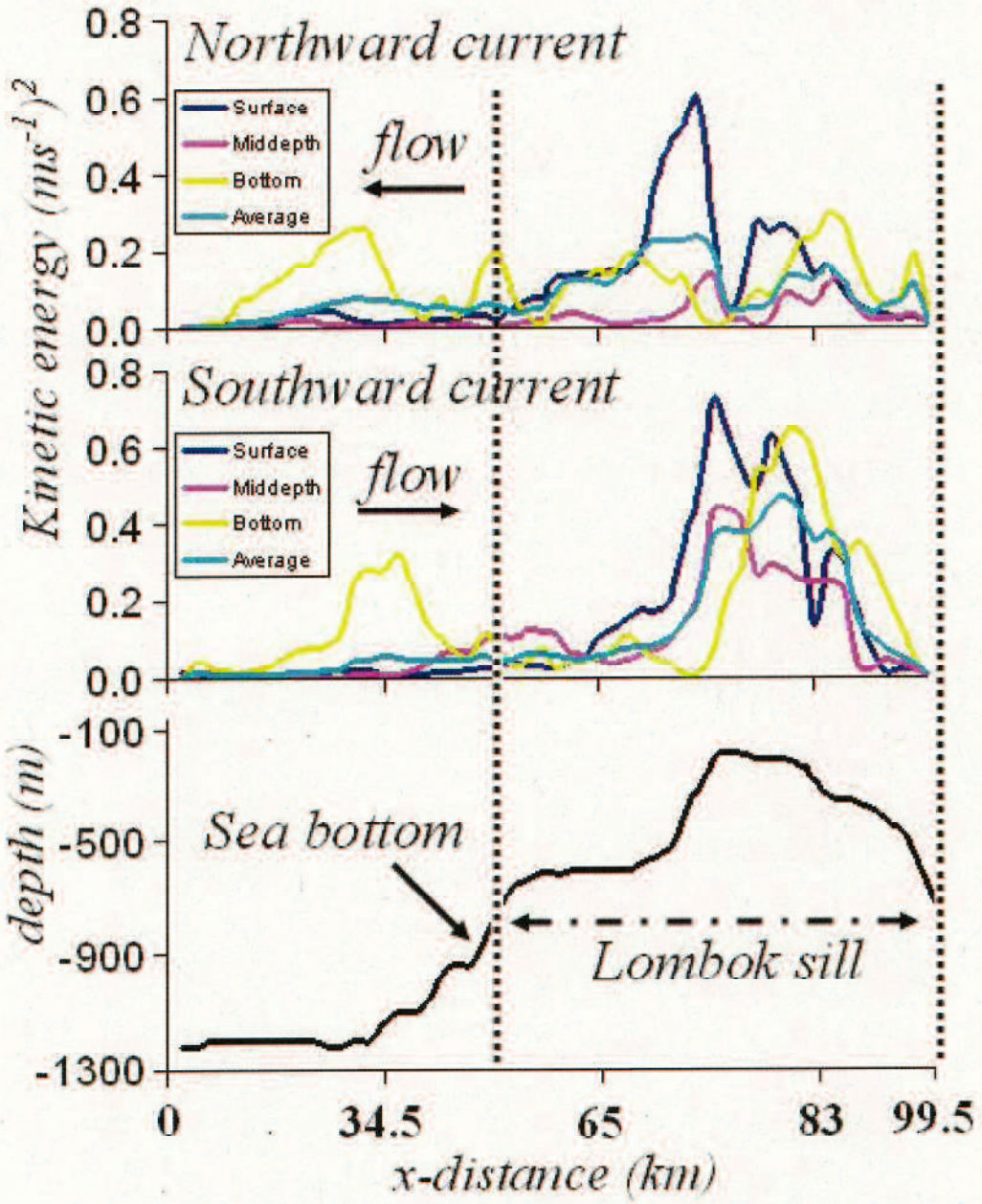

Figure 3.10 Kinetic energy of northward and southward tidal current along Lombok Sill route.

The averaged kinetic energy (averaged from upper layer to the bottom layer) is slightly small from the northern open boundary to the northern side of Lombok Sill. Whereas, the averaged kinetic energy dramatically increase in the vicinity of the

Lombok Sill, especially during the southward tidal current that could reach 0.4 m^2/s^2 and 0.25 m^2/s^2 for the northward current. The fluctuation of kinetic energy indicates the contribution of the sill in order to enhance the tidal flow passing through the Lombok Sill.

5. M2 Tidal Signature

5.1 M2 Tidal Current

The horizontal tidal flows surrounding the Lombok Sills generated by M2 tide were presented by indicating co-amplitude contours as shown in Figure 3.11. It indicates the obvious fact that the eastward flow component (Figure 3.11a) has a relatively smaller velocity compared to the northward flow component (Figure 3.11b). The spatial changes in the amplitude of the northward flow component occur very rapidly over the sill. The stepped form of the bottom topography also evidently contributes to increasing the tidal flow surrounding the sill. The effect is enhanced for the northward and the eastward components flow in the southern side of the sill, especially in the near bottom 50 cm/s for the eastward component and 220 cm/s for the northward component. The strong horizontal flow in the southern sill may be due to the stepped form of the bottom topography. A relatively strong current for the northward component is also generated above the sill. The intensified current in vicinity of the sill could amplify it.

The calculated results of the M2 vertical tidal flow component surrounding the Lombok Sill are shown in the Figure 3.12. The co-amplitude signature for the vertical component surrounding the Lombok Sill (Figure 3.12a) evidently shows the enhancement of the vertical flow over the sill. It also indicates that a strong vertical component is generated in the southern and the northern side of the Lombok Sill, especially near the sea bottom. The amplitude of the vertical flow could reach 6.5 cm/s in the northern side of the sill top and 9 cm/s in the southern side of the sill top.

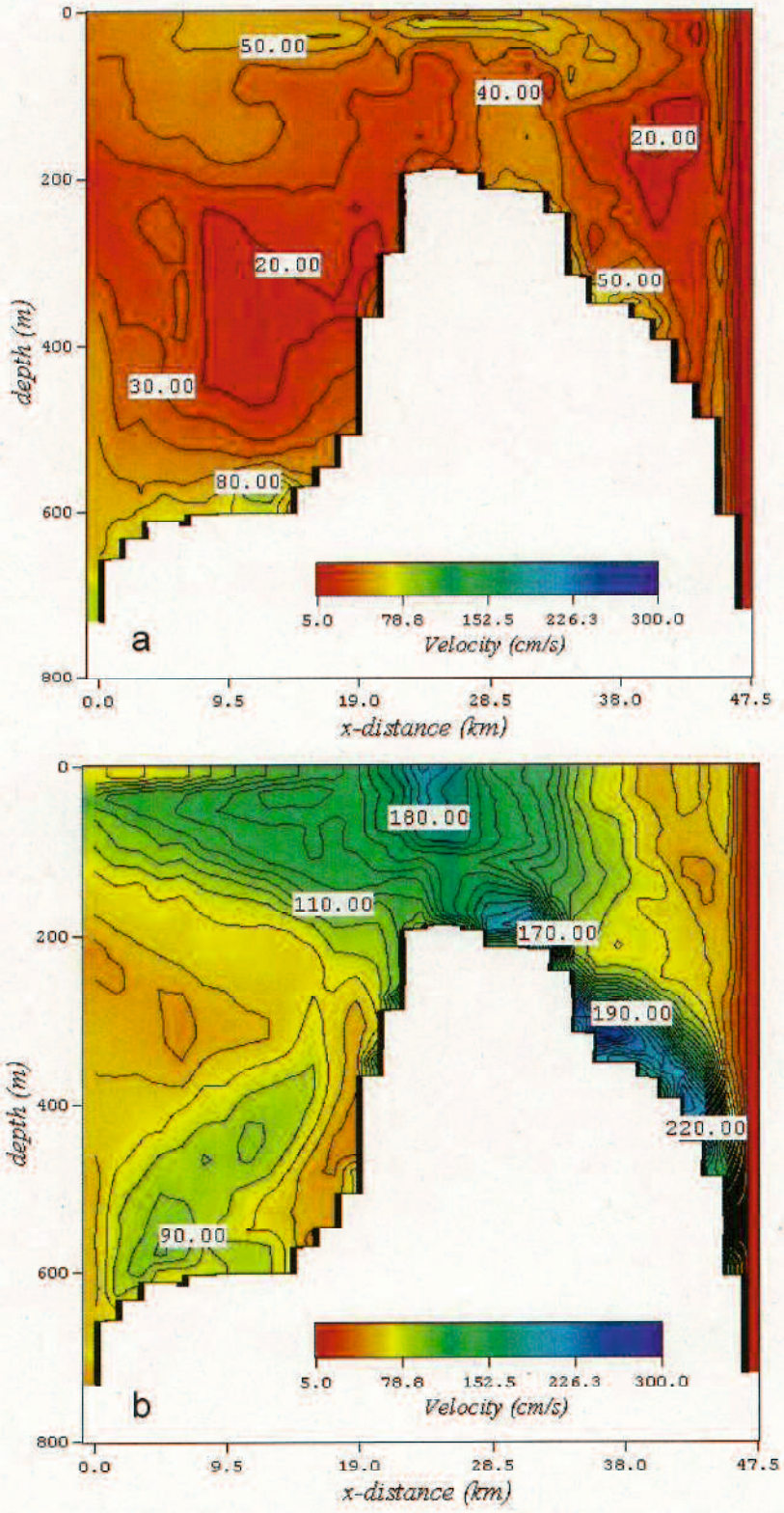

Figure 3.11 Co-amplitude of horizontal velocity over Lombok Sill. The contour scales are 10 cm/s, a) eastward flow-component, b) northward flow-component.

The vertical residual current pattern (Figure 3.12b) shows the role of the Lombok Sill. Strong downward flows occur above of the Lombok Sill. The Lombok Sill has a significant role in vertical mixing. The upward and downward vertical residual currents are changed spatially, and intensified over the sill. The maximum vertical residual velocity is -3 cm/s and 1 cm/s for downward and upward flow respectively, occurs in the surrounding the sill top.

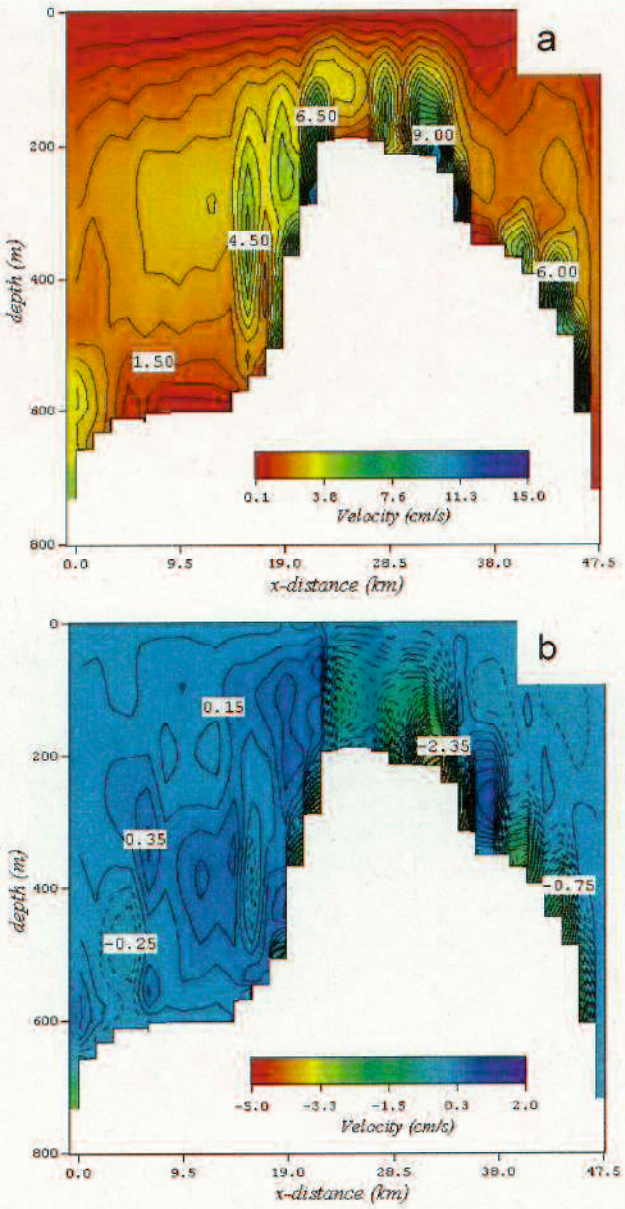

Figure 3.12 Vertical velocities across the Lombok Sill, a) co-amplitude, the contour intervals are 0.5 cm/s, b) vertical residual current, the contour intervals are 0.05 cm/s. The dash line and solid line are negative and positive value respectively

5.2 M2 Tidal Upwelling Signature

The Figure 3.13 shows eight sequential snapshots of the numerical results. These represent the temperature distribution over the Lombok Sill during southward and northward M2 tidal flow. The evolution of temperature perturbation over the Lombok sill is evidently shows during fourth M2 tidal period. The M2 tidal flow has a slightly high amplitude and depression in the upper layer during the southward and northward tidal flow. Those M2 tidal flows are responsible for enhancing the tidal upwelling above the sill. This is indicated by an increasing and decreasing of the seawater temperature in the water column. The upwelling occurred in the northern side of Lombok sill just after northward flow begin where the seawater temperature decreases to 20°C at 400 m depth and increases to 26°C at 300 m depth in the southern side of the sill. After the maximum and the end of the northward tidal flow, the seawater downwelling occur in the northern side of the sill and upwelling in the southern side of the sill. This makes the seawater temperature at 400 m depth in the northern side increases to 22°C, whereas at 300 m depth the temperature in the southern side reduces to 24°C. The upwelling phenomenon is relatively small in the southern side of Lombok sill and a relatively strong downwelling in the northern side of the Lombok Sill during northward tidal flow was observed (Figure 3.13b-d).

During the southward M2 tidal flow, the tidal upwelling evidently can be seen in the northern side of Lombok sill just after southward flow begins, and the seawater temperature decreases until 20°C at 350 m depth. Meanwhile, tidal downwelling occurs in the southern side of the sill (Figure 3.13f) and the seawater temperature becomes 26°C at 300 m depth. The strong tidal upwelling in the northern side of the sill and the strong tidal downwelling in the southern side of the sill occur after maximum southward tidal flow (Figure 3.13g), which causes the temperature in top of the sill to decrease to 22°C. The strong tidal upwelling and downwelling still appear during the weak southward tidal flow. Those upwelling and downwelling phenomena indicate that the M2 tidal current has an important role in the enhancement of the tidal upwelling in the vicinity of the Lombok sill.

In order to understand the movement of waters parcels in the upwelling and downwelling area, 25 particles were released at a depth 400 m after 4th cycle of the M2 tidal period (Figure 3.14). In the northern side of the Lombok sill, the particles move

upward rapidly after one cycle of the M2 tidal period. Some of those particles in the northern side of the sill needed only one cycle of the M2 tidal period to reach the upper layer. Meanwhile, particles moved downward in the southern side of the sill. This is allign with the vertical residual current for both sides of the sill. It also have same tendency with the upwelling and downwelling field surrounding the Lombok sill.

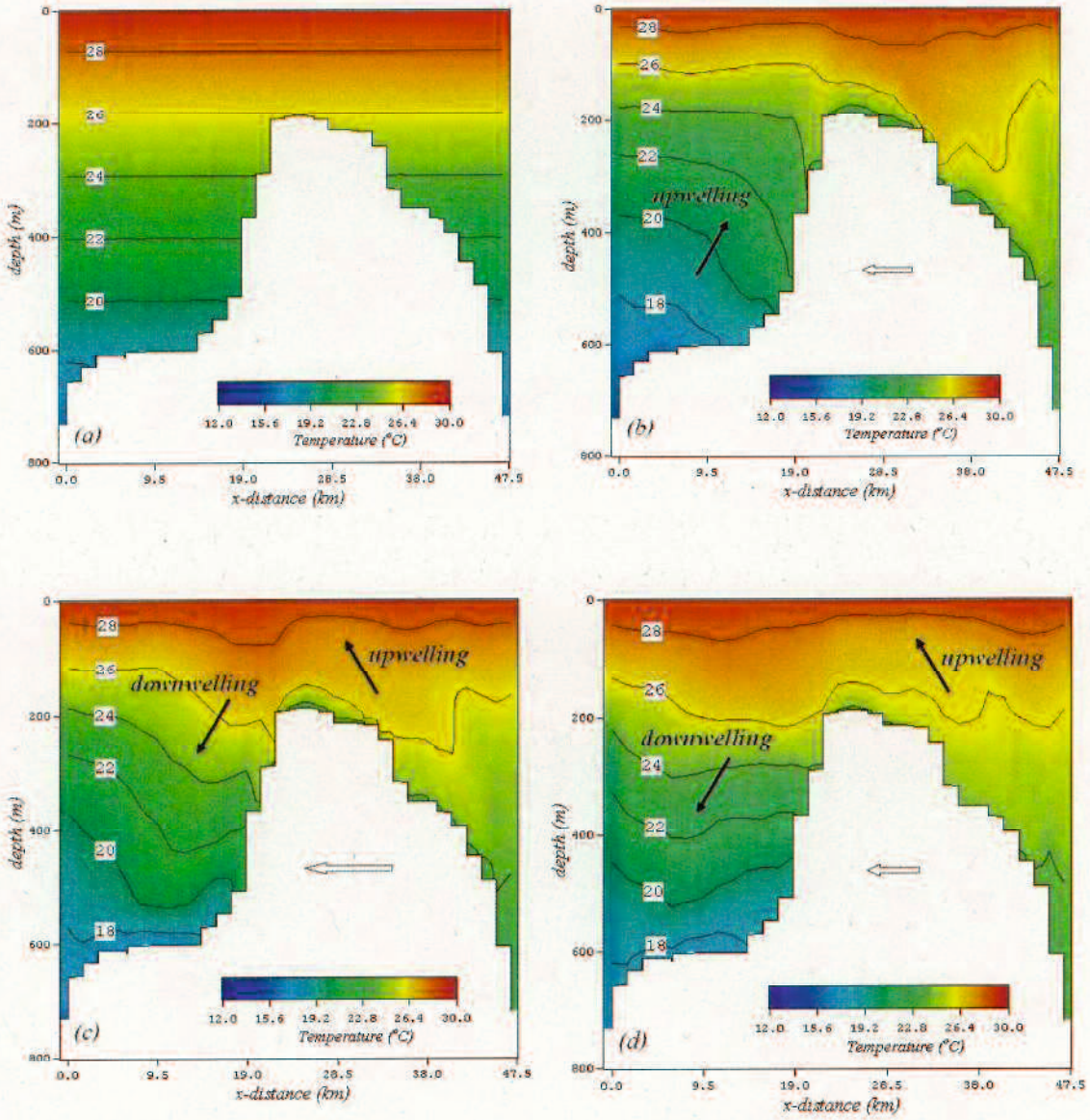

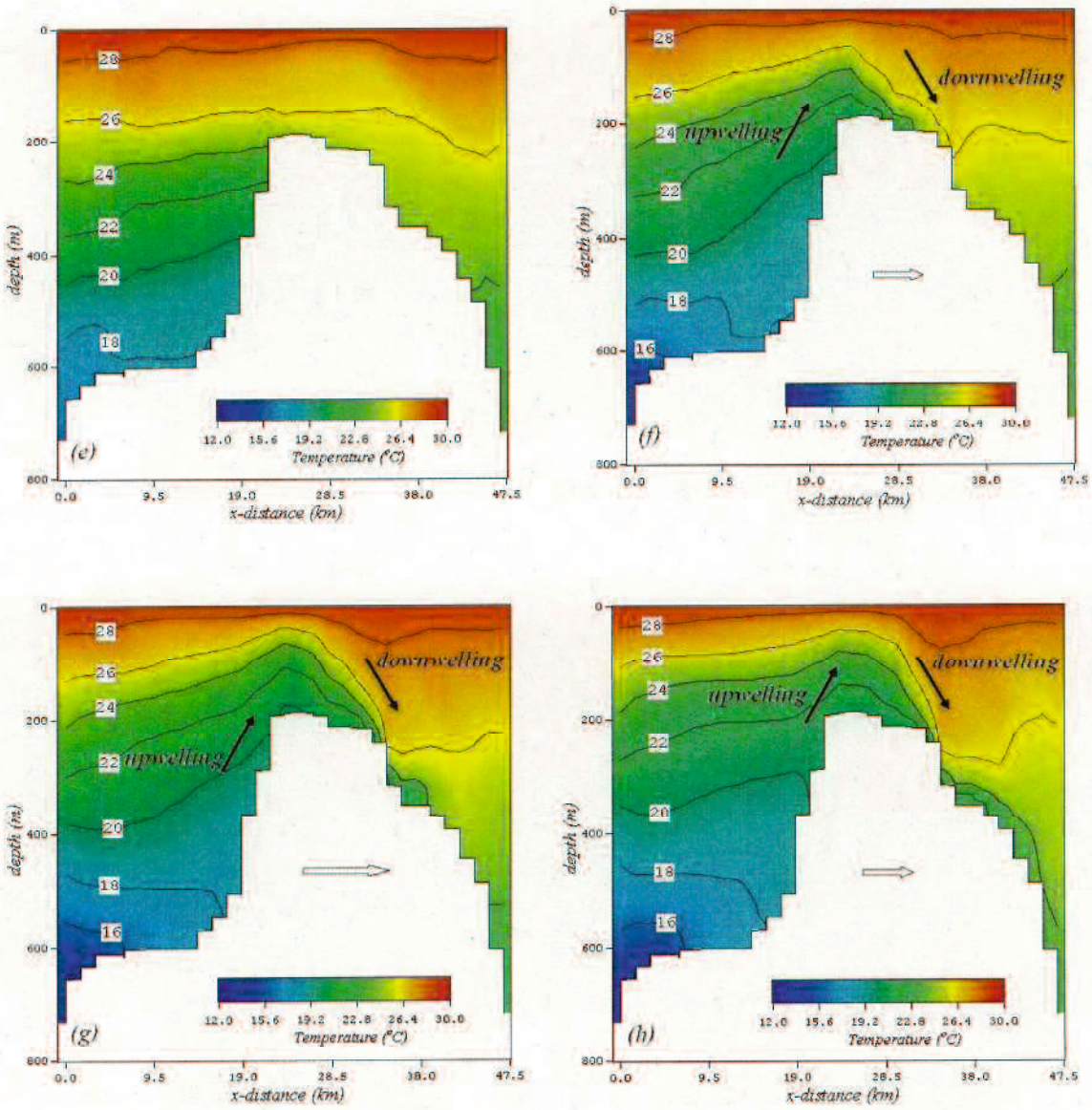

Figure 3.13 Temperature distributions across the sill after 4th cycles of M2 tidal period. The arrow indicated the northward and southward tidal current. a) Initial temperature, b-d) during northward tidal current, e) slack condition, f-h) during southward tidal current. Arrow at the sill denote the amplitude and direction of tidal flow.

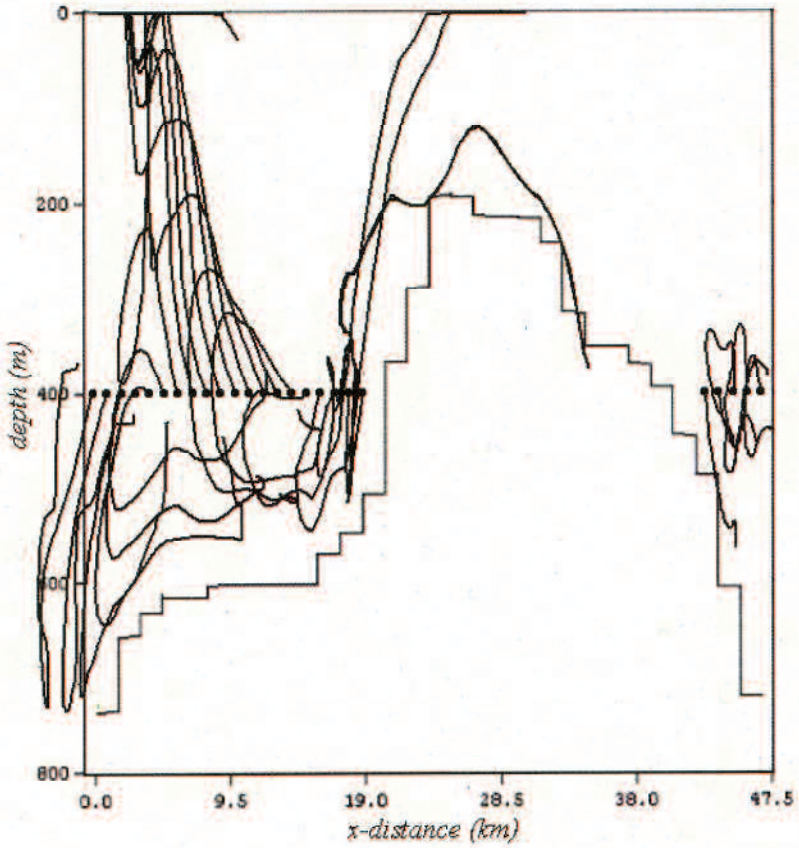

Figure 3.14 Vertical movements of particles that released in the 400 m depth from 3rd until 4th cycles of M2 tidal period, small black circle is the initial position.

6. SUMMARY

Horizontal and vertical flows in the Lombok Strait were discussed with3-D stratified flow model. It is confirmed that present computation of model can well predict the tidal current pattern in Lombok and Badung Strait. The model shows the alongshore current along the coastline of Bali revealed during the northward and southward current. The southward current has a contribution to supply the seawater into the Benoa bay.

The model results indicated the occurrence of tidal upwelling over the sill. Qualitatively, the strong tidal upwelling occurred in the north side of the Lombok sill during the southward current, while the weak tidal upwelling was occurred in the south side of the Lombok Sill during the northward current. The upwelling occurred in the northern side of Lombok sill just after northward flow began where the seawater temperature decreases to 20°C at 400 m depth and increases to 26°C at 300 m depth in the southern side of the sill. After the maximum and the end of the northward tidal flow, the seawater downwelling occurred in the northern side of the sill and upwelling in the

southern side of the sill. This caused the seawater temperature at 400 m depth in the northern side increases to 22°C, whereas at 300 m depth in the southern side the temperature reduces to 24°C.

Just after the southward flow begins, the tidal upwelling in the northern side of Lombok sill occurred, and the seawater temperature decreases to 20°C at 350 m depth. Meanwhile the tidal downwelling occurred in the southern side of the sill and the seawater temperature becomes 26°C at 300 m depth. The strong tidal upwelling in the northern side of the sill and strong tidal downwelling in the southern side of the sill occurred after maximum southward tidal flow. It made the temperature in top of the sill decrease to 22°C.

The vicinity of the sill also enhanced the tidal upwelling confirmed by the relatively strong vertical residual current surrounding the upper layer above the sill and by the rapid particles movement from 400 m depth to the upper layer.

References

Awaji, T., Imasato, N. and Kunishi, H., 1980.Tidal Exchange through a strait: A Numerical experiment using a simple model basin, Journal of Physical Oceanography, Vol.10, pp.1499-1508.

Chen, C., Beardsley, R. C. and Cowles, G., 2006.An unstructured grid,finite-volume coastal ocean model: FVCOM user manual, second edition

Ffield, A. and Gordon, A. L., 1992.Vertical mixing in the Indonesian thermocline, Journal of Physical Oceanography, Vol.22, pp.184-195.

Ffield, A. and Gordon, A.L., 1996. Tidal Mixing Signature in the Indonesian Seas, Journal of Physical Oceanography, Vol. 26, pp. 1924-1937

Galperin, B., Kantha, L. H., Hassid, S., and Rosati, A., 1988. A quasi-equilibrium turbulent energy model for geophysical flows, Journal of Atmospheric Science, Vol.45, pp.55-62.

Gordon, A. L., 2005. Oceanography of the Indonesian seas and their throughflow, Oceanography, Vol.18, pp. 14-27.

Gordon, A.L., McClean, J.L., 1999. Thermocline stratification of the Indonesian Seasm, models and observations. Journal of Physical Oceanography 29, 198–216

Hatayama, T., Awaji, T. and Akitomo, K., 1996.Tidal current in the Indonesian seas and their effect on transport and mixing, Journal of Geophysical Research, Vol.101, pp.12353-12373.

Hatayama, T., 2004.Transformation of the Indonesian throughflow water by vertical mixing and its relation to tidally generated internal waves, Jouranl of Oceanography, Vol.60, pp.569-585.

Lu, X., Qiao, F., Xia, C., Wang, G., and Yuan, Y., 2010 Upwelling and surface cold patches in the Yellow Sea in summer: effects of tidal mixing on the vertical circulation, Continental Shelf Research, Vol.30, pp.620-632.

Matsumoto, K, Ooe, M., Sato, T. and Segawa, J., 1995.Ocean tide model obtained from TOPEX/POSEIDON altimetry data, Journal of Geophysical Research, Vol.100, pp.25319-25330.

Murray, S. P., and D. Arief, 1988: Throughflow into the Indian Ocean through the Lombok Strait, January 1985-January 1986. *Nature*, **333**, 444–447

Murray, S. P., Arief, D., Kindle, J. C. and Hulburt, H. E., 1990.Characteristics of circulation in an Indonesian archipelago strait from hydrography, current measurements and modeling results, The Physical Oceanography of Sea, Vol.318, pp.3-23.

Nakamura, T., Awaji, T., Hatayama, T., Akitomo, K., Takizawa, T., Kono, T., Kawasaki, Y. and Fukasawa, M., 2000.The generation of large-amplitude unsteady lee waves by subinertial K1 tidal flows: A possible vertical mixing mechanism in the Kuril Straits, Journal of Physical Oceanography, Vol.30, pp.1601-1621.

Potemra,J.T., Hautala, S.L., Sprintal, J., Pandoe, W., 2002. Interaction between the Indonesian Seas and the Indian Ocean in Observations and Numerical Models,Journal of Physical Oceanography. Vol. 32, pp. 1838-1854

Qu, T. et al., 2005, Sea Surface Temperature and its Variability in the Indonesian Region, Oceanography Vol. 18, No. 4, pp 50-61

Robertson. R and Amy Ffield. 2005, M2 BaroclinicTide in The Indonesian Seas, Oceanography, Vol. 18, No. 4, pp. 62-73

Schiller A., 2004. Effects of explicit tidal forcing in an OGCM on the water-mass structure and circulation in the Indonesian throughflow region, Ocean Modelling, Volume 6, Issue 1,pp 31-49

Smagorinsky, J., 1963. General circulation experiments with the primitive equation, I.The basic experiment. Monthly Weather Rev, Vol.91, pp.99-164.

Susanto, R. D., Mitnik, L. and Zheng, Q., 2005. Ocean internal wave observed in the Lombok Strait, Oceanography, Vol.18, pp.80-87.

Wenju, C. and Lennon, G.W., 1988. Upwelling in the Taiwan Strait in response to wind stress, Ocean circulation and topography, Estuarine,Coastal and Shekf Sciences, Vol.26, pp.15-31.

CHAPTER 4

SEAWATER EXCHANGE OF BENOA BAY

1. Introduction

Seawater in the coastal area has an important role concerning the sustainability of coastal ecosystem. For instance, the coastal area is used as nursery region and feeding ground for large number of marine species. In the last decades, because of the increased development activities exploiting the coastal areas, the degradation of environmental quality has become a serious issue among researchers. Seawater experiences various contaminants either directly from pollutant sources or indirectly from river discharges. The knowledge of hydrodynamics processes in coastal area has an essential role in any investigation. It can be used to investigate the capability of seawater to assimilate those various pollutants discharged into it. The main flow of seawater in the coastal region is strongly influenced by tidal system (Imasato et al., 1980), in addition to that induced by river flow and wind. Therefore, an accurate study of the tidal flow in coastal waters becomes one of the most important environmental sciences. In the recent years, numerical simulation of the tidal current is widely used for coastal ocean circulation study. However, until now, we have not found any study concerning coastal ocean circulation in Benoa bay, particularly the study that describe and try to measure the seawater exchange system.

As shown in Figure 4.1, Benoa Bay is semi-enclosed water situated in the southern part of Bali-Indonesia. The lateral dimension of Benoa Bay is 10 km x 5 km in the inner part of the bay. Benoa Bay is characterized by a narrow strait in the bay mouth formed by Seranganisland and Benoa Peninsula. The main vessel harbor in Bali, namely Benoa Harbor, is located in the inner part of the bay. Since 1996, Serangan and Bali have been connected by a bridge, and very limited water could pass through under the bridge into Benoa bay.

Benoa bay is important for Bali both from environmental as well as economic points of view. From the environmental point of view, Benoa bay is the area for the mangrove ecosystem but it is also used for the disposal of garbage. From the economic point of view, Benoa bay is used for harbor, oil station, and tourism activities.

Therefore, in order to conserve the marine environment in the bay, understanding of the characteristics of the seawater circulation is imperative.

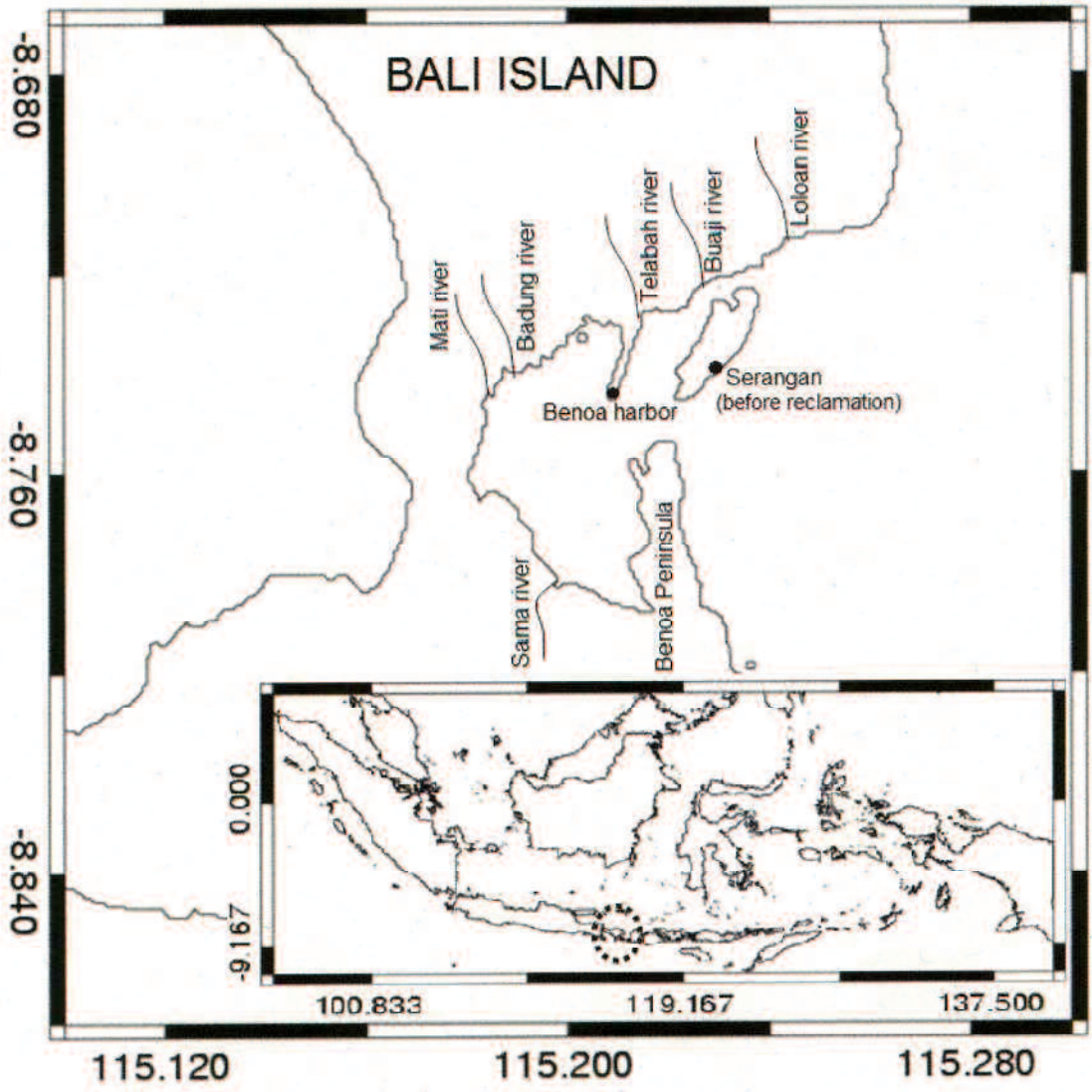

Figure 4.1 Benoa Bay map with scribble black lines indicating river discharge. The inset picture is the Indonesia Archipelago. Benoa Bay is indicated with a circle.

Figure 4.2 shows the bathymetry map that was obtained from Hydro-Oceanography Division Indonesian Navy (DISHIDROS-TNI AL). Benoa bay has a shallow water depth, where the deepest part in the inner part of the bay is less than 15 m and in the outer part (towards the ocean) less than 50m. In the inner part of the bay, particularly in the nearest coastline the water depth varies from about 1m to 5m. The

surroundings of the bay mouth and the east part of Benoa harbor have the stepped bottom topography with depth 10m to 15m.

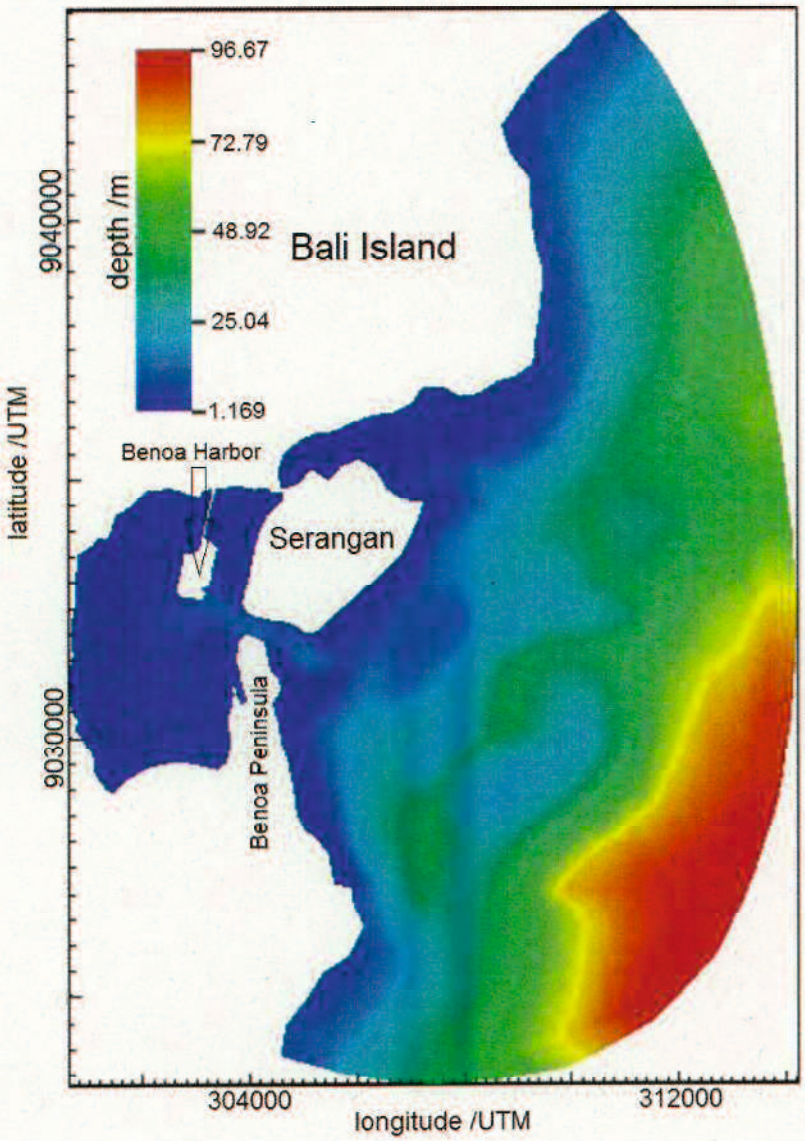

Figure 4.2 bathymetry map

In general, the oceanic circulation within the Benoa Bay is controlled by inflows from Badung strait and Indian Ocean. The tides and tidal currents are typical of water circulation in Benoa Bay, which is mostly impacted by seawater from Badung Strait. The type of tides in Benoa Bay is semi-diurnal, in which the M2 is the dominant tidal component. During spring tide, the sea level in the inner bay can rise to 2.5m and drop 2.1 m during neap tide.

In addition, Benoa Bay is under the influence of the six rivers discharges: Badung, Mati, Sama, Telabah, Lolan and Rangda River. According to the report of Environmental Impact Assessment Agency of Bali Province, the fresher water discharged into the bay is less than $360m^3$/hours in each river discharge. This low salinity of fresher water runoff has a significant effect on the water circulation due to the difference of salinity with the sea water.

It is important to understand the physical process of the tidal current field in order to discuss the water quality and the eco-system in Benoa Bay; particularly the seawater exchange is one of the important physical processes. In order to clarify the mechanism of seawater exchange, we undertake a numerical simulation by tracking the particles released in the current driven by M2 tidal component. Additionally, the seawater-flushing rate is estimated by calculating the time consumed by the particles' movement in box area as a function of the initial condition. Finite Volume Coastal Ocean Model (FVCOM) developed by Chen et al (2003) is used in our study. FVCOM is based on the Finite Volume Method and three dimensional primitive equations. One unique feature of FVCOM is the use of the unstructured grid. The suitability of unstructured grid approach in FVCOM enables us to reproduce coastal ocean currents with high resolution in a complex coastal geometry. FVCOM has been successfully used by many researchers for investigation of the coastal ocean circulation (Chen et al, 2007; Huang et al, 2007) and the physical mechanism for the offshore detachment (Chen et al, 2008). The Lagrangian method was widely used for examining particle tracking and seawater exchange (Chen et al 2008, Bligili et al 2005, Awaji et al 1980).

Through this study, the tidal current mechanism and the particle transport for the existing configuration of Benoa bay will be discussed clearly. Moreover, to comprehend the detail of the tidal current mechanism, the discussion for the past two configurations and changes of present configuration on Benoa Bay is also given. The two past configurations and changes of present configuration on Benoa bay are as follows;

1) Benoa bay with the original configuration of Serangan island (before reclamation) with the existence of Benoa harbor.
2) The original configuration of Benoa bay, i.e.,the original condition of Serangan island and without the Benoa harbor.

3) The change on present configuration by removing the road that connects the main island with Benoa harbor.

2. Numerical Model

The FVCOM used in this research is FVCOM 2.7.1 series. The governing three-dimensional equations consist of the momentum, continuity, temperature, salinity, and density equations as given by Chen et al (2006). The vertical eddy viscosity and the vertical thermal diffusion coefficients are obtained using the modified Mellor-Yamada level 2.5 (MY's-2.5) turbulence closure models (Mellor and Yamada, 1982). The horizontal diffusion coefficients are determined using a Smagorinsky eddy parameterization method (Chen et al, 2003).

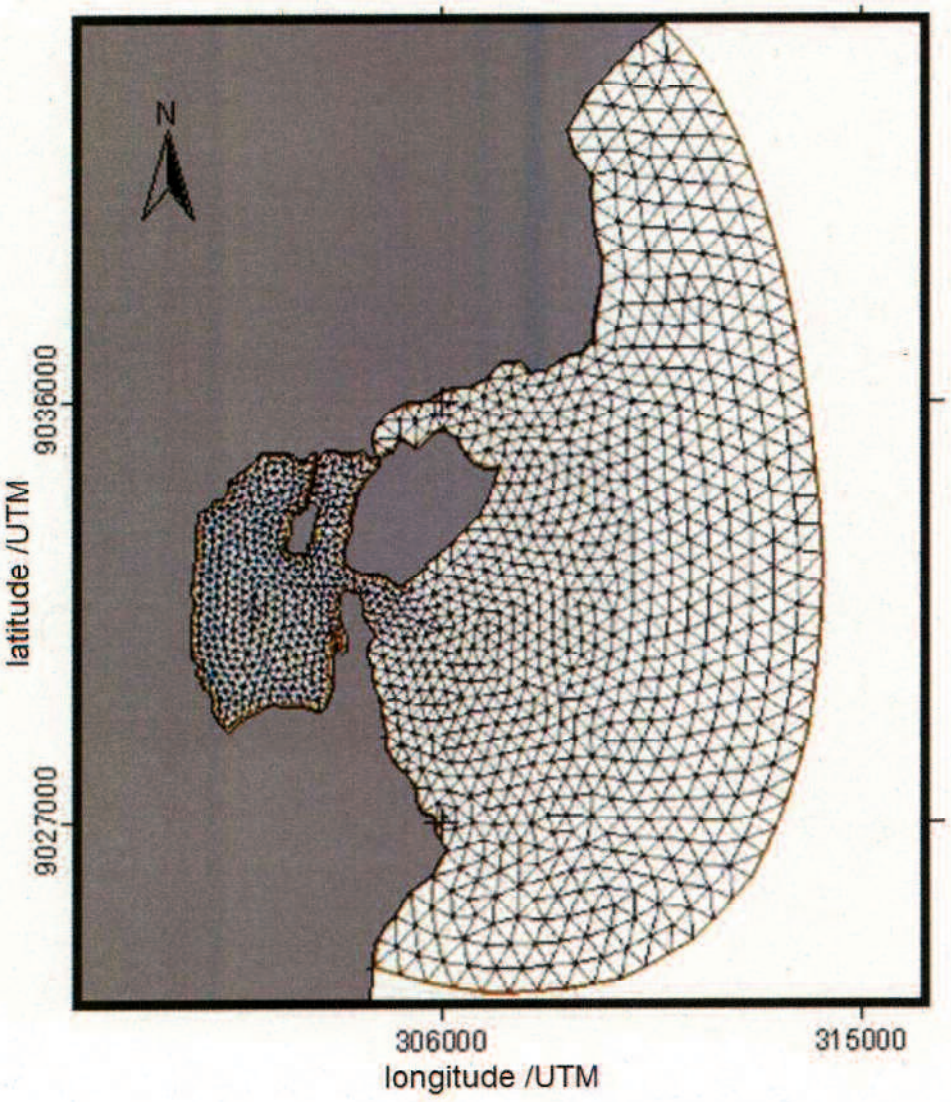

Figure 4.3 Unstructured Triangular grids

FVCOM is composed of the external and internal modes that are computed separately using two split time steps. FVCOM subdivides the horizontal numerical computational domains into a set of non-overlapping unstructured triangular meshes. An unstructured triangle is composed of three nodes, a centroid, and three sides. The scalar variables, such as salinity (S), water elevation (ζ), and vertical velocity (ω) are placed at the nodes, and determined by a net flux through the section linked to centroid and the mid-point of the adjacent sides in the surrounding triangles (Called the tracer control element or TCE). The horizontal velocity u and v are placed at the centroid and calculated on the basis of the net flux through the three sides of that triangle (the momentum control element or MCE). FVCOM uses an exact form of the no flux bottom boundary conditions for temperature and salinity. The bottom slope and gradients of temperature and salinity are calculated using Green's theorem.

In this study, the computational domain is configured with unstructured triangular grids in the horizontal and σ-level in the vertical (Figure 4.3). The grid in the horizontal cases is designed with different resolutions, i.e., 200m in the inner of bay to 600m in the outer of bay and vertical grid was divided into 10 σ-levels.

Table 4.1 The initial set up conditions for the model

Items		Contents
Grid	Number of node	1298
	Number of element	2342
Layers		Uniform layer with 10^{th} sigma layer
Open boundary	Tide conditions	M2 tidal component
	Temperature and salinity	uniform
River discharge		Badung River, Mati River, Sama River, Telabah River, Lolan River and Rangda River
Meteorological condition		uniform
Time step		1.0 second

To consider the wet and dry conditions during ebb tide and flood tide, a wet/dry point treatment method has been incorporated into the calculation. The vertical column thickness is less than 0.05m in the cell during ebb tide and will be designed as a dry cell and its velocity is set to zero. During flood tide where the water level rises, a dry cell becomes wet and its velocity and elevation are computed.

In this study, FVCOM is forced by four river discharges within the bay and two river discharges in the Northern part of Serangan island (See figure 4.1). In the open boundary of the computational domain, M2 tidal component is forced for tidal water circulation, and the temperature is determined to be constant. The computational domain is also forced by fresher water from six rivers which are discharged into Benoa bay. In the surface boundary, the meteorological parameters are determined to be constant. The constant salinity used as an initial condition since no observation data we could obtain in the Benoa bay. This assumption would be fairly acceptable since the water depth of Benoa Bay is shallow. Furthermore, a constant salinity and meteorological data used in this study, since the climatological condition in the Benoa bay does not change significantly for short time (tropical area). The M2 tidal component used in the open boundary was obtained from the tidal model developed by Ocean Research Institute (ORI), the University of Tokyo (ORI-Tide) (Matsumoto et al, 1995). The initial setup conditions are summarized in Table 4.1.

The investigation of the seawater exchange in Benoa Bay was performed using the Lagrangian particle tracking method. The Lagrangian particle tracking solving a nonlinear system of ordinary differential equation (ODE) is as follows (Chen et al (2006):

$$\frac{dx}{dt} = v(x(t),t) \qquad (1)$$

Where$x$ is the particle position at a time t, dx / dt is the rate of change of the particle position in time and v (x, t) is the 3-dimensional velocity field generated by the model. The particles released in the model domain are treated using conserved mass method. In this calculation, the dependence of the velocity field on time has been eliminated since the velocity field is considered stationary during the tracking time interval (Chen et al, 2006). In order to provide a clear analysis of seawater exchange in Benoa Bay, the

model area is divided into five regions as shown in Figure 4.4. In each region, the characteristics of particle transport will be investigated thoroughly to obtain an overall characteristic of the seawater exchange. Seawater exchange in the model domain is also investigated by using the calculated time of particles in residence in the model area.

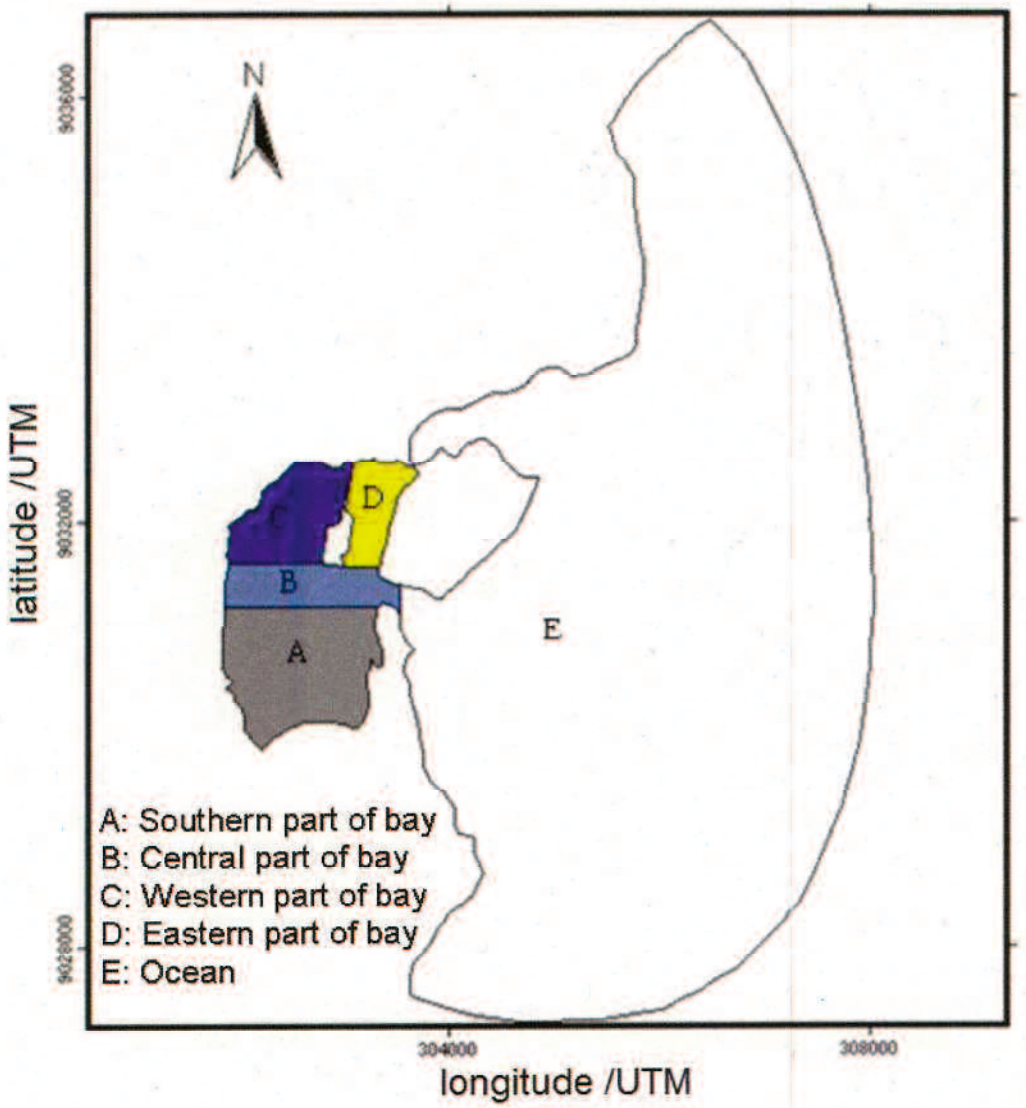

Figure 4.4 Benoa bay divided into five model regions

3. Observation

The observational investigation was performed to measure seawater salinity. Center for Remote Sensing and Ocean Sciences (CReSOS) Udayana University-Bali and Kyowa Concrete Industries Ltd carried out the field observation on May 2005 for salinity using compact CTD. The locations of the observation stations are shown in the Figure 4.5. Eight observation stations were located in the inner part of the bay and five

stations in the outside of the bay. The Salinity parameter was measured at every 2 m depth.

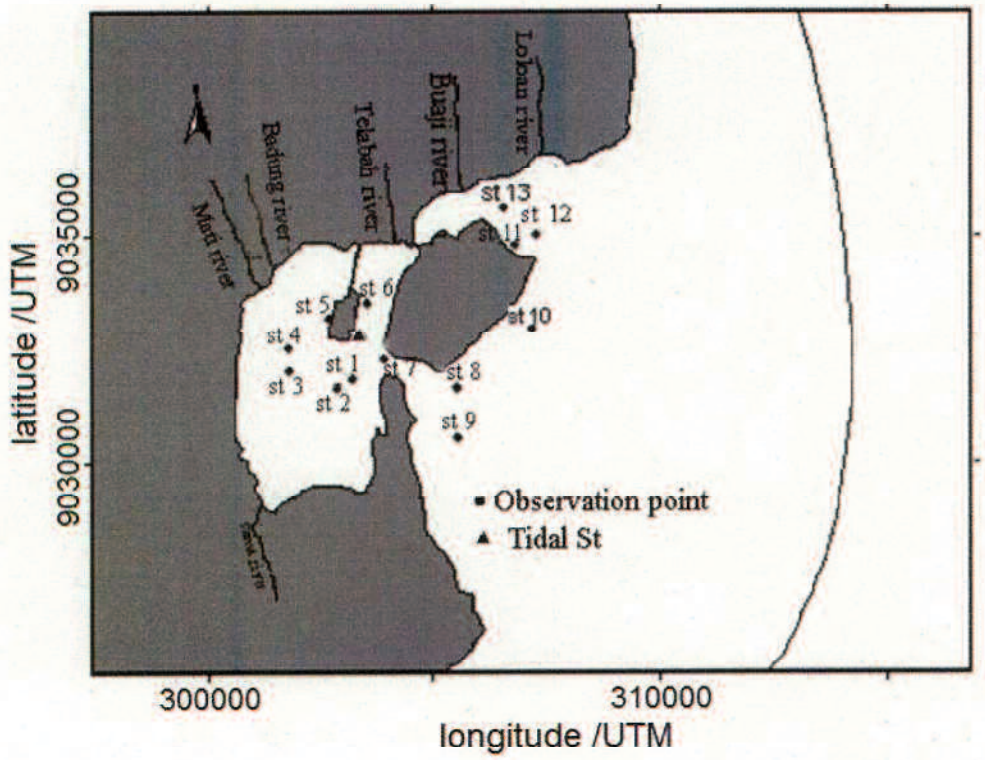

Figure 4.5 Salinity observation station indicated with black circle and tidal measurement station indicated with triangle

Within the bay, there is one tidal observation station that was set up by National Coordinating Agency for Surveys and Mapping (Bakosurtanal) Indonesia to measure the tidal elevation. The measurement of tidal level was recorded every hour. In order to validate the model calculation, M2 amplitude was filtered using the least square analysis method.

Unfortunately, there is no measurement of tidal current available yet in Benoa Bay. Therefore, in this research, we are unable to validate the tidal currents produced by numerical calculation with field data.

4. Results and Discussion

4.1 Tidal level validation

Figure 4.6 shows a comparison between the numerical and observation results for the M2 tidal height and phase lag. The comparison between the observed and the

simulated amplitude and phase lag of M2 tidal component at the tidal measurement station in the inner of Benoa Bay shows a good agreement. Table 4.2 shows small discrepancy in amplitude and phase lag, which are 0.02m and -1.2 degree respectively. The small discrepancy between observation and numerical calculation indicated that FVCOM has a good performance to simulate the seawater level in the model domain.

Table 4.2 Comparison of FVCOM result and observation for M2 amplitude and phase lag

	FVCOM	Observation	Difference (Δ)
Amplitude (m)	0.74	0.72	0.02
Phase lag (degree)	256.8	258.0	-1.2

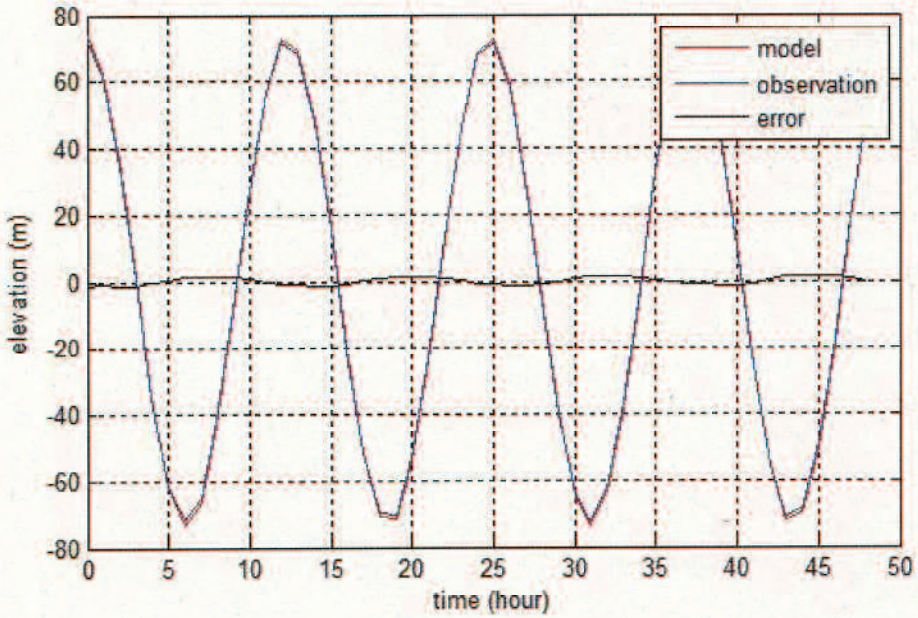

Figure 4.6 Verification of the tidal height

4.2 M2 Tidal Current and M2 Tidal Residual Current

4.2.1 The comparison of M2 tidal current mechanism

The M2 tidal current mechanism in the surface layer for the case of the present configuration, the past configurations, and modification of present configuration (remove the road connecting the Benoa harbor and main island) are shown in the figure 4.7. Case 1 means the present configuration. The original configuration of Serangan island (before reclamation) with the Benoa harbor is called case2, the original

configuration of Serangan island (before reclamation) without the Benoa harbor is called case 3, and changes of present configuration is called case 4.

For case 1, the seawater only has one channel between Serangan Island and Benoa peninsula. Seawater could not be able to exchange in the northern channel causes by the bridge connected the main island with the Serangan island after reclamation. This configuration has blocked the water in the former northern channel from the outer of bay to enter into the inner of bay, and water from the inner of bay into the outer of bay.

In case 2, the water flow is divided into two routes, to the northern channel (between Serangan and the main island) and to the southern channel (between Serangan and Benoa Peninsula).Relatively strong current is occurred in both channels, where the maximum tidal current was 0.45 m/s during ebb tide and 0.3 m/s during flood tide.

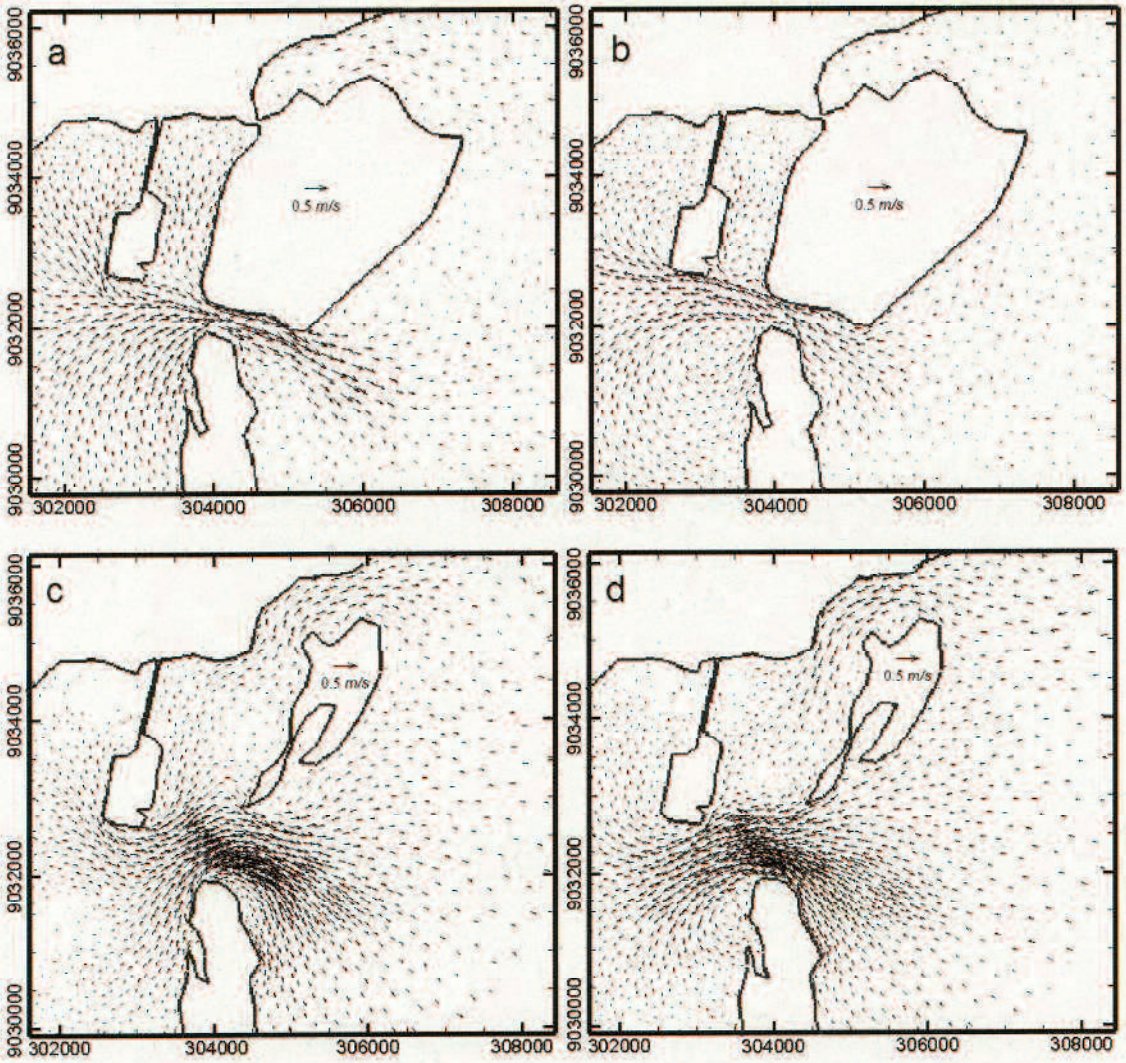

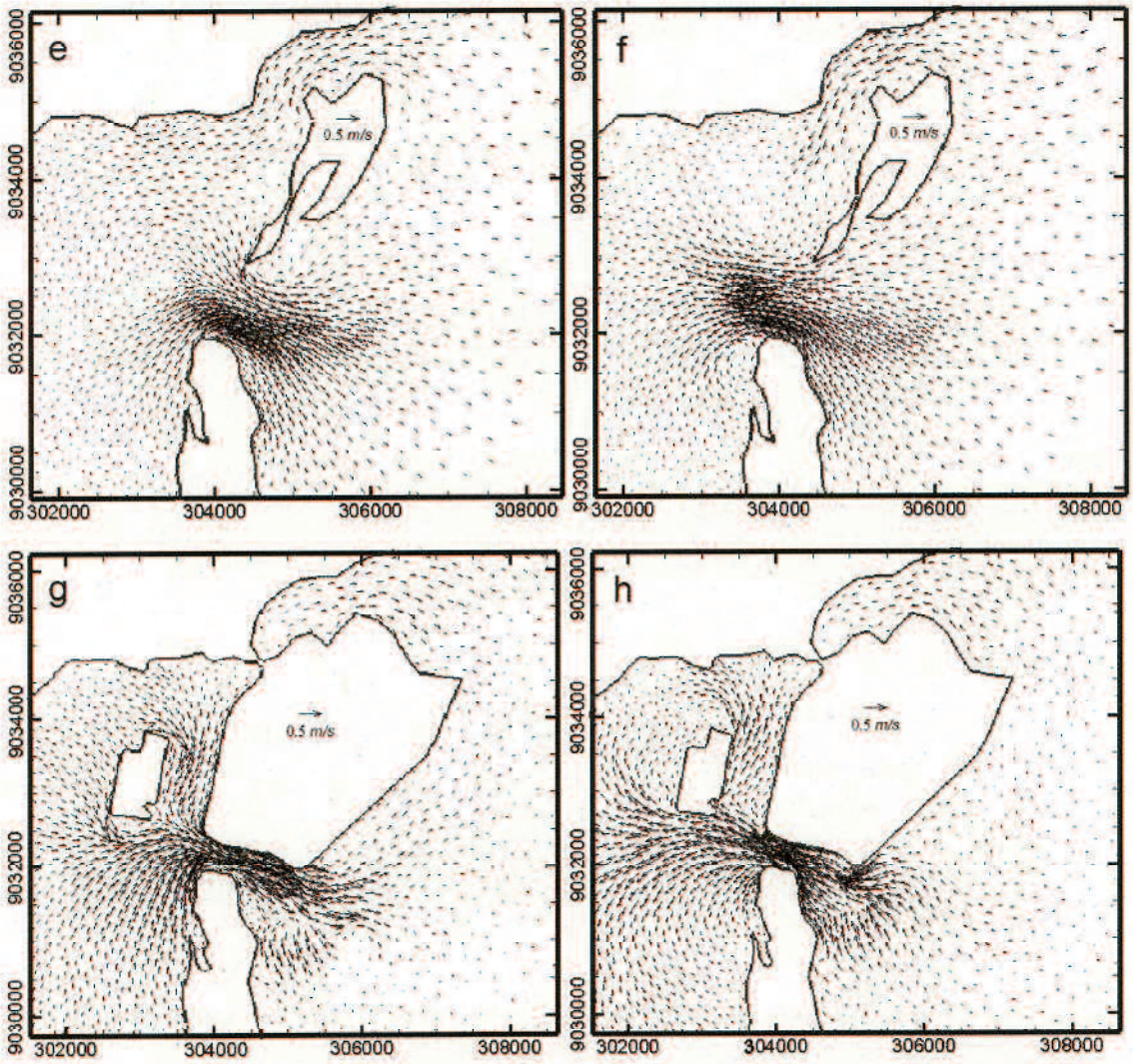

Figure 4.7 Tidal current pattern of Benoa bay in the present, past configuration, and modifed of present configuration for the surface layer; a-b) is case 1, c-d) is case 2, e-f) is case 3, and g-h) is case 4, vector unit are in m/s

Similar mechanism occurs in case 3. It can be seen that there are two routes as in case 2. The seawater is flowing clearly from two channels without any blocking at the bay. It could be a good condition for the water flushing from the inner bay to the outer bay. A good circulation of seawater from the outer bay to the inner bay will influence for the nutrient transportation from the deeper water in the outer bay as a food for the number of organism in the mangrove area. The maximum of M2 tidal current for the original condition is 0.4 m/s during ebb tide, and 0.3 m/s during flood tide.

The seawater circulation mechanism after a change on present configuration was made (case 4), are shown in the Figure 4.7 (g,h). It shows that seawater from the

western part of bay could flow to the outer part of bay from the new channel in the southern part of bay (located between Benoa harbor and the main island) during ebb tide. A similar pattern are also revealed during flood tide; which aside from the seawater that flows directly to the western part of bay; passing through southern part of bay, the seawater also flow to the western part of bay; passing through eastern part of bay. This configuration could give better circulation compared to the present configuration (case 1). The maximum M2 tidal current for case 4 is 0.66 m/s during ebb tide and 0.6 m/s during flood tide.

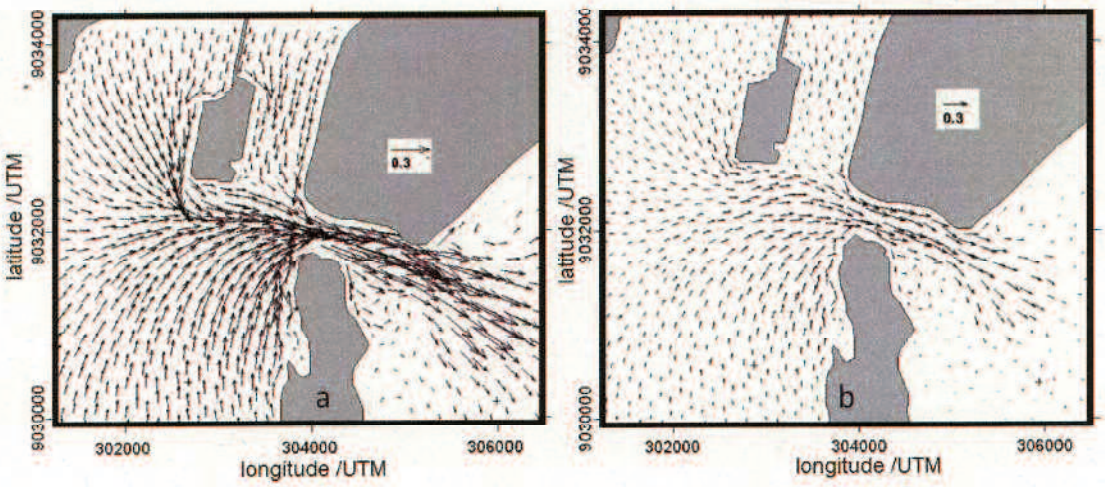

Figure 4.8 Tidal current for the present configuration of Benoa bay at ebb tide; a) surface, b) near bottom layer. the vector unit are in m/s.

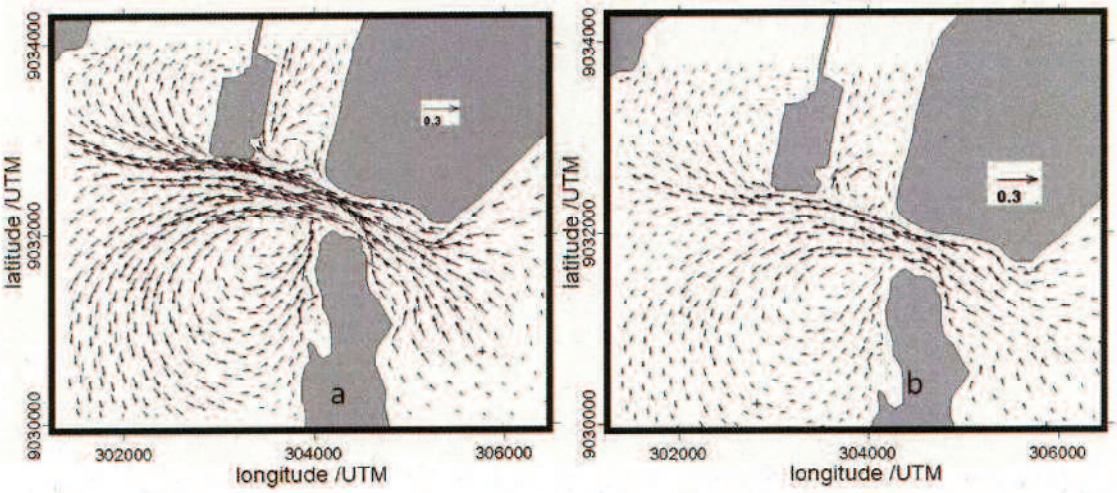

Figure 4.9 Tidal current for the present configuration of Benoa bay at flood tide; a) surface, b) near bottom layer .the vector unit are in m/s.

Figure 4.8 and Figure 4.9 show the tidal current for the present configuration of Benoa bay at the ebb tide and flood tide, respectively. The different mechanism occurred for the existing configuration compared with the past and changes on present configurations. The seawater flow only has one channel, the southern channel with narrower channel. During the ebb tide, the seawater flows out from the inner bay into the ocean. The narrow strait between Serangan island and Benoa Peninsula causes an increase in M2 tidal current. At the narrow strait in the bay mouth, the M2 tidal current reached 0.46 m/s at the surface layer and decreased due to the increased water depth. The maximum of the tidal current was 0.29 m/s near the bottom. In the Northern part of Serangan as well, the tidal current was slightly high which could be caused by the effect of narrow channel formed in that area. During the flood tide, the seawater flows into the bay and developed a small eddy in the surrounding of Western part of Benoa Peninsula. This could occur due to the geometric condition of model area. During flood tide, the M2 tidal current reached 0.31 m/s in the surface layer and 0.19 m/s in the nearest bottom layer. This tidal current is lower than ebb tide condition.

4.2.2. M2 Residual current

The tidal residual current is well defined in a number of papers (Imasato, 1983; Awaji, 1980). In this paper the M2 tidal residual current defined by Eq (4.4) (Imasato, 1983).

$$U_r(x,y) = \frac{1}{T}\int_0^T u(x,y,t)dt \qquad (4.4)$$

Where U_r is the residual current, T is the tidal period, and $u(x,y,t)$ is the velocity for x and y direction at time t.

The tidal residual current patterns for four cases in Benoa bay are shown on figure 4.10. Case 1 has the weakest tidal residual current compared to the three other cases, and in the inner bay part, the vector direction are tend to went onto the inner bay. In case 2, two eddies are formed in the inner bay, and one strongest eddy directed to the outer bay is formed in the bay mouth. This outward direction of residual current in the bay mouth will give better chance for the particle to move onto the outer bay. Similar pattern is also appeared in case 3, where particles in the inner bay could be easily transported for case 3 and case 2 compared to case 1. After making changes for case 1

to become case 4, strong outward of tidal residual current appeared in the outer bay, and the eddies also formed in the inner bay and the northern channel between Benoa harbor and the main island. Maximum tidal residual current for the case 1, case 2, case 3, and case 4 are 0.097 m/s, 0.12 m/s, 0.13 m/s, and 0.15 m/s respectively.

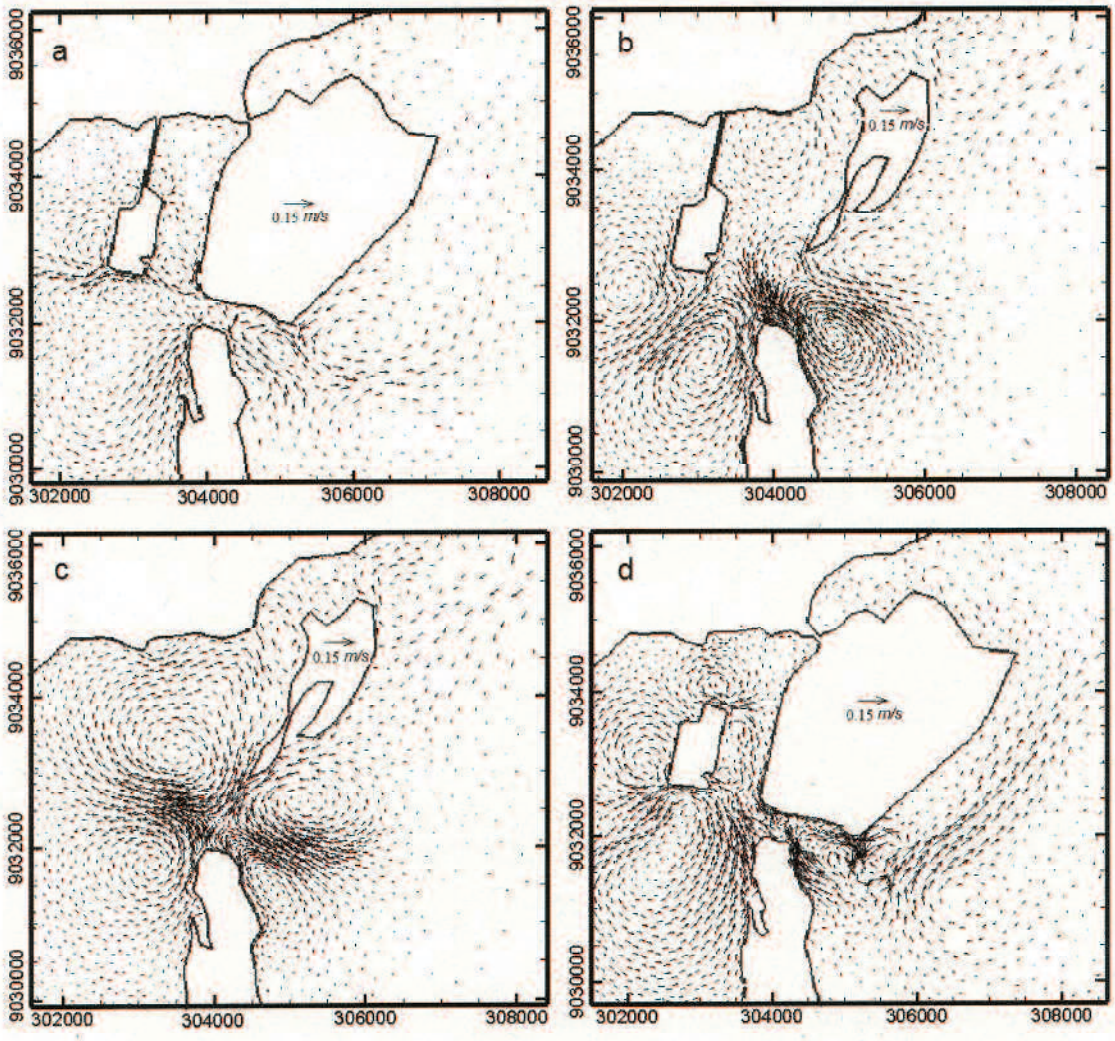

Figure 4.10 Surface tidal residual current; a) case 1, b) case 2, c) case 3, and d) case 4. The vector unit are in m/s.

The weak M2 tidal residual current was revealed in the existing condition of Benoa Bay as shown in Figure 4.11. The maximum velocity of the residual current occurring in narrow strait of bay mouth was 0.097m/s for surface layer and 0.059m/s for the nearest bottom layer. Despite the weakness of tidal residual current, it could play a dominant role in the distribution of passive contaminants in the ocean (Yasuda, 1980).

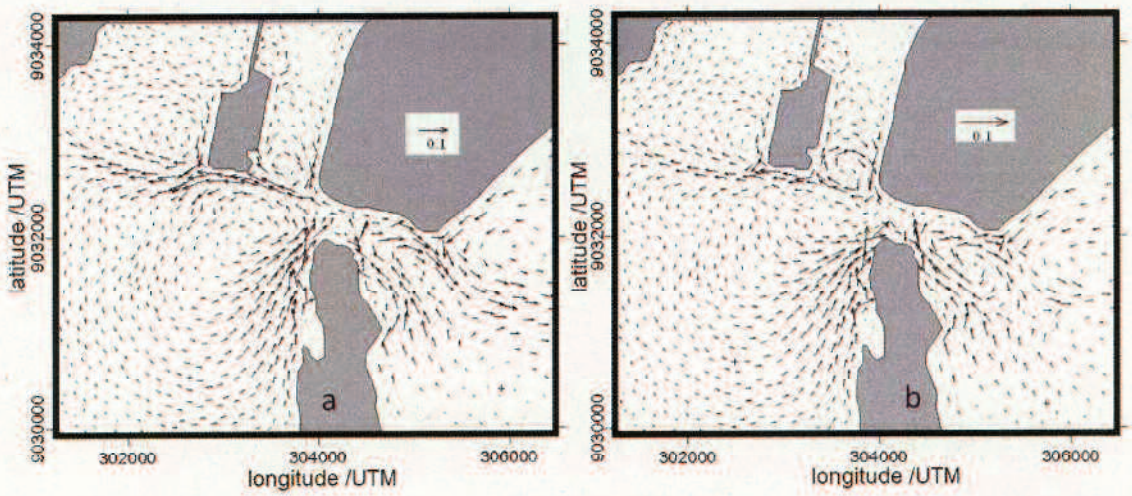

Figure 4.11 Tidal residual current of present configuration; a) surface, b) near bottom layer. The vector unit are in m/s.

Two small eddies within the bay and one small eddy in bay mouth can be seen. These tidal residual circulations are caused by non-linearity, due to the coastal geometry formed by narrow strait in the bay mouth and the bottom topography (Yanagi, 1976; Zhou, 2012). Along the central region of the bay until the bay mouth, the tidal residual currents are slightly higher and had more complicated stream systems than other regions, because the central region of the bay would be the crossing area to the three-stream regions which are the Southern part of bay, Western part of the Benoa Harbor and Eastern part of the Benoa Harbor. The tidal residual current is also obviously influenced by the bottom topography, in which the tidal residual current in the surface layer is relatively higher than in the bottom layer (Yanagi, 1976).The river discharge into the inner of Benoa bay could also influence the tidal residual current as italso suggested by Zhou (2012).

4.3 Salinity distribution for The Existing Condition

Figure 4.12 shows the salinity distribution after 60 days of river discharges. Low salinity appeared in the inner of bay and in Northern part of Serangan island. During ebb tide, the low salinity water in the inner bay is distributed toward the bay mouth. Otherwise, during flood tide, the higher salinity from the Ocean flowed into the bay. It implied that the salinity in the inner bay increased.

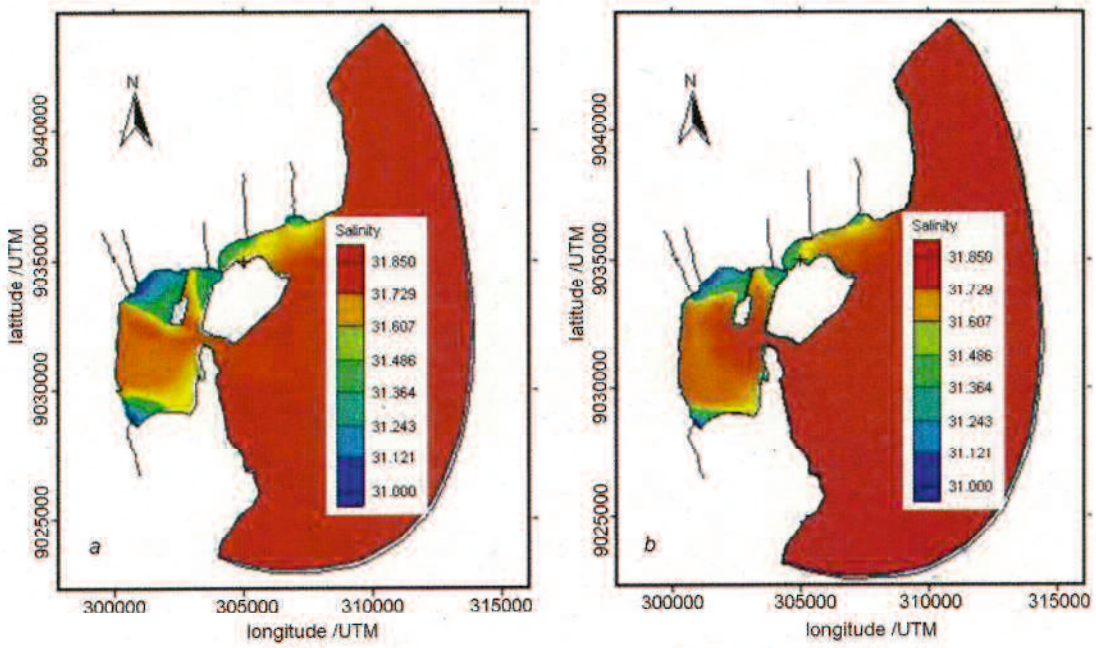

Figure 4.12 Salinity distribution; a) ebb tide, b) flood tide

Figure 4.14 shows the vertical profile of salinity during ebb tide along the cross section that is indicated by straight black line in horizontal topographical figure in the inset figure. It was depicted clearly that the salinity is not well-mixed vertically, especially in the inner bay, whereas a well-mixed vertical distribution can be seen in the outer bay. The vertical salinity distribution at the inner bay showed low concentration in the surface layer (dash circle line in the Figure 4.14a) during the ebb tide. At the same time, relatively higher meridional current velocity component is indicated at the same location (dash circle line in the Figure 4.14c). This meridional current velocity component leads the transportation of fresher water from the Badung River and the MatiRiver to the inner bay. As the zonal current velocity component become weak and the meridional current velocity component become strong (dot circle line in the Figure 4.14b,c). The salinity concentration become high and mixed well in the outer bay (dot circle line in the Figure 4.14a). The weak zonal current velocity component at the outer bay (dot circle line in the Figure 4.14b) leads the low fresher water flowing out from the inner bay. Meanwhile, the strong meridional current velocity (dot circle line in the Figure 4.14c) induced higher seawater salinity transported from the Badung Strait to the outer bay, which lead a well-mixed vertically distribution. The fluctuation of current velocity changes with the time since the meteorological and fresh water inflow also

varies with the time (Lu et al, 2012; Lu et al, 2011). This model indicated that the river discharges into the inner bay do not have a significant influence on seawater salinity in the outer bay.

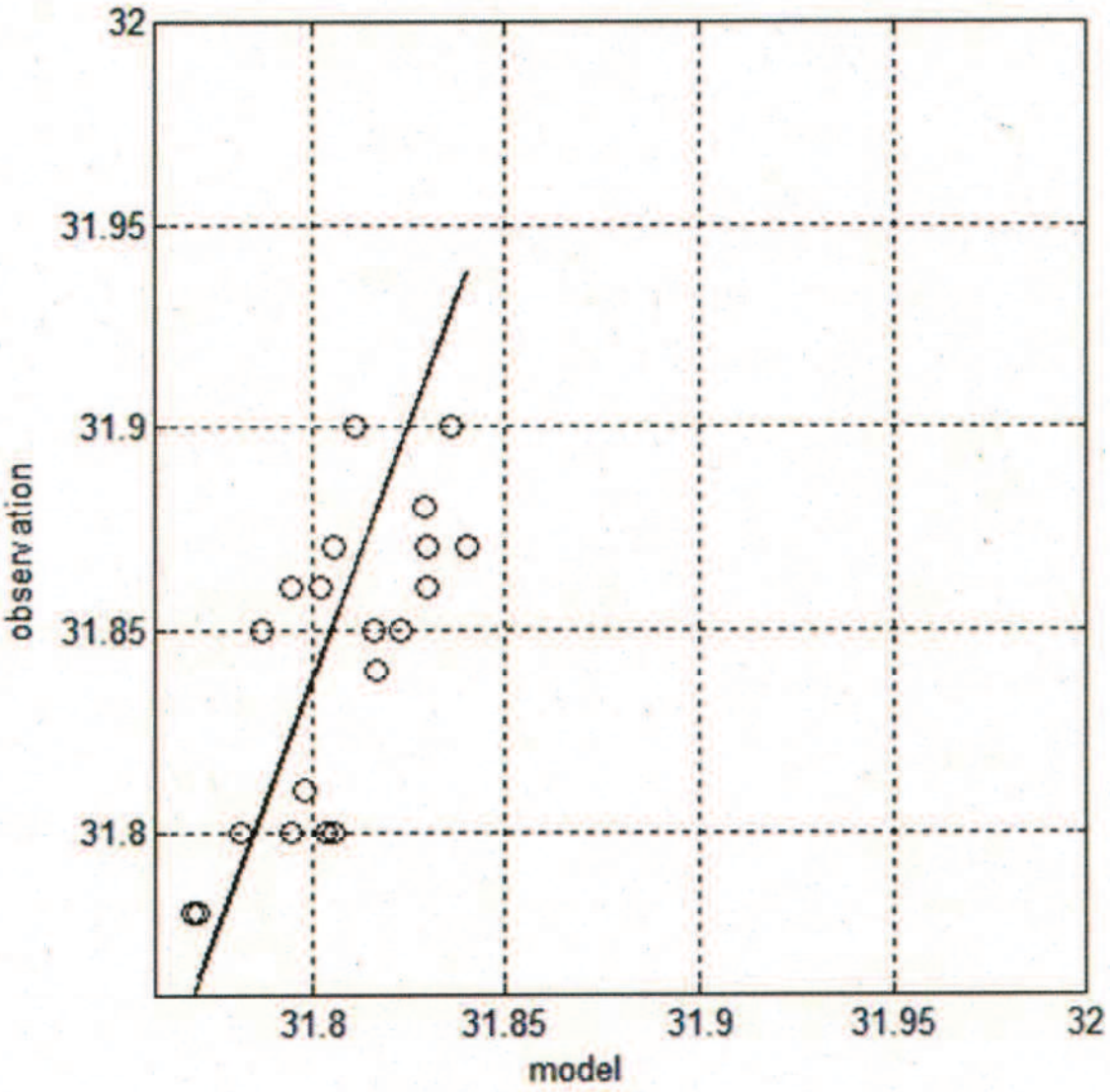

Figure 4.13 Validity of Salinity distribution

The relationship of numerical calculation and observation results for salinity are shown in Figure 4.13. The correlation determination (r^2) given by FVCOM is 0.75. This indicates that the numerical model has a good ability for salinity calculation including fresh water discharges. Salinity discrepancy between the observation and the model caused by spatially salinity distribution in the inner bay was significantly caused only by rivers discharge of the model, while the observation are climatologically considered.

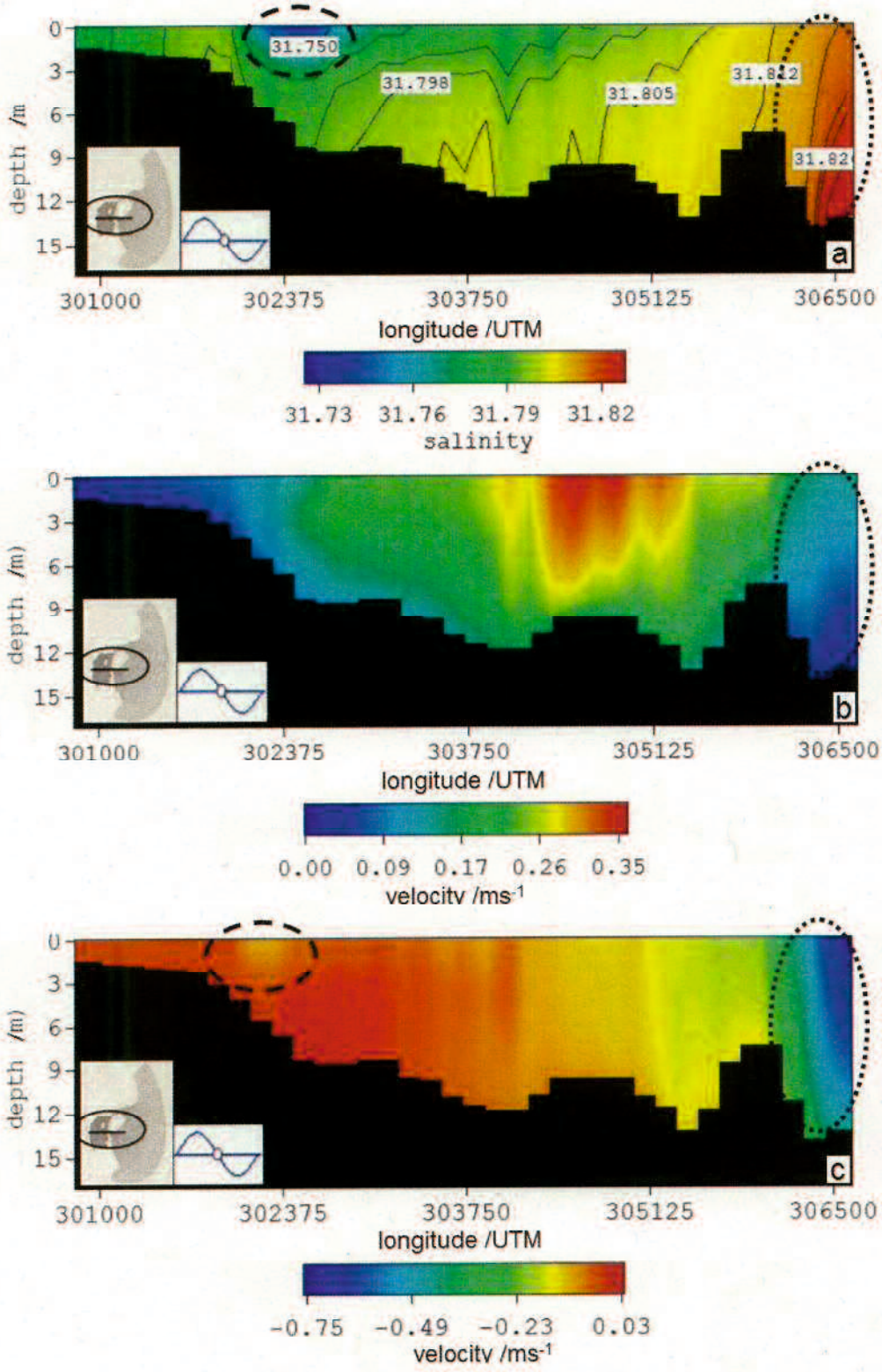

Figure 4.14 Vertical profile of a) salinity distribution, b) zonal (u) current component, c) meridional (v) current component along the cross section, the inset picture in the left is the location of cross section, and the inset picture in the right is the tidal condition for the cross section.

4.4 Seawater Exchange

In order to investigate the seawater exchange in the Benoa Bay, 3-D Lagrangian particle tracking is used. The neutral buoyant particles are released at surface layer. Initially, 144 particles are released uniformly at the maximum flood tide after model calculation become stable. The particles position is calculated over the length of model time step and recorded at 60 min interval. Furthermore, the fraction of particle is calculated based on the particles number and the percentage of particles movement are calculated at a specific time. The particles reaching the bottom are treated to be trapped at the bottom, i.e., the reflection at the bottom is not considered.

4.4.1 The comparison of particle transport mechanism

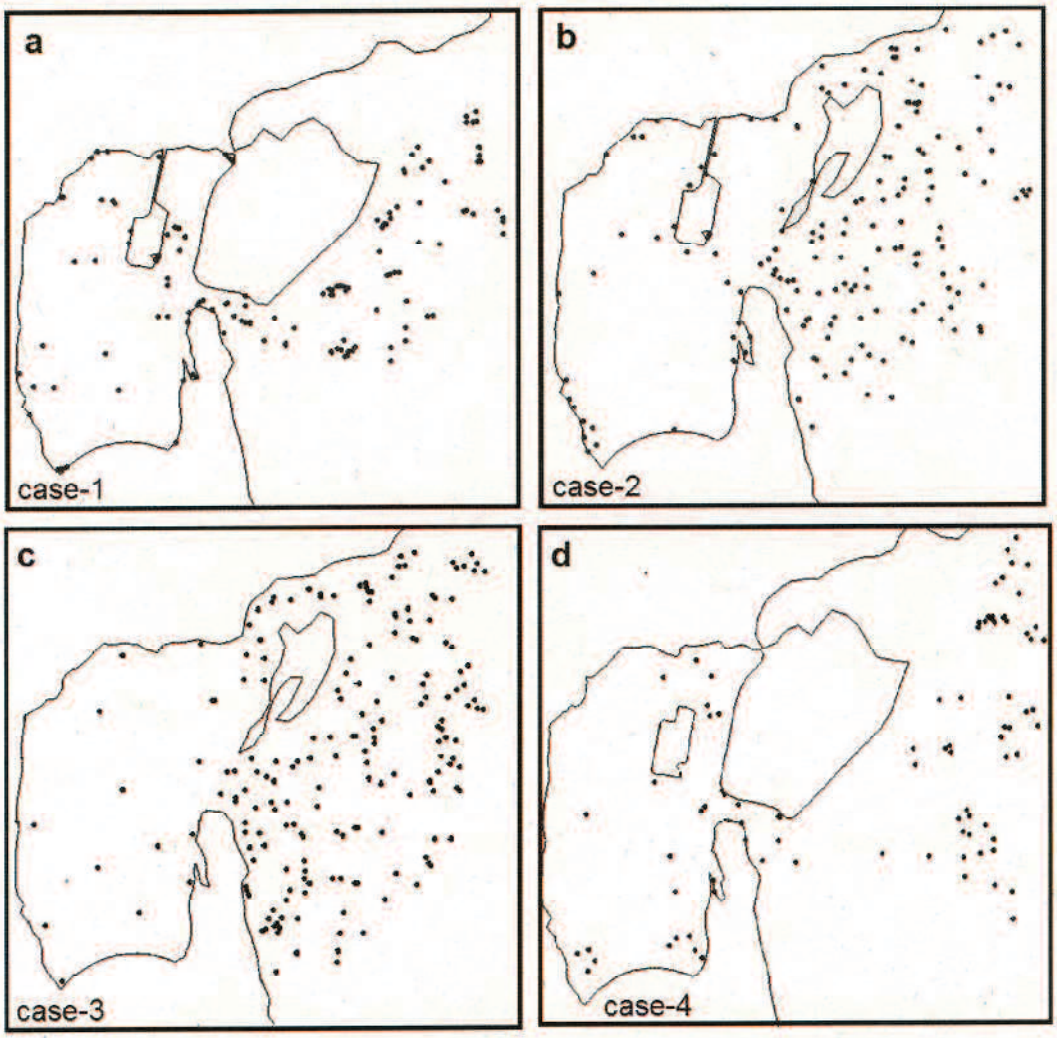

Figure 4.15. Particle transport at 10th tidal cycles; a) case 1, b) case 2, c) case 3, and d) case 4.

Figure 4.15 shows the particles position for model ran at 10th tidal cycles. It is shown in the case-1 the particles in the inner of bay were much more than the other three cases. However after modification of case-1 become case-4, the number of particles in the inner of bay seen much less than compare than case-1. The past configuration, case-2 and case-3 are also shows the number of particle within the Benoa bay are smaller than the present configuration (case-1). It could be explaining by the M2 tidal residual current pattern that can be shown in the previous chapter (chapter 4.2.2).

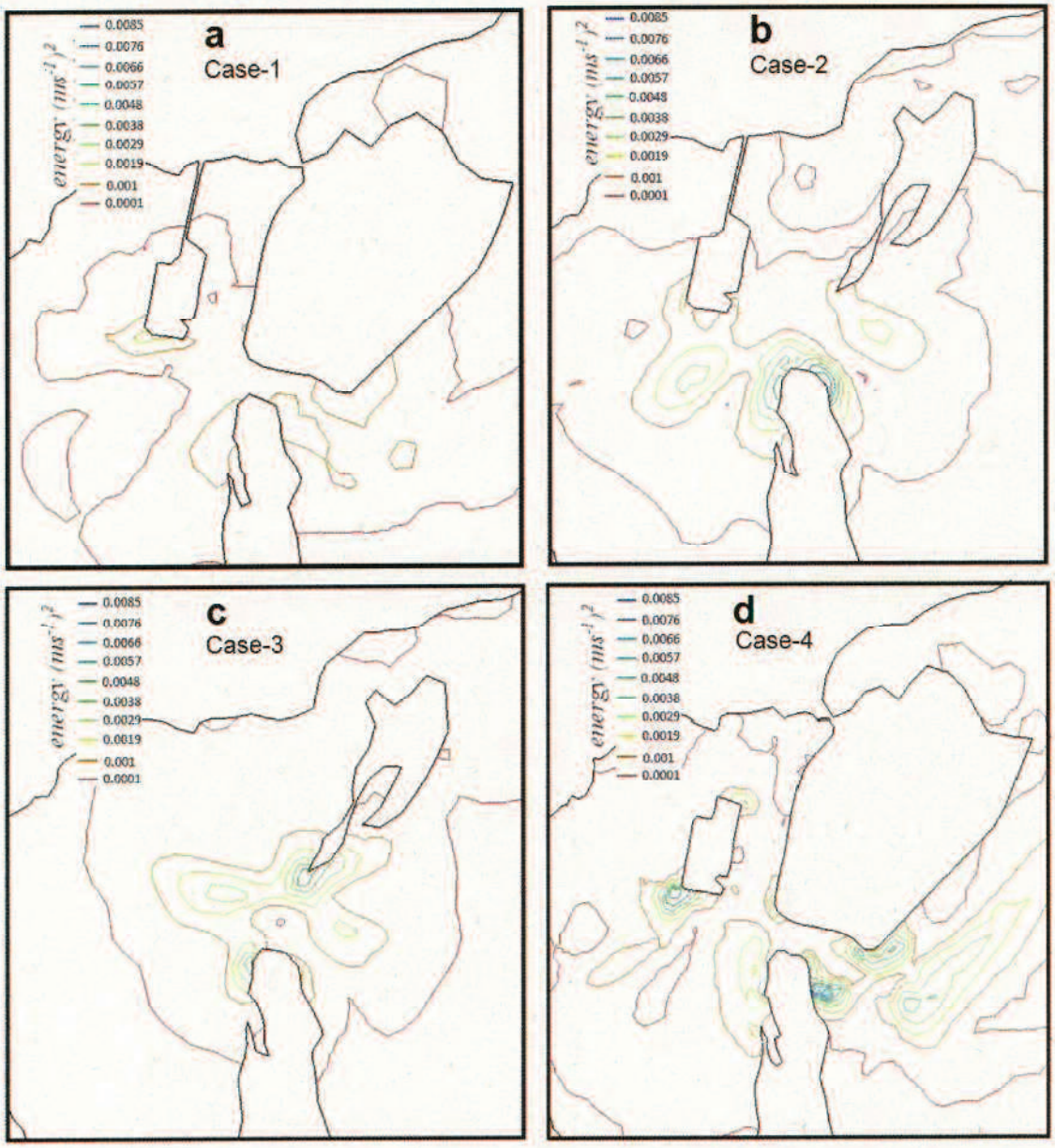

Figure 4.16 Energy of the tidal residual current; a) case 1, b) case 2, c) case 3, and d) case 4.

The comparison of four cases of energy on residual tidal current is shown by figure 4.16. From those figures, it is shown that case 1 has the weakest energy on residual tidal current compared to the other three cases. In case 2, the strongest energy is revealed in the inner bay and in the tip of Benoa peninsula. For case 3, the highest energy is mostly revealed in the bay mouth, and for case 4, the highest energy is revealed in the bay mouth and in the outer bay. From these results, changes of present configuration had presented better condition for the water circulation compared to the present configuration of Benoa bay.

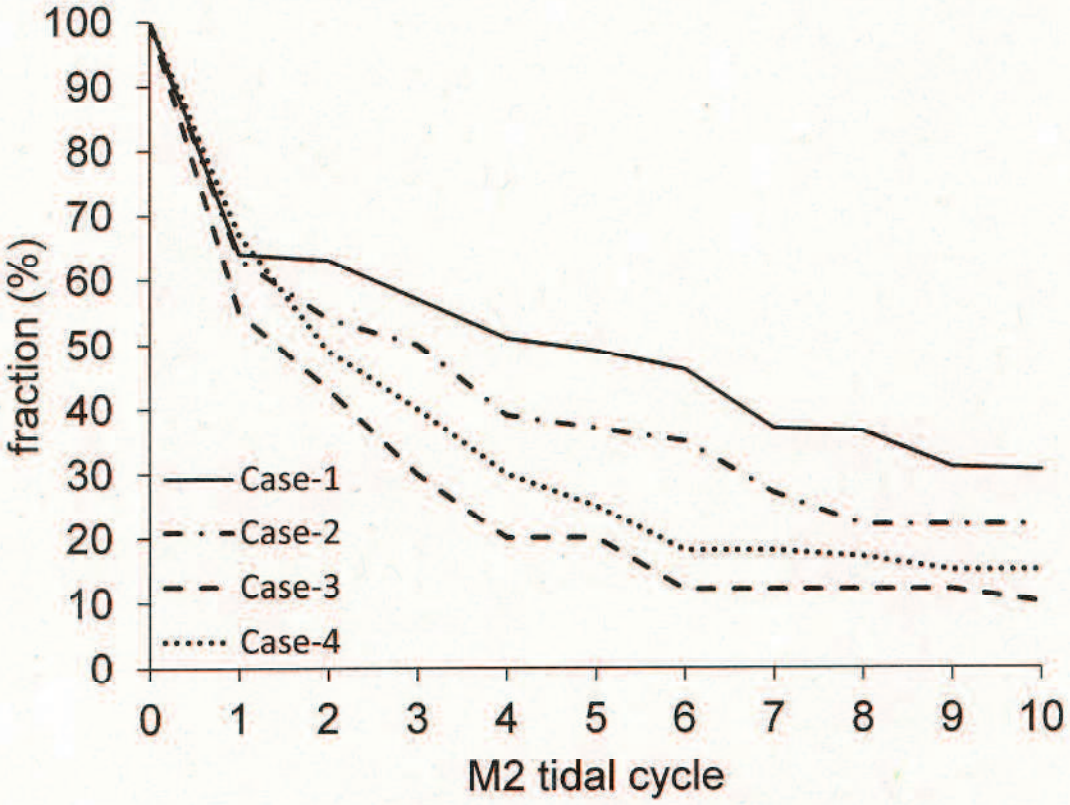

Figure 4.17 Overall particles remaining inside of bay

The overall of seawater exchange for the existing Benoa bay configuration can be seen in Figure 4.17.

In case 1, the particles are transported rapidly to the ocean. 37% of particles are exported to the ocean immediately after they are released. Furthermore, 50% of the particles are exported to the ocean after four tidal cycles and increased 70% after nine tidal cycles. Based on the exponential decay equation of the particle movement, more

than 95% of particles predicted will be exported to the outer sea after 30 tidal cycles. It means that the particles initially laid down within the bay will be nearly completely transported to the ocean after one month.

We can see the difference mechanism in case 3. The particles shortly move into the outer sea. It takes only four tidal cycles to exported 80% particles from the inner of bay to the ocean, and the particles remain are only 10% after 10 tidal cycle.

In case 2, the particle movement is slower than case 3, but faster than case 1. The particles take eight tidal cycles to export 80% particles to the ocean and 20% particles remain within the inner bay after ten tidal cycles. As a result of this simulation, it is found that the construction of Benoa harbor and reclamation of Serangan island affect the seawater exchange in the Benoa bay significantly. The change of configuration of the bay makes it difficult for the particles to move to the outer bay, so if Benoa bay receives pollutants from the river discharge or other activity in the inner of bay, the contaminated water is hardly exchanged with outer sea and the water quality becomes worth.

In case 4, after changes were made, present condition shaped with no bridge connecting the harbor to the main island, where particle that moved to the outer bay is better than that in case 1 and case 2. This is clearly shown from the sea water circulation and the tidal residual current pattern above. The particles are exported 30% after it released, and more than 80% particles are transported to the outer bay after 6 tidal cycles. This case can give better seawater exchange compared to case 1 and case 2.

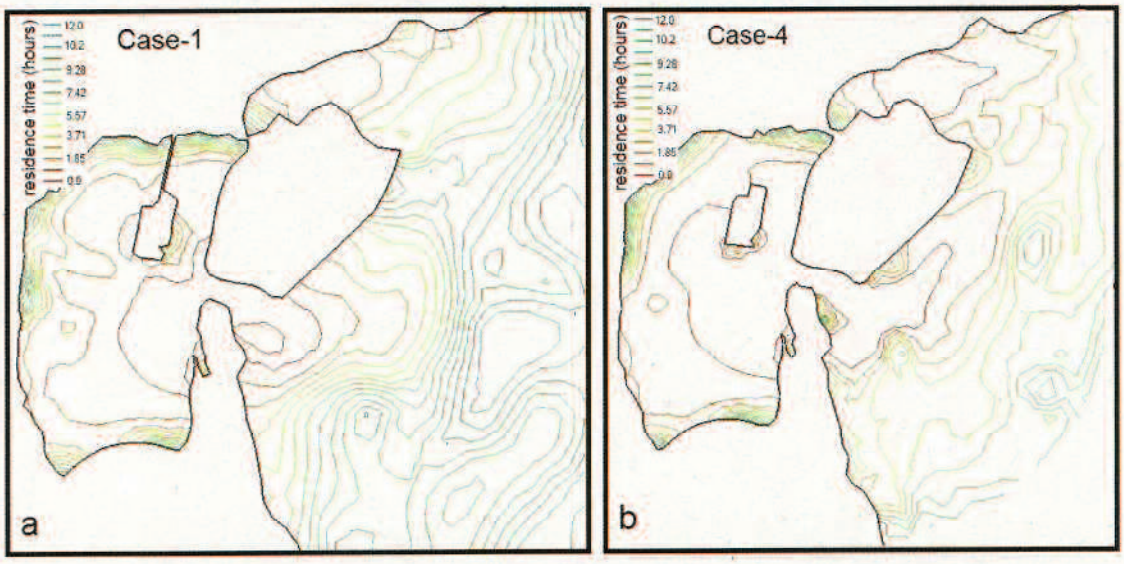

Figure 4.18 Residence time of; a) Case-1, and b) Case-4

Another way to investigate the seawater exchange in Benoa Bay is by calculating the residence time. The residence time of particles could be known by seeing how long particles reside in a specific area that was about to be flushed. In this study, we used a 300 m x 300 m moving box to estimate the residence time (Bilgili et al, 2005). Figure 4.18 shows the time particles spend in these box regions as a function of their initial conditions.

For the case-1 (Fig. 18a), the particles spend one to five hours in the inner of bay, and particles spend more than five hours in the edge of the bay, especially in the southeastern edge, southwestern edge, western edge, and northeastern edge of bay. In the bay mouth and outer of bay, the particles have a shorter residence time, it spend about one to two hours. Waters that surround bay mouth, such as the south edge of eastern part region, the east edge of southern part region and a few areas in the western part region (red color), have a shorter residence time. For the case-4 (Fig. 18b), the particles spend one to three hours in almost of the inner bay. The particles spend more than three hours in the small area within the bay, especially in the southeastern edge, southwestern edge, western edge, and northeastern edge of bay. In the bay mouth to the outer bay and extending to the northeast area the particles have a shorter residence time.; which corresponds to a relatively high energy of tidal residual current. The Figure 4.18 has give a good impression in residence time for the case on modification configuration of present condition. The faster residence time are revealed after removing a road connecting the harbor with main Bali island.

4.4.2 The particle transport mechanism of existing condition

Figure 4.19 depicts the particles remaining at each region in the bay in case 1. As shown in the western part region (black dot-line) and the central part region (green dot-line), the particles are transported rather rapidly to another region than in the eastern part region (blue dot-line) and southern part region (red dot-line). In the western part region, more than 90% of the particles are transported after four tidal cycles and after two tidal cycles for the central part region. However, the particles in the southern part region are transported rather slowly than in both of the previously mentioned regions. More than 90% of the particles are exported to another region after nine tidal cycles. In

the eastern part region, the particles were transported very slowly than in other regions. It takes more than ten tidal cycles to transport the particles into other regions.

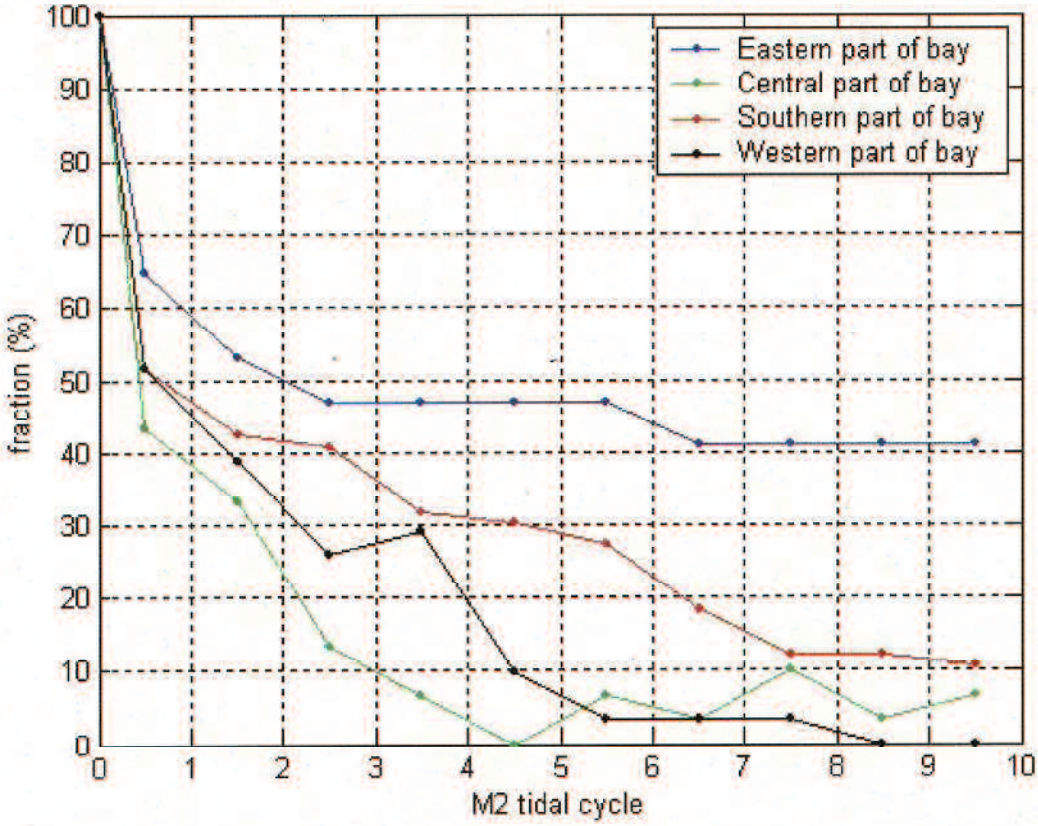

Figure 4.19 Particle remaining in each model region

Figure 4.20 shows the particles transport for each model regions. In western part region (the upper-left frame), about 40% of the particles initially in western part region are transported to the ocean after nine tidal cycles, while more than 40% of the particles are transported to the central region just after particles are released. However, after three tidal cycles it decreased to 20% and increased to 40% after nine tidal cycles. The particles from the western part region were also connected with those in the southern part region. The southern part region received particles from western part region after one tidal cycle and increased to 40% after four tidal cycles. Some particles from the western part region are transported directly to the ocean that is connected by the central region, while some particles are transported to the southern part region first before finally transported into the ocean.

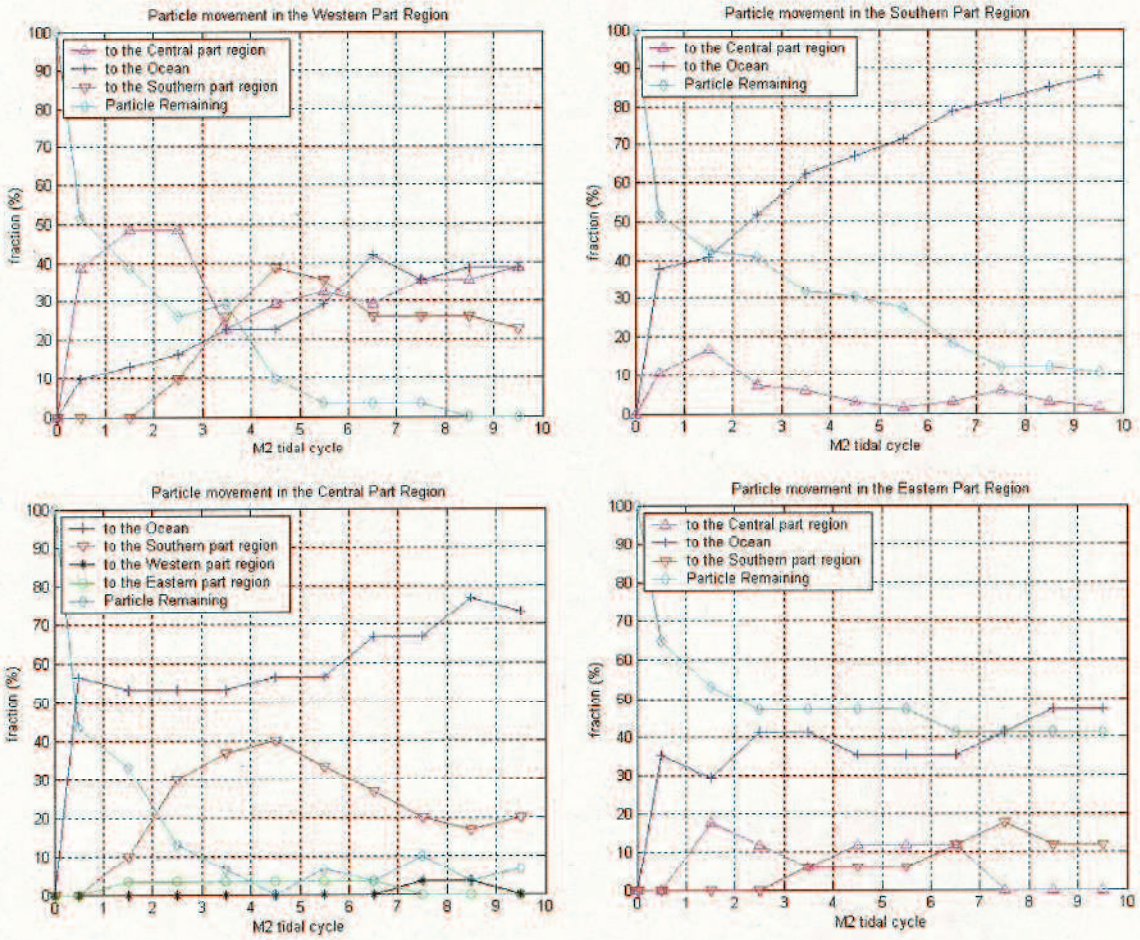

Figure 4.20 Particles transport characteristics in each region

As shown in the southern part of the bay (the upper-right frame), more than 80% of the particles are transported to the ocean and less than 20% of the particles remained in the central part of the bay during nine tidal cycles. The particles from the Southern part region are not connected with those in the western region and the eastern region. It seems that the particles are directly transported from the southern region into the central part of the bay and transported to the ocean (Figure 4.21).

The particles in the eastern part region (the lower-right frame), roughly more than 30%, are transported into the ocean immediately after the particles are released, and increased nearly 50% after nine tidal cycles. The particles from this region are also related to those in the southern part region. More than 10% of the particles are transported after four tidal cycles. The eastern part region trapped 40% of the particles after sixth tidal cycle. This gives an impression that the particles cannot be transported to another region in the model domain. This is the result obtained by investigating the

residual current pattern. It suggests that the residual current in the eastern part region went to the north. Additionally, the tidal current in bay mouth strongly flowed to the west-east direction. Therefore, it will be difficult to exchange the seawater in this region to other regions.

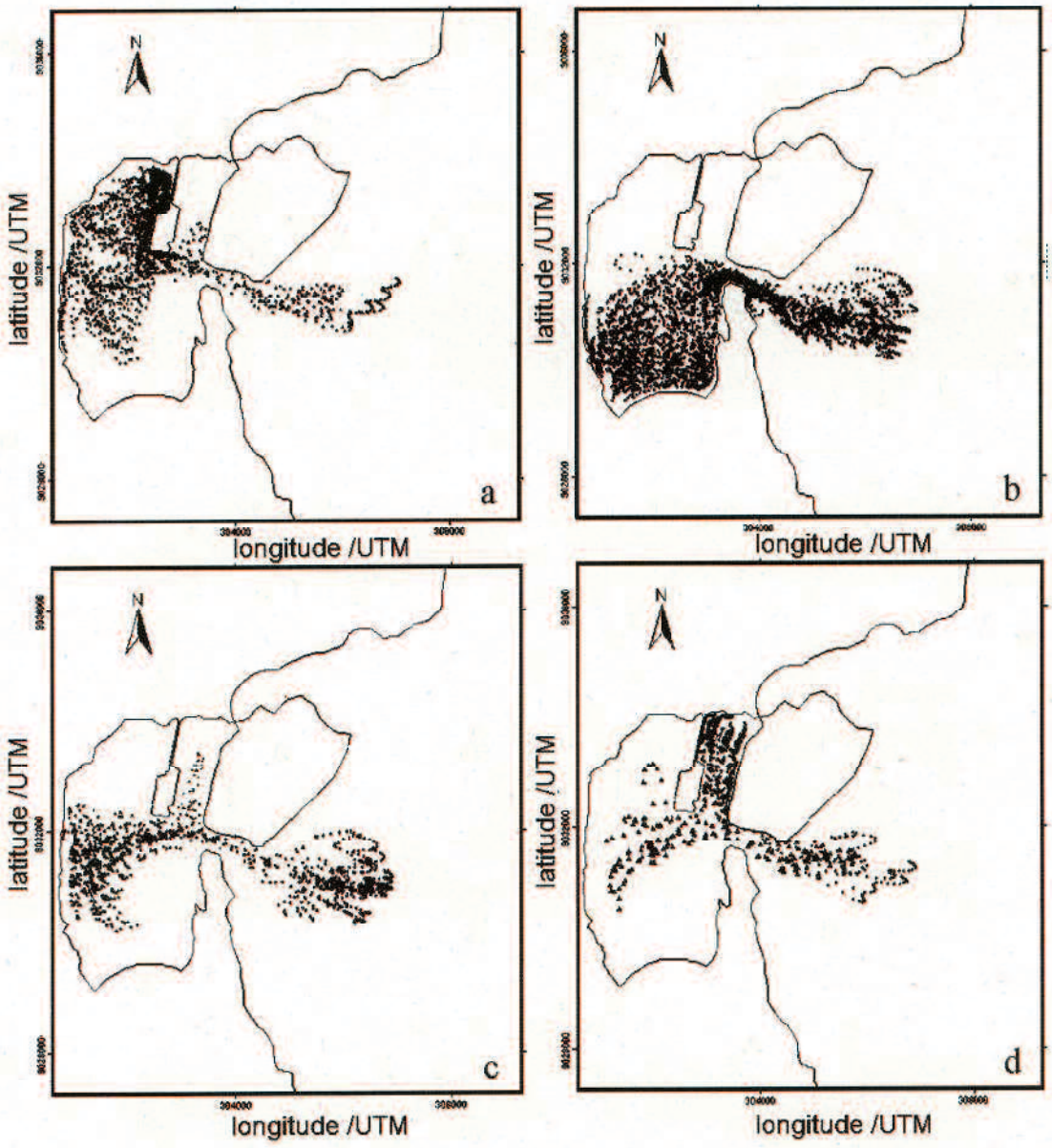

Figure 4.21 Particle tracking, a) Western part region, b) Southern part region, c) Central part region, d) Eastern part region

Finally, more than 50% of particles are directly transported from the central part of the bay (the lower-left frame) into the ocean immediately after the particles are released and increase to above 70% after eight tidal cycles. Some particles are also

transported into the southern part region, which more than 20% transported after two tidal cycles. It is obvious that the increasing particles transported to the ocean will be accompanied by decreasing particles transported to the southern part region. A few particles are also transported to the western part and the eastern part region.

In the Figure 4.20 revealed the general characteristics of the seawater exchange in Benoa bay. In general, the fraction of particles has two ways to find the gate into the ocean. In the first way, the particles are directly transported into the ocean from each region, and in the other way the particles transported to the southern part of the bay and then exported to the ocean (Figure 4.21). However, the particles in the eastern part of the bay are not transported into the ocean easily compared with other regions. This could be caused by the residual current (Zhou, 2012). The residual circulation near the open boundary of the eastern part of the bay can be seen in Figure 4.11. The particles in the eastern part would be trapped by this circulation. This is the reason why the particles cannot move to the ocean easily.

5. Summary

The M2 tidal current patterns are clearly depicted by the numerical calculation with FVCOM. The past configurations of Benoa bay show the seawater has two channels to flow from inner or outer bay, they are northern and southern channel. The two channels would make the seawater flow easier to bring the water mass from the inner of bay to the outer of bay. The past configurations of Benoa bay without the harbor and with the harbor have a maximum M2 tidal current during ebb tide 0.4 m/s and 0.45 m/s respectively. The significant change of M2 tidal current mechanism occurred for the existing configuration. The seawater only has one channel to flow from the outer or from the inner of bay with the narrower channel. The narrower channel has increased the maximum M2 tidal current during ebb tide and reached 0.48m/s. After present configuration changed, the seawater could flow from the northern channel of Benoa harbor and the main island to outer (inner) bay during ebb (flood) tide, and the tidal current increase in the bay mouth has become 0.66 m/s during ebb tide.

A weak M2 tidal residual current is revealed in whole model domain for the existing configuration of Benoa bay. However, M2 tidal residual current are stronger in the past configuration of Benoa bay. Changes of present configuration on Benoa bay

could also change M2 tidal residual current, which is better than the present configuration.

The characteristics of the seawater exchange are clearly depicted by using Lagrangian particle method. The particle transport has a different mechanism for the four cases. The original configuration of Benoa bay, i.e., case 3 could transport 80% particle from the inner of bay to the outer of bay only bay four M2 tidal cycles. However, the particles only exported 60% and 50% for the case of Benoa bay with case 1 and case2. After changes for present configuration (case 1) were made and turn it into case 4, the particles that could be exported are 80% into the outer bay by only six tidal cycles. It gives an impression that changes of present configuration would give better seawater exchange for Benoa bay, and will give more contribution for better condition of ecosystem in Benoa bay.

References

Awaji T, et al. 1980. Tidal exchange through a strait: A numerical experiment using a simple model basin. Journal Physical Oceanography, 10:1499-1508.

Bilgili A, et al. 2005. Estuary/Ocean Exchange and Tidal Mixing in Gulf of Maine estuary: A Langrangian Modeling Study, Estuarine. Coastal and Self science, 65: 607-624

Chen C, Liu H. 2003. An unstructured grid, finite-volume, three-dimensional, primitive equations ocean model: Application to coastal ocean and estuaries. Journal of Atmospheric and Oceanic Technology, 20: 159-186

Chen C, et al. 2006. An Unstructured Grid, Finite-Volume Coastal Ocean Model (FVCOM) user manual.

Chen C, et al. 2008. Physical mechanism for offshore detachment of the Changjiang diluted water in the east China Sea. Journal of Geophysical Research, 113: 1-17

Haidvogel DB, et al. 2000. Model evaluation experiments in the North Atlantic Basin: Simulation in nonlinear terrain-following coordinates. Dynamical Atmosphere and Ocean, 32: 239-281

Huang H, et al. 2008. A numerical study of tidal asymmetry in Okatee Creek, South Carolina. Estuarine, Coastal and Shelf Science, 78:190-202

Imasato N, et al. 1980. Tidal Exchange through Naruto, Akashi and Kitan Straits. Journal of the Oceanographical Society of Japan, 36:151-162

Lu S, et al. 2012. Upper ocean near-inertial response to 1998 Typhoon Faith in the South China Sea, ActaOceanologicaSinica, 31: 25-32

Lu S, et al. 2011. A case study of near-inertial oscillation in the South China Sea using mooring observations and satellite altimeter data, Journal of Oceanography, 67:677-687

Marshall J, et al. 1997 .A finite-volume, incompressible Navier-Stokes model for studies of the ocean on parallel computers. Journal of Geophysical Research, 102: 5753-5766.

Matsumoto K, et al. 1995. Ocean tide model obtained from TOPEX/POSEIDON altimetry data, Journal of Geophysical Research, 100:25319-25330

Yanagi T. 1976. Fundamental study on the tidal residual current-I, Journal of the Oceanographical Society of Japan, 32:199-208

Yasuda H. 1980 .Generating Mechanism of the Tidal Residual Current due to the Coastal Boundary layer. Journal of the Oceanographical Society of Japan, 35: 241-252

Zhou W, et al. 2012. Saltwater intrusion in the Pearl River Estuary during winter, Aquatic Ecosystem Health & Management Volume: 15: 70-80

CHAPTER 5
CONCLUSIONS

1. Conclusions

This study was conducted to detect the characteristics of the tidal currents in Benoa bay and Lombok strait. It is found that in relation to the rough bottom topography, the tidal current has an ability to produce an upwelling and downwelling mechanism in the Lombok strait, especially at the top of Lombok sill. The upwelling mechanism in the Lombok strait can be important information for the fishery point of view. The upwelling occurred in the Lombok strait would bring the high nutrient from the deeper water to the surface. This high nutrient area can serve as good places for fishery. In addition, the tidal upwelling in the Lombok strait brings the cooler water from the deeper water to the surface. This cool water reduces the evaporation, and it could impact the local weather/climate.

The tidal current patterns and the water exchange abilities of Benoa bay were investigated. The tidal current pattern in the Benoa bay depends on the configuration of the bay. The current patterns between the original configuration of Serangan with the Benoa harbor (case 2) and without the Benoa harbor (case 3) are quite different, though there are two routes to sea water flow, which are the northern channel and the southern channel. The maximum tidal currents during ebb tide are 0.45 m/s and 0.4 m/s in case 2 and case 3, respectively. The significant change of M2 tidal current mechanism can be seen in the existing configuration. The seawater only has one channel to flow from the outer or from the inner of bay with the narrower channel. The narrower channel enhanced the maximum M2 tidal current during ebb tide. It reached 0.48m/s. After present configuration changed, the seawater could flow from the northern channel of Benoa harbor and the main Bali island to outer (inner) bay during ebb (flood) tide, and the tidal current increase in the bay mouth has become 0.66 m/s during ebb tide.

For the overall of seawater exchange in case 1, the particles were exported 70% to the outer bay after nine tidal cycles. The difference of mechanism can be seen in case 3. The particles shortly moved to the outer bay for this case. It take only four tidal cycle for the particles to export 80% from the inner bay to the outer bay, and the particles

remain only 10% after 10 tidal cycles. The particle movement in case 2 is slower than that in case 3, but faster than that in the present configuration (case 1). The particles take eight tidal cycles for the particles to export 80% to the outer bay and the particles remain 20% particles within the inner bay after ten tidal cycles. After changes for present configuration (case 1) were made and turn it into case 4, the particles that could be exported are 80% into the outer bay by only six tidal cycles. The modification of present condition (case-4) is also generated shorter residence time in comparison with the present configuration (case-1), especially in the inner and outer of bay. It gives an impression that changes of present configuration would give better seawater exchange for Benoa bay, and will give more contribution for better condition of ecosystem in Benoa bay.

2. Future Study

In the present study, the model is restricted only used the tidal generated current and uniform of meteorological parameter. This is due to the lack of measurement data in Benoa bay. The possible improvement by using enough observation data involving in the model could bring the model nearer to reality. In the future, an attempt to collect observation data either spatial or temporal will clearly explains the characteristics of water circulation in the Benoa bay. Since Benoa bay is located in the tropical area, then the knowledge of temporal variability, seasonal or annual variability is important. On the other hand, In the future, the study concerning to the ecological impact of the reclamation and related to that for the major ecosystem (mangrove, coral reef, and sea grass) within the Benoa bay need to be consider.

Since the Benoa bay is located directly related with Badung strait and Lombok strait, therefore the deep investigation concerning to the interaction of Lombok strait and Badung strait with the Benoa bay are needed. This investigation would be very important for the fishery, aquaculture, and tourism activity.

Bali local government should be very careful in making some modification and/or conversion of Benoa bay. From the model, we showed the impact of Benoa bay modification that lead to retain the particle to reside in the inner bay longer than the original shape. Some modifications would have an important role for the ecology (mangrove ecosystem, coral reef, and sea grass) and tourism activity.